PREFACE

We would like to offer the readers the scientific activity report of the Frank Laboratory of Neutron Physics for 2010. The first part of the report presents a brief review of the experimental and theoretical results achieved in the main scientific directions – condensed matter physics, neutron nuclear physics and applied research. The second part includes the reports on the modernization of the IBR-2 pulsed reactor. The third part is concerned with the development and creation of elements of neutron spectrometers for condensed matter investigations. The fourth part presents the experimental reports that cover the main scientific directions in greater detail. The list of publications for 2010 completes the report.

In 2010 the main achievements of the Laboratory were:

- physical start-up of the IBR-2 reactor after a four-year period of modernization;
- modernization of some spectrometers at the IBR-2 reactor and continuation of the development of new facilities for neutron studies in condensed matter physics;
- 800-hour operation of the IREN facility for experiments;
- development of scientific experiments at local facilities and in collaboration with other scientific centers in Russia and abroad.

FLNP has cooperation agreements in the field of neutron investigations with almost 200 scientific institutes and universities from 40 countries from all over the world. A significant contribution to this cooperation is made by the JINR Member States.

The FLNP staff consists of more than 400 employees. The scientific staff includes 43 Ph.D. and 14 D.Sci. researchers and more than 50 researchers and specialists from the JINR Member States (besides the Russian Federation) with almost half of them under 35 years of age.

The organization of annual conferences and schools covering all research fields of FLNP activities helps to recruit young specialists — one of the top priority tasks of the FLNP Directorate.

All these facts confirm that the Laboratory continues to develop successfully and dynamically, carrying out investigations in the interests of the JINR Member States.

A.V.Belushkin
Director

1. SCIENTIFIC RESEARCH

CONDENSED MATTER PHYSICS

The main objectives of research in the framework of the theme involved the application of neutron scattering techniques and complementary methods to investigate the structure, dynamics and microscopic properties of nanosystems and novel materials, which are of great importance for the development of nanotechnologies in the fields of electronics, pharmacology, medicine, chemistry, modern condensed matter physics and interdisciplinary sciences. In view of the IBR-2 reactor shutdown for modernization, the experimental activities conducted by the personnel of the FLNP Department of Neutron Investigations of Condensed Matter (NICM) were carried out in neutron and synchrotron centers in Russia and abroad. These activities were performed in accordance with the Topical Plan for JINR Research and International Cooperation under the existing cooperation agreements and accepted beam time application proposals. The activities on the IBR-2 reactor were carried out in accordance with the modernization program plan for the spectrometers. Most attention was given to the realization of the top priority projects (construction of the new DN-6 diffractometer for studying microsamples, multipurpose GRAINS reflectometer and modernization of the SKAT/EPSILON spectrometers for geophysical research).

Within the framework of investigations under the theme, the employees of the NICM Department maintained broad cooperation with many scientific organizations in Russia and abroad. The cooperation, as a rule, was documented by joint protocols or agreements. In Russia, particularly active collaboration was with the thematically close organizations, such as RRC KI, PNPI, MSU, IMP, ISSP RAS, IC RAS, and others.

A list of main scientific topics studied by the employees of the NICM Department includes:

- Investigation of structure and properties of novel crystal materials and nanosystems by neutron diffraction;
- Investigation of magnetic colloidal systems in bulk and at interfaces;
- Investigation of structure of carbon nanomaterials;
- Magnetism of layered nanostructures;
- Investigation of supermolecular structure and functional characteristics of biological, colloidal and polymeric nanodispersed materials;
- Investigation of nanostructure and properties of lipid membranes and lipid complexes;
- Investigation of atomic dynamics of nanosystems and materials by neutron inelastic scattering;
- Investigation of texture and properties of minerals and rocks;
- Analysis of internal stresses in bulky materials and factory-made goods.

Scientific results.

Structure investigations of novel oxide materials.

The magnetic and crystal structures of the complex cobalt oxide $Pr_{0.5}Sr_{0.5}CoO_3$ have been studied using neutron diffraction and synchrotron radiation in the temperature range from 1.5 to

1120 K. Unlike other $Ln_{0.5}Sr_{0.5}CoO_3$ compounds, it exhibits both a paramagnetic-ferromagnetic transition at $T_C \approx 226$ K and one more magnetic phase transition at $T_A \approx 120$ K accompanied by a change in the behavior of magnetization in external magnetic fields and an anomalous behavior of elastic properties of the material. Successive structural transitions with the reduction of the crystal symmetry from cubic (space group $Pm\bar{3}m$) to rhombohedral ($R\bar{3}c$), then to orthorhombic (Imma) and triclinic ($P\bar{1}$) are detected at temperatures of about 800, 300 and 120 K (**Fig. 1**). The obtained results have helped to refine the earlier suggested models of the crystal structure of various phases. The anomalies in the temperature behavior of some interatomic distances and angles, as well as the reorientation of cobalt magnetic moments are observed at the transition to $P\bar{1}$ phase.

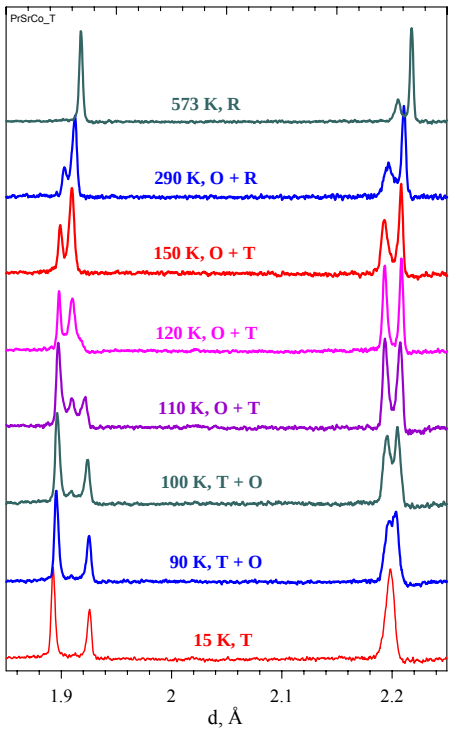

Fig. 1. A characteristic section of the diffraction spectrum of $Pr_{0.5}Sr_{0.5}CoO_3$ measured on the HRFD diffractometer at various temperatures. The temperature (from 15 K to 573 K) and corresponding structural phases: R = $R\bar{3}c$, O = *Imma*, T = $P\bar{1}$ are indicated.

The atomic and magnetic structures of $La_{0.5}Ca_{0.5}CoO_3$ cobaltite have been studied by the neutron diffraction technique at high pressures of up to 4 GPa in the temperature range from 10 to 300 K [1]. The Curie temperature increases with the pressure with the coefficient $dTC/dP = 1$ K/GPa, demonstrating the stability of the ground ferromagnetic (FM) state. The pressure dependence of the ground FM state in $La_{0.5}Ca_{0.5}CoO_3$ is in drastic contrast with that for $La_{1-x}Ca_xCoO_3$ at a lower calcium content ($x < 0.3$). For the latter compound, under pressure the suppression of the ground FM state and a large negative pressure coefficient of the Curie temperature ($dT_C/dP < 0$) are observed. The pressure dependences of the structural parameters have been obtained.

The structural and magnetic phase transitions in the multiferroic $BiMnO_3$ complex oxide have been studied at high pressures (**Fig. 2**) [2]. A unique feature of this compound as compared to other multiferroics is the combination of magnetoelectric effects with ferromagnetic ordering. A structural phase transition between two monoclinic modifications of *C2/c* symmetry was observed at a pressure of 1 GPa, which was accompanied by a significant change in the parameters of the unit cell and some interatomic distances. The structural phase transition occurs with a change in the character of

magnetic ordering from ferromagnetic (T_C = 100 K) to antiferromagnetic (T_N = 90 K) one with a

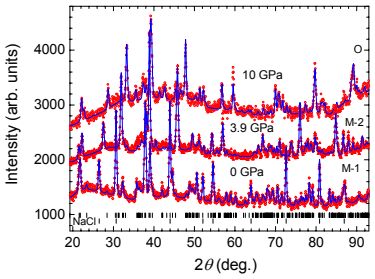

Fig. 2. Neutron diffraction spectra of $BiMnO_3$ obtained at various pressures and room temperature at the HRPT diffractometer (PSI, Switzerland) and treated by the Rietveld method (left). Magnetic structure of the high pressure monoclinic phase of $BiMnO_3$ (right).

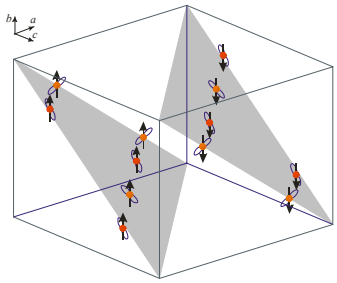

propagation vector k = (½ ½ ½). With a further increase in pressure at $P \sim 8$ GPa a structural phase transition to an orthorhombic phase of *Pbnm* symmetry was observed. The obtained results made it possible to reveal the role of competing superexchange interactions in the mechanism of occurrence of magnetoelectric phenomena.

Investigations of magnetic fluids.

Within the framework of the Helmholtz Association (Germany)-RFBR (Russia) Joint Research Groups (project HRJRG-16) structural characteristics of biocompatible ferrofluids synthesized for treating human brain cancer tumors have been determined using small-angle neutron scattering [4, 5]. The double layers of myristic (MA+MA) or lauric (LA+LA) acids were used to stabilize magnetite nanoparticles (size of ~10 nm, polydispersity > 50%) in a liquid medium. Despite rather large volume fractions of dispersed magnetite ($\varphi_m \sim 10$ %) on retention of a high stability the presence of nanoparticle clusters with a characteristic size of 30-40 nm has been revealed in the samples. The use of the contrast variation (H_2O/D_2O mixtures) and the application of the method of modified basic functions have allowed us to determine the cluster characteristics related to their inner structure. In particular, a significant difference in the surfactant fraction in the clusters has been observed for the samples of two types. It has been found that the clusters in the samples of the LA+LA type consist of magnetite particles completely coated with a surfactant shell about 3.5 nm thick, while in the samples of the MA+MA type the clusters comprise magnetite particles partially coated with the surfactants (**Fig. 3**). This indicates that more significant aggregation of the surfactant with a larger length decreases MA adsorption on the magnetite surface during the preparation. This conclusion is consistent with the fact that the synthesis of stable aqueous ferrofluids with the use of longer surfactants from the series of monocarboxylic acids (palmitic and stearic acids) is impossible. Other important characteristics obtained in the research are the temperature stability of the clusters and the absence of micelles of free (non-adsorbed) surfactants, which distinguishes the systems under study from the previously studied technical water-based ferrofluids stabilized by dodecylbenzenesulphonic acid, where fractal aggregates and significant surfactant excess with the micelle formation were observed.

The contrast variation in small-angle neutron scattering (Helmholtz Centre Geesthacht) using the method of modified basic functions has been applied in research of biocompatible ferrofluids prepared by the replacement of sodium oleate with polyethyleneglycol when stabilizing magnetite in water (Institute of Experimental Physics, Kosice, Slovakia) [6].

The cluster reorganization has been revealed depending on the amount of the polymer added to the system. In particular, under sufficient polymer concentration in the initial ferrofluid compact clusters (size 40 nm) transform to extended fractal clusters (size above 120 nm).

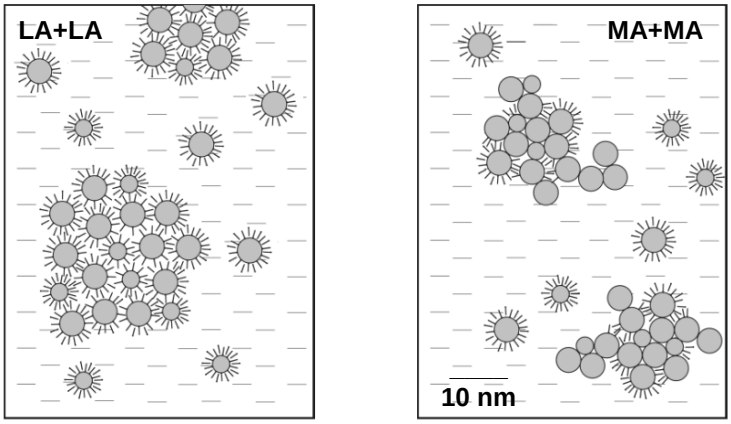

Fig. 3. A schematic representation of the cluster structure in two biocompatible aqueous ferrofluids with double layer stabilization of magnetite nanoparticles by lauric (LA+LA) and myristic (MA+MA) acids on the basis of contrast-variation small-angle neutron scattering data. Illustration by Yu.I.Emelina (FLNP JINR).

Along with this, the thickness of the stabilizing shell changes slightly, which is indicative of the polymer adsorption in the flat configuration on the magnetite surface. Taking into account a decrease in the saturation magnetization of the new fluid it is concluded the observed reorganization is related to the lowering of the system stability.

Investigations of carbon nanomaterials.

In the frame of the research of fullerene solutions with moderate polarity (dielectric constant 10–50) the C_{60}/N-methyl-pyrrolidone (C_{60}/NMP) system has been thoroughly investigated. The solution is characterized by the formation of large (size up to 500 nm) but stable clusters of fullerene molecules within about one month after the dissolution. In particular, it has been proposed [7] to follow the cluster growth by means of the extraction into an organic solvent immiscible with NMP (e.g. hexane) (**Fig. 4**). The cluster formation is correlated with the temporal solvatochromic effect (change in UV-Vis absorption spectrum with time). It has been shown that after the dissolution C_{60} is extracted from C_{60}/NMP (mauve color) to hexane (mauve color of lower intensity) in the molecular state. The extraction decreases with time and finally shows that all C_{60} in C_{60}/NMP (brownish yellow color) transfer to the unextractable clusters. The transition from a molecular to a colloidal (cluster) solution is reflected in mass-spectra of dried solutions. On addition of water (immiscible with hexane either) to the system the extraction resumes, which suggests that the clusters are destroyed as a result of the detachment of single C_{60} molecules. The appearance of separate molecules in the solution has been testified by mass-spectrometry, and a decrease in the cluster size has been detected by small-angle neutron scattering. It has been shown that along with this, water molecules chemically bind fullerene (charge-transfer complex). So, basing on the complex analysis and combining various methods, the solvatochromic effects in the C_{60}/NMP and C_{60}/NMP/water systems have been explained: together with the cluster development the initial fullerene-solvent complexes change with time (preferably on the cluster surface), thus favoring the fullerene dissolution in the NMP/water mixture.

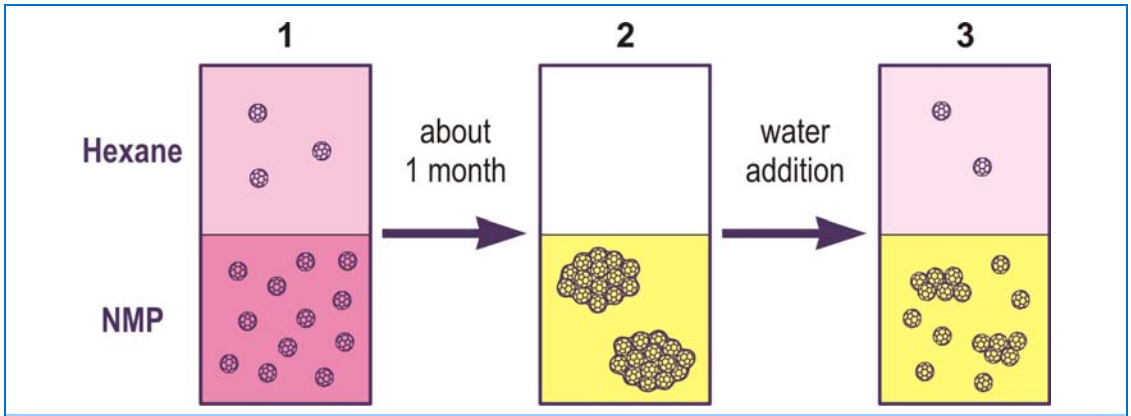

Fig. 4. A schematic representation of various stages in the extraction of fullerene C_{60} from C_{60}/NMП and C_{60}/NMП/H_2O solutions using the data of complementary structural methods. Cluster sizes are in the ranges of 100-500 nm (stage 2) and 10-100 nm (stage 3). Illustration by Yu.I.Emelina (FLNP JINR).

The theoretical model of the cluster formation in polar solutions of fullerene C_{60} has been developed [8]. The experimental data for C_{60}/NMP solution have been analyzed in terms of the kinetic theory of nucleation. It has been shown that in the frame of the nucleation theory, similar to the case of non-polar C_{60} solutions, the application of the cluster drop model results in fast phase separation in the system. The use of estimated thermodynamic parameters for the solution C_{60}/NMP in the kinetic equations gives ~10 μs for the duration of the independent growth stage. In contrast to non-polar solutions, the limited growth model, which limits the cluster size (the aggregation number), is inapplicable from the physical viewpoint. For the qualitative description of the processes in the system an alternative mechanism of the limited growth has been proposed. It assumes that the gradual formation of donor-acceptor complexes C_{60}-NMP restricts the growth of fullerene clusters. The corresponding model takes into account the assumed change of the C_{60}-NMP complexes with time.

Investigations of magnetic layered nanostructures.

The experimental investigations of the predicted inverse proximity effect for a superconductor-

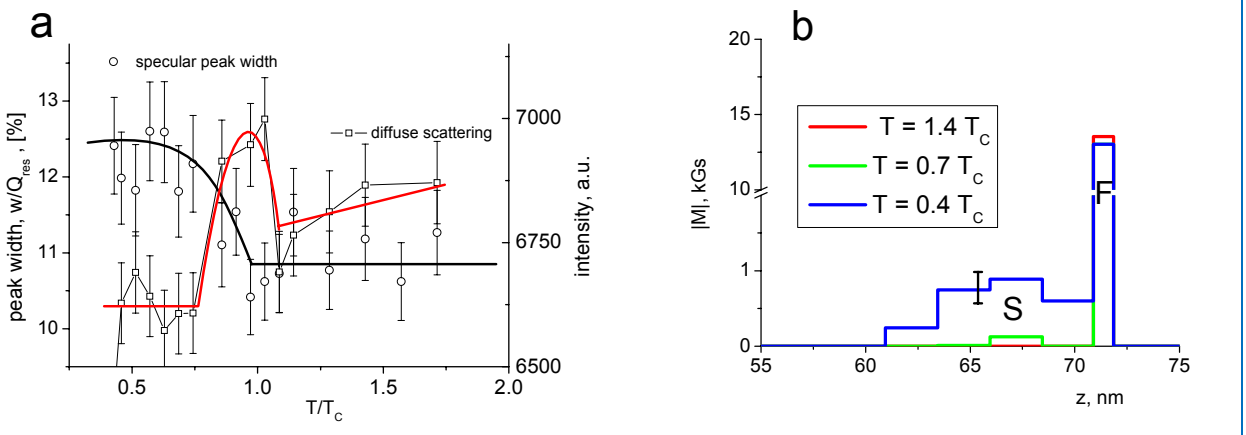

Fig. 5. a) Temperature behavior of magnetic scattering intensities near the superconducting phase transition.
b) Magnetic profile of the system above and below the transition temperature.

ferromagnet bilayer of the V/Fe nanostructure, which consists in the appearance of magnetization in the superconductor (**Fig. 5**) have been carried out. Theoretical predictions gave both the positive (in respect of ferromagnetic magnetization direction) and negative magnetization of the superconductor. The studies of the V/Fe bilayer have revealed the inverse proximity effect [9]. It has been found that below the superconducting transition temperature the superconducting layer is magnetized positively and the ferromagnetic layer — negatively, so the whole bilayer increases its magnetic moment.

Investigations of lipid membranes and lipid complexes.

Aqueous solutions of multilamellar vesicles (MLV) of the membranes modeling the lipid component in the mucous membranes of the oral cavity of mammals based on ceramide-6 and membranes in its structure (mixtures of sphingomyelin/dipalmitoylphosphatidylcholine/ dipalmitoylphosphatidylethanolamine with ceramide-6), have been investigated by means of synchrotron radiation diffraction in the temperature range of 20 - 80 (90)^{o}C (**Fig. 6**).

It has been found that at high temperatures (70-80 ^{o}C) the mixture of sphingomyelin /phospholipids tends to form an inverse hexagonal phase. Ceramide-6 at a mole fraction of 0.2-0.3 increases the repeat distance in MLV of the sphingomyelin/phospholipids mixture by ~1 Å and hinders the formation of the inverse hexagonal phase at high temperatures.

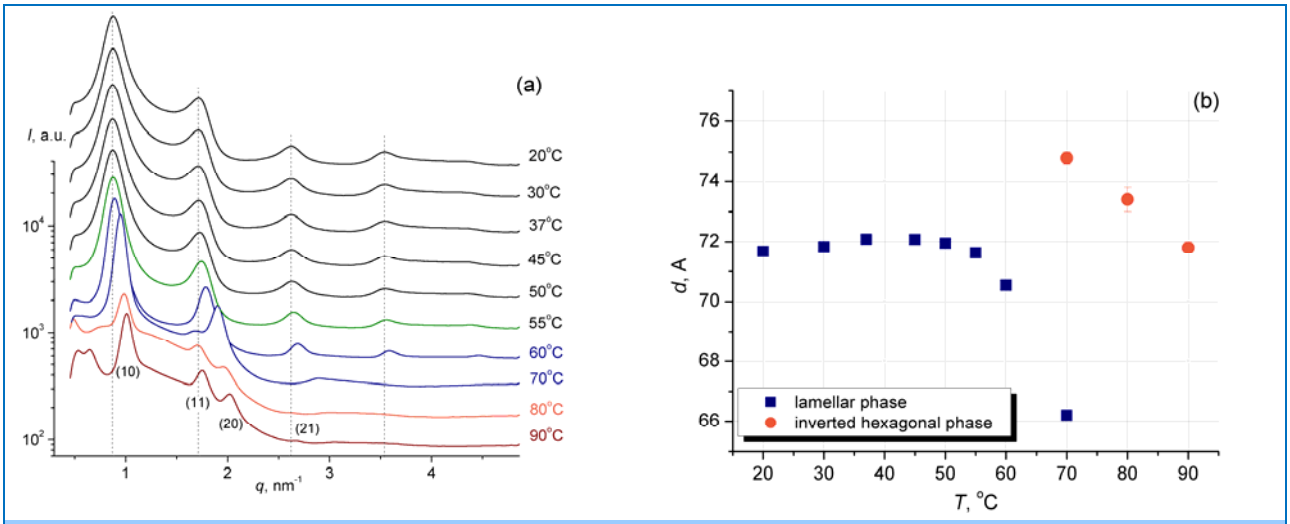

Fig. 6. (a) Diffraction spectra of the lamellar structure of MLV of sphingomyelin/DPPC/DPPE = 1/2/2. (b) Temperature dependence of the repeat distance (d) of the lamellar phase (■) and the parameter ($a = 2d/\sqrt{3}$) of the inverted hexagonal phase (●) of MLV of sphingomyelin/DPPC/DPPE = 1/2/2

As a result of the performed studies of the membranes composed of ceramide 6/cholesterol/ palmitic acid/cholesterol sulfate it has been found that the phase state of the membrane depends not only on the temperature, but also on the pH of water used in their preparation. At low pH values (5-7), the lipid bilayer is in the L_{φ} crystal phase and with increasing pH up to 9 there occurs a phase transition to the L_{β} gel phase while the degree of order of hydrocarbon tails decreases significantly and the membrane becomes single-phase.

The preparation phosphogliv dissolved in water has been studied. It has been determined that the lipid fraction of phosphogliv exists in an aqueous phase in the form of multilamellar liposomes with a repeat distance of 47.1 Å, which consist of the mixture of phosphatidylcholine (PC) and glycyrrhizic

acid (GRA). In the precipitate liposomes with repeat distances of 47.1 Å (mixture of PC and GRA) and 62.8 Å (pure PC) have been found.

The phospholipid transport system developed in the Institute of Biomedical Chemistry of the Russian Academy of Medical Sciences has been investigated. Samples were prepared by dissolving a lyophilized preparation in water with a drug concentration of 25 %. This concentration corresponds to the medical recommendation on the use of the medicine. The studies have demonstrated that 25 % solution of PTNS in water is a vesicle system of low polydispersity and the relative standard deviation in size is 20-30 %. The average radius of the vesicle is 160 Å, which corresponds to the PTNS nanoparticle size of 320 Å. The morphology of PTNS has been determined. It has been proved that the phospholipid transport system is a vesicle system with a low level of polydispersity at its 25 % concentration in water.

Investigations of polymer and colloidal nanosystems.

In cooperation with the Enikolopov Institute of Synthetic Polymer Materials of RAS and Bogoliubov Laboratory of Theoretical Physics (BLTP) of JINR the investigation of structural features of dendrimers — polymers combining properties of hyperbranched macromolecules and particles — has been continued [10]. For small-angle neutron scattering using the contrast variation technique the average scattering density of dendrimers has been determined and the invariants have been calculated. It has been shown that the scattering density distribution in the dendrimer volume is uniform within the experimental error. The upper estimate of the inhomogeneity of the scattering density of the dendrimers has been obtained. The possibility of the penetration of the solvent into the dendrimers has been demonstrated and the quantitative estimate of the volume accessible for the penetration of the solvent has been given. Some generalizing conclusions about the structure and properties of the specified kind of dendrimers from lower to higher generations have been made. In the dendrimer-solvent system at various concentrations and external conditions the existence of a structural factor, which is not typical for the «rigid sphere» systems has been revealed down to the lowest concentrations.

Theoretical calculations on the simulation of small-angle scattering from deterministic fractals — generalized Cantor fractals — have been performed in cooperation with BLTP JINR (**Fig. 7**) [11]. Deterministic fractals are a model of strictly self-similar structures of nano-objects, which nowadays can be obtained due to the development of modern nanotechnologies. The fractal dimension can vary from zero to three depending on the degree of its packing, which is controlled by the dimensionless scaling factor. The form-factor of the generalized Cantor fractal has been calculated analytically for arbitrary values of the wave vector and any finite iterations of the fractal, which makes it possible to use it for describing small-angle neutron and X-ray scattering from orientationally-ordered sets of fractals. For randomly oriented mono- and polydisperse fractals the scattering intensity has been obtained in the form of simple integrals. The values of the asymptotes for the fractal structure factor have been calculated and the radius of gyration has been obtained analytically for arbitrary iteration. The “shelf” behavior of the small-angle scattering curve has been explained. The possibility to estimate the number of particles from which the fractal is formed has been demonstrated.

In the framework of the study of surfactant solutions used for stabilizing ferrofluids, the structure and interaction parameters of micelles of dodecylbenzenesulfonic acid (DBSA) in deuterated water have been studied by small-angle neutron scattering (Helmholtz Center Geesthacht) [12]. The dependences of the micellar aggregation number, fractional charge, charge per micelle and surface potential on the surfactant concentration are analyzed. A typical increase in the micelle size with the

growth in the acid content has been found, which can be related to the transition from spherical to rod-like micelles.

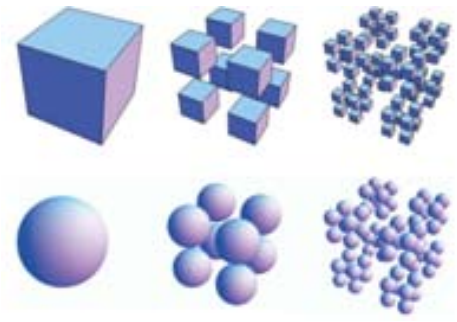

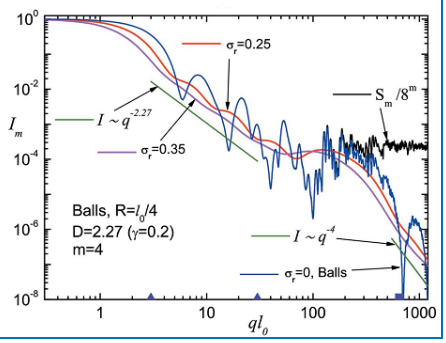

Fig. 7. Model representation of zero, first and second iterations for the generalized Cantor set composed of cubes and balls (left) and model intensity curves with the fractal dimension D = 2.27 with regard to polydispersity (right).

The obtained data have been used for estimating concentrations of micelle and free surfactant in bulk of aqueous ferrofluids (magnetite in water with a double shell of DBSA under excess).

Atomic dynamics.

The spin dynamics in the $Ce_{(1-x)}Y_xAl_3$ system at a transition from a heavy fermion (HF) state at x=0 to a mixed valence (MV) state at x=0.5 has been investigated by inelastic neutron scattering [13] (**Fig. 8**). It has been shown that the substitution of yttrium for cerium results in a strong transformation of spectrum components of the magnetic response due to an increase in the *k-f* hybridization.

The dynamics of uranium mononitride, which is considered to be a basic material for the creation of combined fuel for fast neutron reactors has been investigated. The inelastic neutron scattering spectra of UN have revealed quasi-resonant peculiarities in the region of the gap between acoustic and optical vibrations, which can be explained by solitons and nonlinear localized modes.

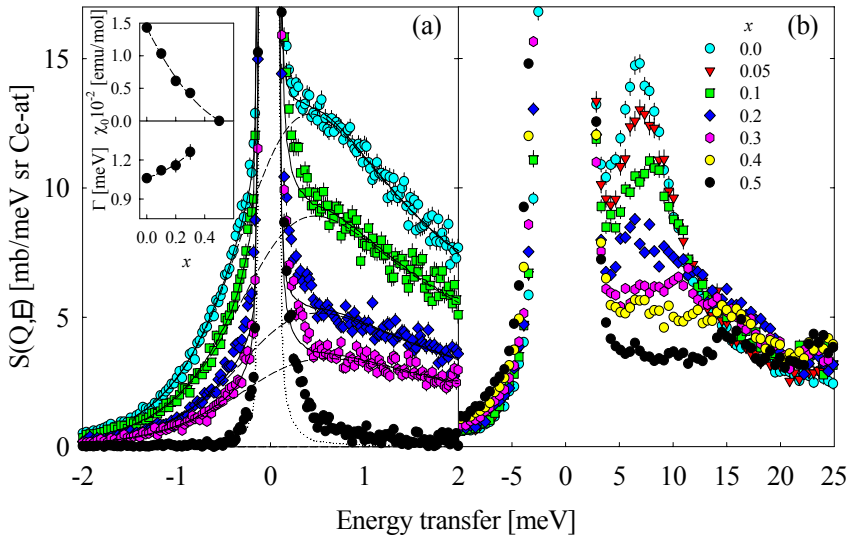

Fig. 8. S(Q,ω) of $Ce_{1-x}Y_xAl_3$ as a function of yttrium concentration "x":

a) measured on IN6 (ILL, France) at an average scattering angle of 60° and an incident energy of 3.12 MeV. The solid lines are fits to a quasielastic Lorentzian lineshape (dashed line) and an elastic peak (dotted line) convolved with the resolution function. The inset shows the dependence of yttrium concentration "x" on the values of the static susceptibility, ω_0, (top inset) and the half-width, $\Gamma/2$, (bottom inset) of the quasielastic peaks.

b) measured on LRMECS (ANL, USA) at an average scattering angle of 15° and an incident energy of 35 MeV.

Atomic structure and lattice dynamics of nickel hydroxide, $Ni(OH)_2$, an electrode material for chemical current sources, have been investigated by incoherent inelastic neutron scattering. The

comparative analysis of the vibrational spectra and lattice dynamics of nickel and magnesium hydroxides has been performed on the basis of inelastic incoherent neutron scattering data as well as Raman and IR-spectroscopy [14]. Optical phonon spectra have been calculated using the methods of the density functional theory and agree well with the vibrational spectroscopy data. The analysis of the calculated force constant matrix has made it possible to suggest the interpretation of the main features in the spectra of these compounds. The density functional method provides an insight into the peculiarities of interatomic interactions characteristic for these layered compounds and shows the important role of the spin-spin interactions in nickel hydroxide. It has been demonstrated that this method can be successfully applied to the investigation of the atomic structure and lattice dynamics of the β-NiOOH phase.

Applied research.

Among traditional applied investigations in the Department of Neutron Investigations of Condensed Matter are the experimental studies of internal stresses and texture of rocks and minerals, determination of internal stresses in bulk materials and products, including engineering materials and components of machines and devices. For the most part, these investigations are carried out using neutron diffraction.

Experiments to study elastic wave propagation in model inhomogeneous anisotropic media —

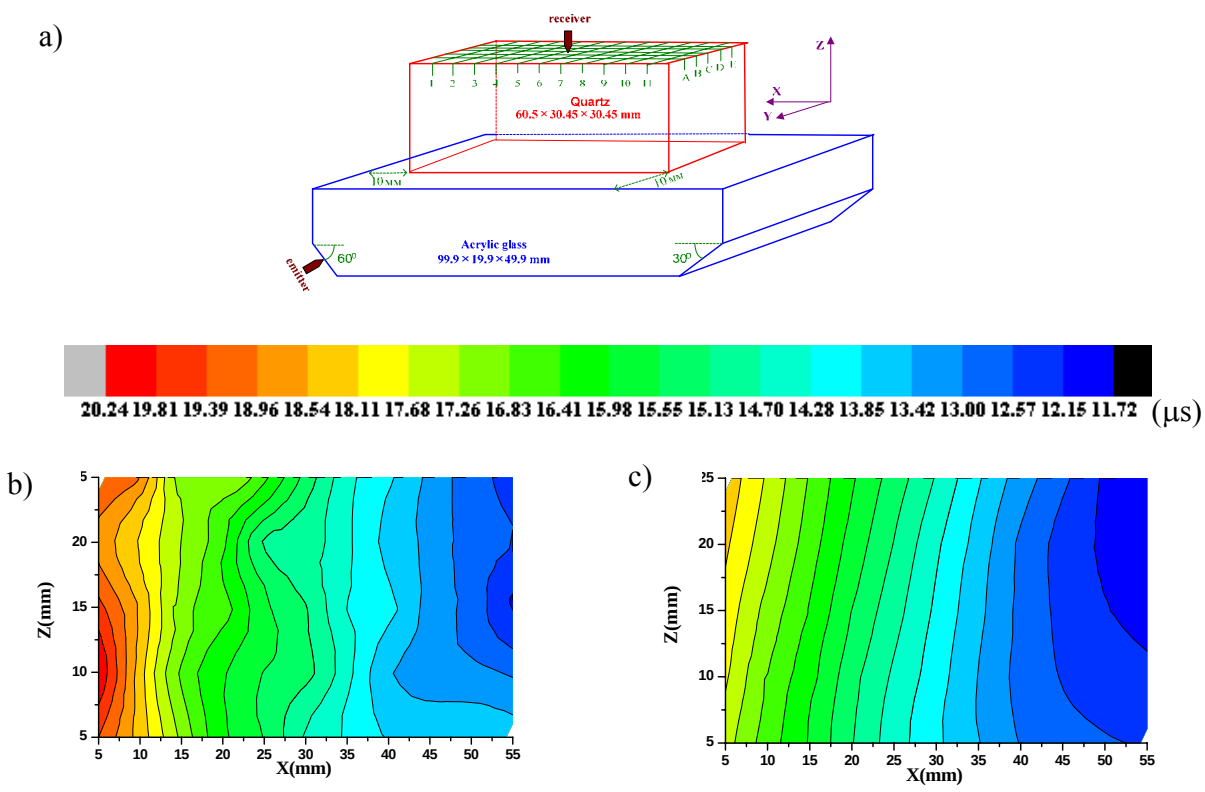

Fig. 9. (a) Scheme of a two-layer model of acrylic glass and quartz with the indicated location of ultrasound emitters and receiver. Isoline distribution maps of travel times of quasi-compressional waves in the model of acrylic glass and quartz. The quartz single crystal is in contact with the glass surface by the **XZ** plane; the emitter is attached to the side cut of the glass plate made at an angle of 60° to the horizontal surface: b) ultrasound frequency is 200 kHz; c) ultrasound frequency is 5 MHz.

samples of acrylic glass + single-crystal quartz, acrylic glass + polycrystalline graphite (with the known texture), epoxy resin + biotite — have been carried out (**Fig. 9**). It has been shown that in the model materials of "epoxy resin + biotite" differing by an order of magnitude in the grain size of biotite (0-0.4 mm and 2-5 mm), the velocities of longitudinal elastic waves with various frequencies coincide. It has been suggested that the discrete wavelet-transform method be used for the analysis of acoustic signals and determination of transverse elastic wave velocities. The comparison of theoretical calculations with the ultrasonic data from physical models has been conducted and a satisfactory agreement of the results has been obtained.

Neutron diffraction studies of residual stresses in a cross-shaped sample of austenitic stainless steel AISI 321 (**Fig. 10**) subjected to biaxial stress-strain cycling have been carried out. Under the action of plastic deformation the austenite matrix underwent partial transformation, which caused the formation of a new ferromagnetic martensitic phase in the sample. The total residual stresses in both phases of the cycled sample were measured using the time-of-flight neutron diffraction technique. Their analysis in the planar approximation has made it possible to determine macrostresses (similar in both phases) and microstresses (in each phase separately) as well as the contribution of hydrostatic pressure to the total phase stresses. In addition, it has been found that during planar cycling there occurs a partial transition from the martensitic phase to the austenitic one, which is connected with a plastic deformation of the material.

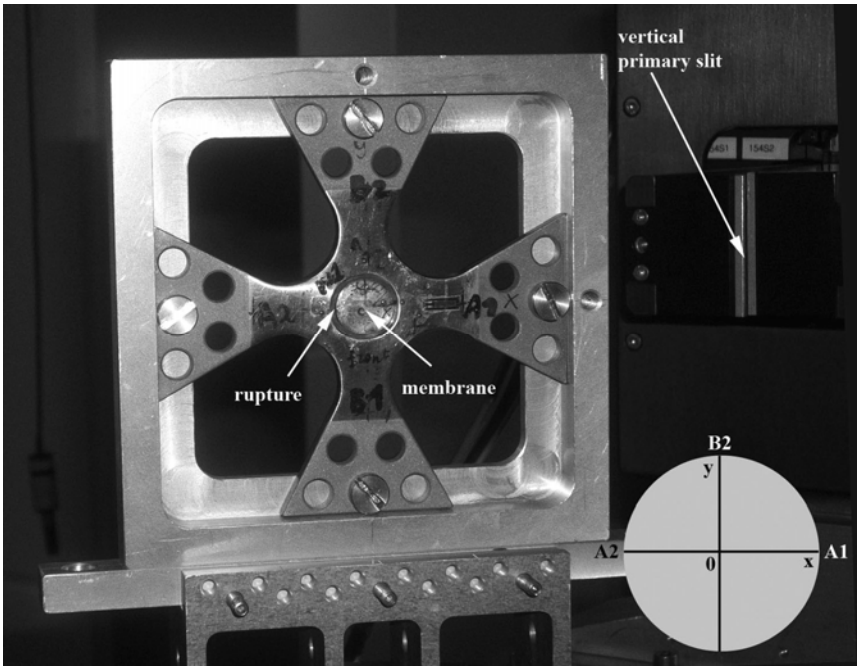

Fig. 10. A photo of the cross-shaped sample of austenitic stainless steel AISI 321 prepared for measuring internal stresses at the POLDI spectrometer (PSI, Switzerland). A vertical beam-forming slit is indicated by the arrow.

The studies of crystallographic texture and residual stresses in reactor materials, specifically in cylindrical fuel plugs made of E-110 alloy for the VVER-1000 reactor have continued. It has been demonstrated that the manufacturing process of parts by rotational swaging results in the formation of an axial crystallographic texture, which undergoes significant changes at annealing. Residual stresses of the first kind in cold-worked (strain of ≈ 150 MPa in a radial direction) and annealed (residual stresses are close to zero) fuel plugs have been calculated.

Using the data analysis of the texture measurement of polyphase granite gravel from the Erzgebirge, the magmatic flow and oriented crystal growth in an anisotropic stress field have been demonstrated to be the major texture formation processes. Texture measurements of rock salt from different sources in North Germany have been performed to study active deformation mechanisms. Despite the presence of external deformation, preferred grain orientations have not been determined. It has been concluded that during deformation processes texture does not develop or previously existing texture is destroyed because of the grain boundary migration processes.

The modeling of elastic wave velocities in rocks on the basis of the texture data of rock samples has shown that the elastic properties of rocks are independent of the influence of crack formation at high pressures. The experimental estimates of elastic wave velocities at low pressures have been compared with the crack formation effects, the extrapolation on high pressures is necessary to evaluate pressure conditions at very great depths. The further investigations have confirmed that all the model functions used are inapplicable for extrapolation. A refinement procedure for a model function, which will result in a better extrapolation of velocities has been suggested.

A texture study of marble samples using the neutron diffraction technique has been performed on TEX-2 (FRM-I) of the GKSS Research Center and STRESS SPEC (FRM-II) of the Technical University of Munich, Germany. The marble samples are from the Carrara region (Italy). This is a topical problem, since it is necessary to establish the reason for deformation and decay of the plates made of this kind of marble. These plates are widely used in Germany for cladding buildings (for example, the University Library building in Göttingen). The decay is caused by the accumulation of

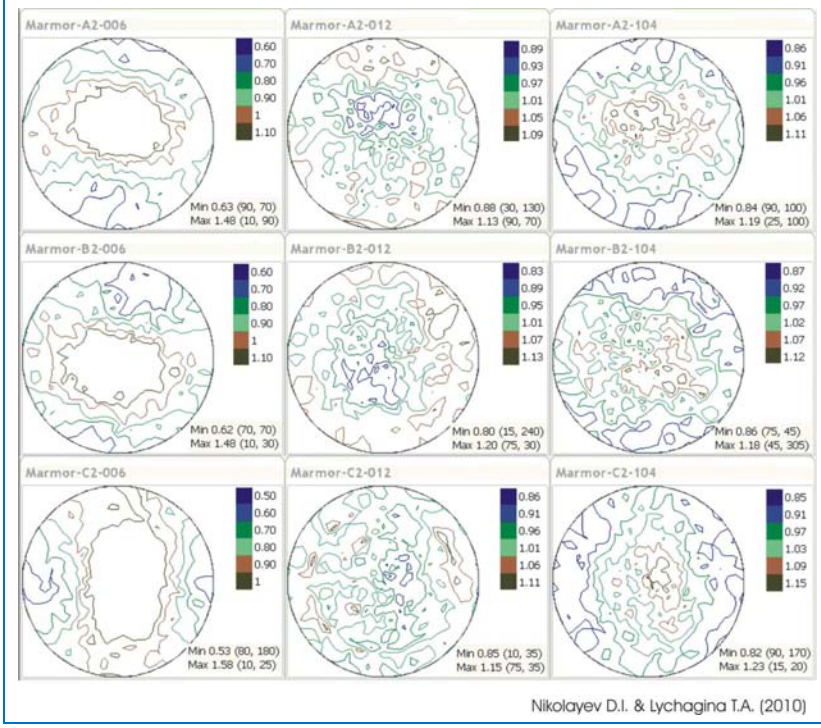

Fig. 11. Pole figures of the marble sample from the Carrara region (Italy) obtained using the diffraction data measured on the TEX-2 diffractometer (FRM-II, Germany).

residual stresses under cyclic deformation (as a result of the action of seasonal temperature gradients).

On the basis of the performed investigations (**Fig. 11**) it has been concluded that the texture sharpness

in the marble samples under study is insufficient to have a significant effect on the formation of the residual stress distribution. Nevertheless, the deformation and decay of marble plates is observed and it is necessary to find the reason for these phenomena; for this purpose it is planned to carry out a number of experiments and simulation studies.

Instrument development.

The installation of the beam chopper and the head part (**Fig. 12**) of the mirror neutron guide for the new DN-6 diffractometer for microsample investigations has been completed on beam 6b of the IBR-2 reactor. The manufacturing of mirrors for the tail part of the neutron guide has continued. The technical documentation for manufacturing the mechanical part of DN-6 has been prepared. The manufacturing of a gas position-sensitive detector has started in the FLNP Spectrometers' Complex Department (SCD).

Fig. 12. The head part of the mirror neutron guide installed on beam 6 of the IBR-2 reactor in the framework of the realization of the project of construction of the new DN-6 diffractometer for microsample investigations.

The installation of the head part (**Fig. 13**) of the new multifunctional reflectometer GRAINS on beam 10 of the IBR-2 reactor has been completed. The vacuum housing (**Fig. 13**) of the beam-forming system has been manufactured, assembled and tested for vacuum. The manufacturing of the background neutron drum chopper with a horizontal slit and the construction of an autonomous vacuum

Fig. 13. The head part of the GRAINS reflectometer installed in the ring corridor of the IBR-2 reactor (left) and the ready-assembled vacuum housing of the beam-forming system (during tests for vacuum in SPA «Atom», right).

system for the reflectometer have continued. The designing and manufacturing of a control system for stepper motors of the instrument and the software for the reflectometer has started. A 2D position-sensitive neutron detector has been manufactured and tested (in cooperation with SCD).

The effect of gravity on the resolution function of a reflectometer with a horizontal sample plane has been studied. The dependences of gravitational distortions of the specular reflection coefficient on various parameters of the reflectometer (collimation, sample sizes, relative distances between the elements of the reflectometer) have been obtained and analyzed.

The activities to install and vacuumize the splitter (**Fig. 14**) on beam 7 of IBR-2, which splits an initial neutron beam into three independent beams for the EPSILON, SKAT and NERA spectrometers, have been completed. A new background chopper with a wide window for three neutron guides has been installed, assembled and tested (in cooperation with SCD). Three lambda-choppers for the 7A-1 (EPSILON), 7A-2 (SKAT) and 7B (NERA) neutron guides have been manufactured and delivered. The technical documentation and the contract to manufacture 80-m sections of a mirror vacuum neutron guide for the NERA spectrometer have been prepared. The activities to modernize the spectrometers on beam 7 are carried out in cooperation with SCD.

Fig. 14. The splitter dividing the initial neutron beam into three independent beams for the EPSILON, SKAT and NERA spectrometers (left) and the new background chopper (right) on beam 7 of the IBR-2 reactor.

Work on the installation and adjustment of mechanical units and mirror segments of a neutron concentrator for the DIN-2PI spectrometer has been completed.

A project of the creation of a neutron spectrometer for studying transient processes in real time at the IBR-2 reactor has been prepared.

Theoretical and experimental activities to substantiate a new method of studying nanostructures — neutron magnetic resonance — have been conducted. The method is based on the phenomenon of neutron wave splitting in the processes of reflection and refraction of neutrons in a static collinear magnetic field and oscillating magnetic field perpendicular to it, which is connected with a gain (loss) of a quantum of an electromagnetic wave to (from) a neutron. This phenomenon in the neutron reflection channel was discovered in the measurements on the REMUR spectrometer in 2006 and verified in 2010 in the investigations in Germany (Munich). At the same time it has been shown that the reflection has a resonance character (intensity of off-specularly reflected neutrons depends on the frequency of the oscillating field and grows at a frequency equal to the Larmor frequency of the neutron spin precession around the magnetic field induction vector in a film).

The development work on the production of polarized neutron microbeams to study local inhomogeneities of nanostructures has been performed (**Fig. 15**). In conventional neutron experiments the information obtained on the object under study is averaged over the width of the incident beam (size of 0.1-1 mm). Layered waveguides, which are a three-layer film structure that transforms a rather wide (0.1 mm) and collimated (0.01°) beam into a narrow (0.1 μm) and divergent (0.1°) one, hold much promise for producing narrower neutron beams (neutron probe). Using layered waveguides the polarized neutron microbeams 0.15 μm wide have been produced for the first time. The neutron beam has the form of an elongated slit, therefore it may be most effectively used for one-dimensional lattices in the form of strips of magnetic materials.

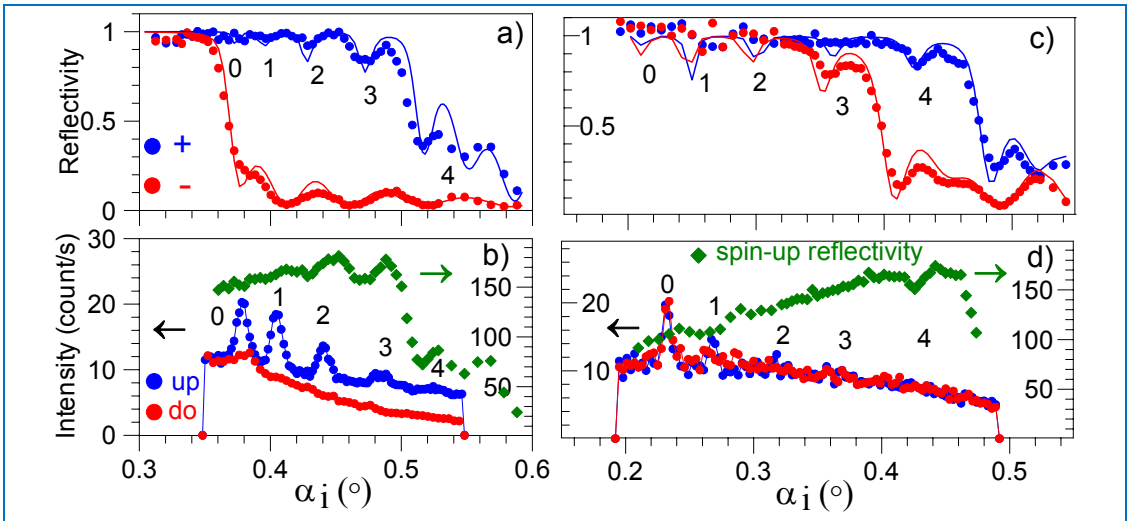

Fig. 15. Production of polarized neutron microbeams using magnetic layered structures. Left column: polarizing waveguide FeO_x(5.4 nm)/Fe(15 nm)/Cu(136 nm)/Fe(51 nm)//glass. Right column: non-polarizing waveguide Py(13 nm)/Al(141 nm)/Py(48 nm)//glass. Top: Reflection coefficients of spin states «+» and «–». The dots are the experimental data; the lines are the fits of the model structure. Indices denote minima that correspond to the resonances of the neutron wave function in the waveguide layer of Cu or Al. Bottom: maxima of the neutron microbeam as a function of the grazing angle of the initial neutron beam. For comparison purposes the intensity of the specularly reflected beam is given. The position of maxima of the microbeam corresponds to the position of minima of the specularly reflected beam. The width of the microbeam is equal to the width of the waveguide layer of Cu(136 nm) and Al(141 nm).

The experimental study of the influence of the finite thickness of spin-flippers with rotating magnetic fields on their efficiency has been carried out at the FRMII reactor, Germany. Similar devices can be used in spin-echo spectrometers of a new type. The finite thickness of the flippers makes it impossible to produce an exact neutron spin flip by 180°.

The automatic high-hydrostatic-pressure device at the YuMO spectrometer for carrying out volumetric studies in the pressure range of 0-4 kbar and in the temperature range of 5-200 °C has been modernized. First P-V-T experiments with water solutions of dimyristoylphosphatidylcholine have been conducted.

References

1. N.O.Golosova, D.P.Kozlenko, E.V.Lukin, B.N.Savenko. "Effect of high pressure on the crystal and magnetic structures of $La_{0.5}Ca_{0.5}CoO_3$ cobaltite", JETP Letters, v. 92, pp. 114-118 (2010).

2. D.P.Kozlenko, A.A.Belik, S.E.Kichanov, I.Mirebeau, D.V.Sheptyakov, Th.Straessle, O.L.Makarova, A.V.Belushkin, B.N.Savenko, E.Takayama-Muromachi. "Competition between ferromagnetic and antiferromagnetic ground states in $BiMnO_3$ at high pressures", Phys. Rev. B 82, 014401 (6 pp.) (2010).

3. A.V.Belushkin and D.P.Kozlenko Structural organization of nanomaterials and nanosystems: neutron scattering insight, Advances in Natural Sciences: Nanoscience and Nanotechnology 1, 023002 (8 pp.) (2010).

4. M.V.Avdeev, B.Mucha, K.Lamszus, L.Vekas, V.M.Garamus, A.V.Feoktystov, O.Marinica, R.Turcu, R.Willumeit. "Structure and in vitro biological testing of water-based ferrofluids stabilized by monocarboxylic acids". Langmuir, 26 (2010) pp. 8503-8509.

5. M.V.Avdeev, V.L.Aksenov. "Small-angle neutron scattering in structure research of magnetic fluids. Review", UFN, v. 180, №10, pp. 1009-1034 (2010).

6. M.V.Avdeev, A.V.Feoktystov, P.Kopcansky, G.Lancz, V.M.Garamus, R.Willumeit, M.Timko, M.Koneracka, V.Zavisova, N.Tomasovicova, A.Jurikova, K.Csach, L.A.Bulavin. "Structure of water-based ferrofluids with sodium oleate and polyethylene glycol stabilization by small-angle neutron scattering: contrast-variation experiments". J. Appl. Cryst. 43 (2010) 959–969.

7. O.A.Kyzyma, M.V.Korobov, M.V.Avdeev, V.M.Garamus, S.V.Snegir, V.I.Petrenko, V.L.Aksenov, L.A.Bulavin. "Aggregate development in C_{60}/N-metyl-2-pyrrolidone solution and its mixture with water as revealed by extraction and mass spectroscopy", Chem. Phys. Lett. 493, 103–106 (2010).

8. M.V.Avdeev, T.V.Tropin, V.L.Aksenov. "Models of cluster formation in solutions of fullerenes", Russian Journal of Phys. Chem. 84(8), 1273–1283 (2010).

9. V.L.Aksenov, Yu.N.Khaidukov, Yu.V.Nikitenko. "Peculiarities of magnetic states in "Ferromagnet-Superconductor" heterostructures due to proximity effects", Journal of Physics: Conference Series, 211, 012022-012027 (2010).

10. A.V.Rogachev, A.I.Kuklin, A.Yu.Cherny, A.N.Ozerin, A.M.Muzafarov, E.A.Tatarinova, V.I.Gordeliy. "Structure of organosilicon dendrimers of higher generations", Physics of the Solid State, 52, № 5, 1045-1049 (2010).

11. A.Yu.Cherny, E.M.Anitas, A.I.Kuklin, M.Balasoiu and V.A.Osipov. "Scattering from generalized Cantor fractals". J. Appl. Cryst. 43, 790–797 (2010).

12. V.I.Petrenko, M.V.Avdeev, V.M.Garamus, L.A.Bulavin, V.L.Aksenov, L.Rosta. "Micelle formation in aqueous solutions of dodecylbenzene sulfonic acid studied by small-angle neutron scattering", *Coll. Surf. A* 369 (2010) 160–164.

13. E.A.Goremychkin, R.Osborn, I.L.Sashin, P.Riseborough, B.D.Rainford, D.T.Adroja, J.M.Lawrence. "Transition from heavy-fermion to mixed-valence behavior in Ce_{1-x} Y_xAl_3: a quantitative comparison with the Anderson impurity". Phys. Rev. Lett. 104, 176402 (4 pp.) (2010).

14. V.Yu.Kazimirov, M.B.Smirnov, L.Bourgeois, L.Guerlou-Demourgues, L.Servant, A.M.Balagurov, I.Natkaniec, N.R.Khasanova, E.V.Antipov. "Lattice dynamics of Ni and Mg hydroxides". Solid State Ionics, 181, 1764-1770 (2010).

2. NEUTRON SOURCES

THE IBR-2 PULSED REACTOR

1. In January-February, 2010, after completion of the adjustment work on the sodium cooling system of the reactor, the heating of the sodium circuits and filling of the Ist and IInd cooling loops with sodium were performed successfully and the circulation of sodium was started in a standby mode. The purification of the coolant with the help of cold traps, calibration tests of the level gauges of the expansion tanks and vessel of the reactor, calibration of the flowmeters were carried out.
2. After installation of actuating mechanisms (AM) of the Safety Control System (SCS) A3-1, A3-2, KO-1, KO-2, PP and AP at regular places, the adjustment of the system controlling the movements of the actuating devices was performed. The emergency protection system of the reactor was tested in the forced operation mode (actuated by a stepper motor and an accelerating spring) and in the mode when its operation was triggered only by a spring. The obtained results are positive and meet the design requirements. Movement ranges of all actuating devices were determined – the setting of the up and down limit switches; the stability of their operation was checked. No faults in the operation of AM were revealed. The SCS AM were tested for electromagnetic compatibility, i.e. for the effects of various disturbances (radio interferences, electrostatic discharges, magnetic fields, etc.). The results of these tests are positive.
3. Installation, adjustment and tests of the Automatic Safety Control System (ASCS-12R). The equipment for ASCS-12R was delivered from SNIIP-SYSTEMATOM in April, 2010 with a delay of 15 months. The installation of the equipment took 3 months and was followed by the adjustment and tests of the complex. In November the ASCS-12R complex was presented to the Working Commission for carrying out the physical start-up of the reactor.
4. The spent IBR-2 fuel assemblies were removed from the main storage facility to an additional one. The main fuel assembly storage is ready for the physical start-up.
5. A start-up neutron source was loaded into the reactor core.
6. All technological systems of the reactor passed complex tests before the physical start-up.
7. A large amount of work on the preparation of the commissioning documentation for the physical start-up was carried out. The reactor successfully passed the inspection by the Working Commission for readiness for physical start-up.

The modernized IBR-2 reactor physical start up was commenced according to the plan.

IREN FACILITY

In accordance with the decision of the JINR Directorate to realize the IREN project in several stages, the construction of the electron accelerator and the nonmultiplying neutron-producing target complex has been completed. Since the beginning of 2009 the carrying out of experimental investigations on newly constructed source has been started. IREN operated around 800 hours for experiment in 2010. Neutron yield raised up to 10^{11} n/s at 100 ns pulse width.

3. NOVEL DEVELOPMENT AND CONSTRUCTION OF EQUIPMENT FOR THE IBR-2 SPECTROMETERS' COMPLEX

In 2010, work in the framework of the theme was focused on several activities connected with the construction and modernization of the equipment, electronic data acquisition and accumulation systems as well as the information-computation infrastructure of the IBR-2 spectrometers' complex.

Cryogenic moderators.

A full-scale test stand of a cryogenic moderator has been developed and assembled in the IBR-2 experimental hall. A functional scheme has been developed; electronic modules and control equipment have been purchased and installed; and the software for a control system for monitoring different parameters of the stand has been created. The system includes various sensors (15 pieces altogether), a gas blower motor drive controller and a controller of the stepper motor of the bead charging device, etc. The system makes it possible to control the main parameters of the moderator test stand: transport of beads through the pneumatic conveying pipe; filling of the moderator chamber with beads; gas flow rate; pressure and temperature of helium. At present, the test stand and the control system undergo trial operation. A number of experiments have been performed at the test stand, which have made it possible to adjust and improve the technological control system, to choose optimum working temperature range for the prototype, to determine the helium flow rate in the inner pneumatic conveying pipe, the optimum rate of feeding beads from the charging device and the total load time of the simulation chamber. Also, in the course of the experiments the simulation chamber has been partially filled (~70% of the volume, **Fig. 1**). A detailed description of the test stand is given in the section "Experimental Reports".

Fig. 1. A photo of beads taken by the Web-camera.

New Fourier diffractometer.

At present, at the IBR-2 reactor a new high resolution Fourier diffractometer is being constructed on the basis of the units of the FSS (Fourier Stress Spectrometer) spectrometer, which had been used in the GKSS Research Center (Germany) for a long time. The layout of the FSS units on beam 13 of IBR-2 has been developed **(Fig. 2),** which only slightly differs from the layout used earlier in GKSS. The necessity for changes is caused mainly by geometrical constraints existing on beam 13 of IBR-2. With the help of the new diffractometer the internal stresses in constructional materials and industrial products will be studied; it is also planned to organize educational process of training

specialists and to test new equipment for further development of the Fourier correlation method for analysis of elastic neutron scattering by crystals (increase of luminosity, improvement of resolution, etc.). This beam is also intended to be used for testing detectors and other spectrometer elements developed in FLNP, i.e. it will serve as a test beam.

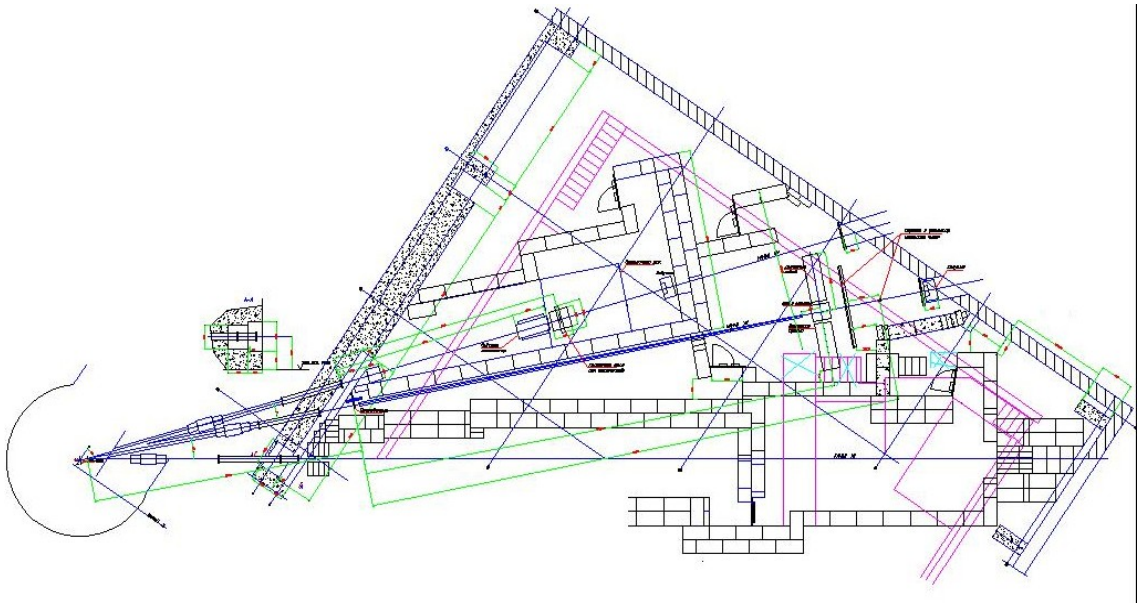

Fig. 2. The layout of the FSS diffractometer on beam 13 of IBR-2.

Neutron beam-forming systems.

In cooperation with the German Institutes and PNPI (Gatchina) the reconstruction of neutron guides for beam 7 of IBR-2 and the modernization of the EPSILON and SKAT diffractometers (in accordance with the plan-schedule of the BMBF-JINR project) continued. The head part of the neutron guide system (splitter, **Fig. 3**) was assembled, optical elements were adjusted and covered by a shielding material, and the debugging of the vacuum system is under way.

Fig. 3. Splitter.

Fig. 4. First sections of the curved neutron guides for EPSILON (yellow) and SKAT (blue).

Vacuum casings and beam-positioning support pillars for the outlet part of the EPSILON and SKAT neutron guides were manufactured. The installation of curved neutron guides for the EPSILON

and SKAT diffractometers (**Fig. 4**) and of vacuum equipment, as well as the vacuumization of the neutron guides are in progress.

Work on the reconstruction of the neutron guide for the NERA-PR spectrometer has started. Working drawings of the new neutron guide have been developed and the old neutron guide has been dismantled.

Choppers and actuating mechanisms.

The choppers of beams 4, 7 and 8 with new TOSHIBA variable-frequency drives have been tested in the phase stabilization mode. Tests of the drum-type DC-motor-based choppers (**Fig. 5**) manufactured in the Scientific Production Association «Atom» have been carried out in the ring corridor on beams 6a and 6b. The phase stabilization accuracy was 25-50 μs.

Fig. 5. A drum-type DC-motor-based chopper.

The modernization of the sample-changing system on beam 4 (YuMO) at IBR-2 has been carried out. The modernization project for the control system of a goniometer and a platform with a detector on the REMUR spectrometer has been developed. Within the framework of the project a structural scheme of the unified control system of stepper motors and systems of data acquisition from sensors has been proposed (**Fig. 6**), which can be used for the modernization of control systems of actuating mechanisms (AM) on other IBR-2 spectrometers as well.

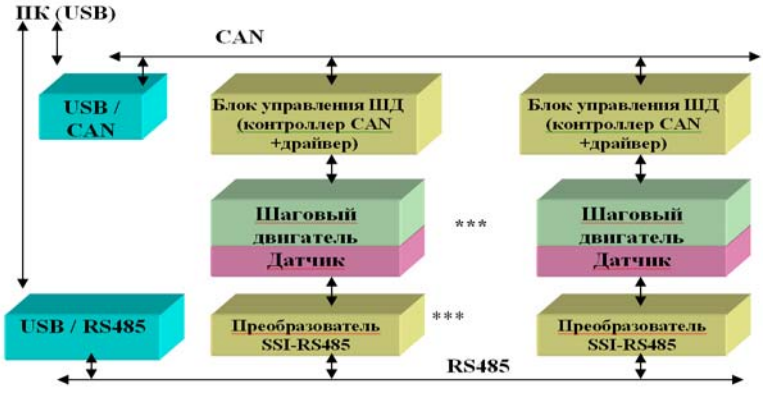

Fig. 6. The structural scheme of the control system of stepper motors and data acquisition from angular sensors.

It seems reasonable in the process of modernization of AM control systems to keep the division between an integrated controller/driver and a stepper motor, since this simplifies the problem of changing the type of a motor or a controller. It is suggested to widely use CAN controllers/drivers of stepper motors with currents of 1-8 A, and absolute multi-turn angle sensors consisting of a one-revolution sensor (12-16 bits) and a sensor of revolutions (12-16 bits). They can be used to control both angular and linear movements.

Calculations and simulation of spectrometers.

In close cooperation with the Munich branch of the Research Centre FZ-Juelich in FLNP the development and support of the software package VITESS (Virtual Instrument Tool European Spallation Source), as well as the calculations and simulations of new devices and spectrometers for both the IBR-2 and the FRM-2 reactors are under way.

The calculations of neutron spectra and optimization of beam geometry from the moderator to a sample for the spectrometers located on beams 4 and 10 of the IBR-2 reactor have been completed:

- The simulation and optimization of the extraction system for beam 4 (YuMO) and a new small-angle instrument with two consecutive collimation systems (divergent neutron guide + multislit collimator: grids) have been completed. This made it possible to increase the sizes of samples in use and at the same time to reduce Q_{min} (and as a result to increase the instrument resolution) as compared to the available YuMO spectrometer. The extraction system allows neutrons to be collected and used from both moderators (cold and thermal).
- The simulation of the prototype of a new instrument with polarized neutrons GRAINS has been performed. The comparison of the simulation results with the analytical calculations has been performed. Particular attention has been given to the proper consideration of the influence of gravitational effects on the resolution function of the instrument, as well as on the distribution of neutron flux on a sample. The results of the simulation have practically coincided with the analytical results. Also, the algorithm for gravitation simulation in VITESS has been improved.

New modules for the VITESS software package have been developed:

- The development and testing of the module for simulating an adiabatic radio-frequency flipper have been completed. The simulation of a spin-echo machine with 4 flippers has been carried out.
- A new special module for simulating moving round grids has been developed with due regard for neutron attenuation in materials. The module can simulate grids at the nanoscale. It is intended to simulate one of the variants of the Neutron Spin Echo Machine. The development and testing of a new module for simulating neutron refraction prisms and systems of prisms have started as well. Both of the above-mentioned modules are being developed in cooperation with A.Ioffe (JCNS-Munich, Germany).
- A module for simulating a universal polarizing mirror for the new GRAINS reflectometer has been developed.

For all the above-listed modules the agreement between the simulation results and theoretical calculations is good.

Detectors.

For the PSD of the GRAINS spectrometer work on the optimization of the firmware for a new electronic block of acquisition and accumulation of data from the detector has been completed and the development of PC software has started. This detector has also been tested with De-Li-DAQ1 electronics on beam 4 of the LVR-15 reactor at the Nuclear Research Institute (NRI) in Řež (Czech Republic). The measurements were carried out for several days with the use of various slit masks, scatterers and so forth. Image Plate and 1D PSD Ordella detectors were used for calibration purposes. The results of the measurement of basic characteristics of the detector coincide with the results obtained last year at the IR-8 reactor in the RRC "Kurchatov Institute" and correspond to the design values. **Figure 7** illustrates the spectrum for a thick alpha-Fe sample (measured in NRI with the GRAINS PSD). Using the same detector, neutron beam profiles were measured on two channels of the IREN facility. Thus, the GRAINS PSD has passed thorough testing in various operation conditions and can be used in experiments at IBR-2.

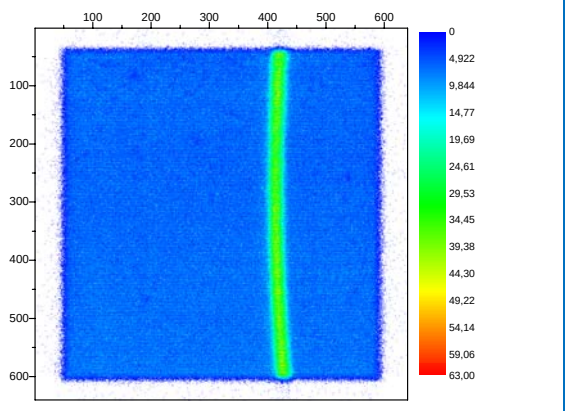

Fig. 7. Spectrum for a thick alpha-Fe sample (distance to the sample is 45 cm, measurement time is 300 s).

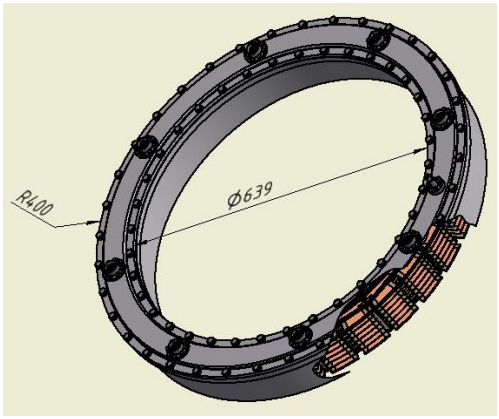

Fig. 8. A ring-shaped multi-section detector of thermal neutrons.

Since 2010, the specialists from NRI (Řež) have been participating in the development and construction of a **ring-shaped multi-section detector (RSD)** of thermal neutrons **(Fig. 8)** for the DN-6 diffractometer. A grant was allocated for this project within the framework of the program of cooperation between JINR and Czech Republic, and this made it possible to prepare the design documentation for mechanical units of the detector, as well as to produce and test the prototype of one section of RSD (test module).

The detector is divided into sections (16 or 32), which share the same gas volume. The casing and the cover of the detector are made of Al-Mg alloy ensuring hermeticity and mechanical strength of the device. Each section in its turn is divided into 6 cells along the generator of the cylindrical surface. The sections and cells are mechanically bounded by 1-mm-thick plates of foil-clad textolite. The dimensions of one cell are 15×30×80 mm^3. Signals from cells are taken from independent anode wires, which are in the geometric centers of the cells. Preamplifiers are located inside the detector gas volume, which allows us to minimize noise. Individual data readout from each cell provides necessary flexibility in adjusting and positioning the detector.

Because of the curved shape of the electrodes, the electric field distribution inside the detector will differ from the electric field distribution in flat chambers. To evaluate the influence of the

curvature of the detector, a test module has been made. An external view of the module is shown in **Fig. 9**. It imitates one section of a 32-section curved detector.

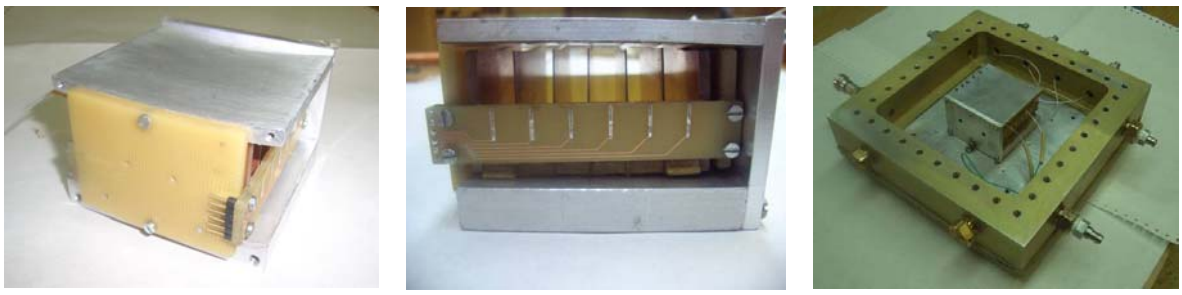

Fig. 9. The test module. Side view, front view, ready-assembled test module.

Gold-plated tungsten anode wires are stretched in the center of the cells between the top and bottom curved cathodes. Several variants of the cells with wires of various diameters (10, 25 and 50 μm) have been tested. The distance from a wire to the curved cathodes at the edges is ~15 mm. The top curved cathode has a radius of 330 mm and a thickness of 5 mm. The radius of curvature of the bottom cathode is 371 mm; it has flat basis, which simplifies the process of manufacturing and does not affect the characteristics of the module. A schematic view of the module is given in **Fig. 10**.

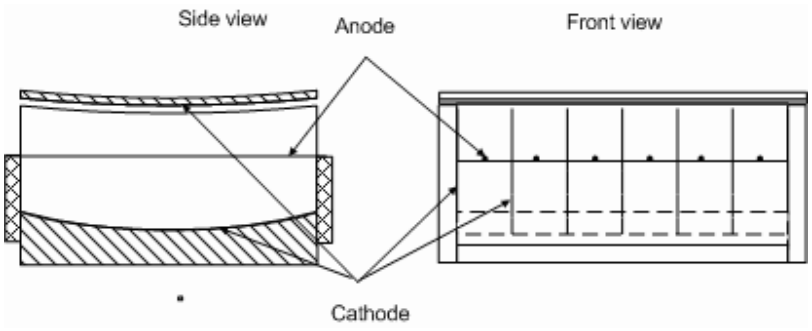

Fig. 10. A schematic of the test module.

The measurements were carried out with a ^{252}Cf neutron source. Amplitude spectra and count rate characteristics were obtained for various gas mixtures. Amplitude spectra of signals from the test module and from a standard helium counter SNM-17 are presented in **Fig. 11**.

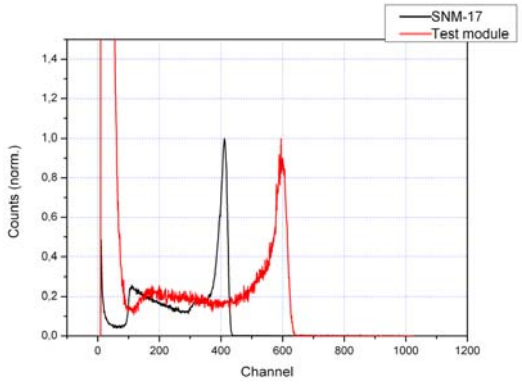

Fig. 11. Comparative amplitude spectra for a SNM-17 counter and the test module. For illustration purposes the spectra have been normalized to unity.

It has been found that signal acquisition in the test module proceeds a little bit more slowly than in SNM-17, which is due to the elongated shape of cells. The energy resolution of the detector is comparable to the resolution of a standard counter. A signal-to-noise ratio is slightly worse, however, signals from neutrons can be reliably separated from noise. Since it is expected that the ring-shaped detector will operate at light loads and in a "clean" beam, we can state that on the whole the characteristics of the test module meet the requirements imposed on the detector.

At present, the design documentation has been forwarded to the SPA «Atom» to produce the mechanical units of the detector.

An advanced version of a high-speed neutron counter with a peak load of up to $3 \cdot 10^6$ n/s (see Annual Report for 2009) has been produced and successfully tested in ILL.

In view of the existing problems with the helium-3 supply, the design of a helium-3 purification system (**Fig. 12**) has been done. The drawings have been forwarded to the SPA «Atom» for production.

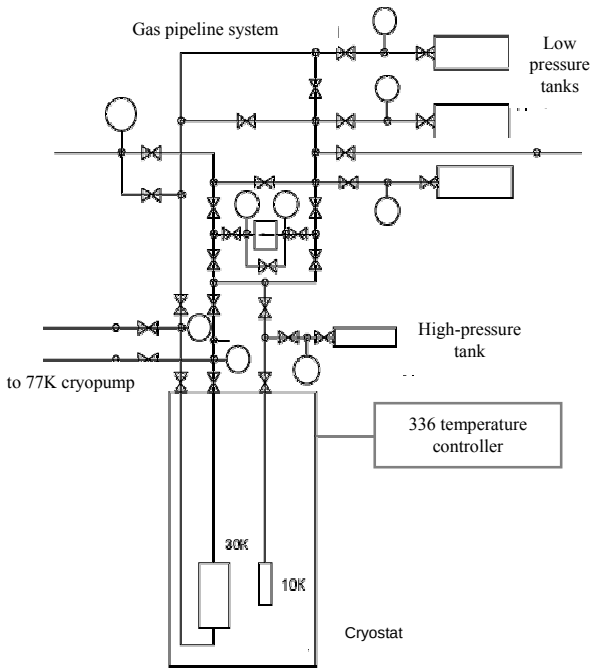

Fig. 12. A general scheme of the helium-3 purification facility. At the preliminary stage helium-3 is purified by a cryopump at the temperature of liquid nitrogen. At the second stage the purification is performed in a cryostat. The cryostat contains two sorption pumps at 30K and 10K. The first pump makes it possible to remove hydrogen from helium-3, the second one serves to compress helium-3, which is fed to a high-pressure cylinder.

Necessary calculations and design works have been performed to create the next module of the scintillation detector “Astra” for the FSD diffractometer. The components necessary for assembling the module have been ordered and partially delivered. The order to manufacture the detector elements has been placed at the SPA «Atom».

Electronics.

Preamplifiers and discriminators for the RSD of the DN-6 diffractometer have been developed, manufactured and tested with a test module.

The architecture and electrical circuits of a unified block for data acquisition and accumulation (DAA) from neutron counters of the EPSILON diffractometer and the ring-shaped detector of DN-6 have been developed. The basic design parameters are as follows:

- time discretization frequency of all signals (detector, reactor start, etc.) – programmable (maximum of 62.5 MHz);
- maximum number of detector elements – 96 (192);
- maximum count rate – $5 \cdot 10^6$ events/s (~$5 \cdot 10^4$ for one detector element);
- PC interface – USB 2.0;
- internal histogram memory of the accumulation block – 64 Mbyte;
- maximum delay of the registration start relative to a reactor burst – 0.268 s (programmable, time step – 16 ns); with the same accuracy the channel width for histogram memory and the width of a time window within which neutrons are registered, can be programmed.

A test generator imitating the operation of the data accumulation system without connection of detector elements is built into electronics. This will make it possible to make a fast check for the serviceability of the equipment before a session and also to perform its autonomous debugging.

Data transmission between the data acquisition electronics and USB interface will be carried out via a serial fiber-optic line at 1.25 Gbit/s.

Structurally the DAA system consists of the above-mentioned programmable block with FPGA and three input converter blocks, in each of which the transformation of signals and transition from a 32-pin LEMO connector to a ribbon cable are carried out. The main difference between the DAA systems for the EPSILON and DN-6 diffractometers is that for the EPSILON diffractometer in a histogram accumulation mode the neutron time focusing operations are required to be performed. Specific features of each spectrometer are taken into account in programming FPGA.

At present, a prototype of the DAA system for 16 detector elements (DAA-16) has been developed and constructed. It is intended for use at the REFLEX spectrometer and can be employed at other instruments, where the number of detector elements does not exceed 16. By the end of the year it is planned to test it.

The data acquisition block De-Li-DAQ2 for PSD has been debugged. Drivers and controllers of spin-flippers (2 sets) have been developed, manufactured and adjusted for the REFLEX spectrometer.

In accordance with the schedule the routine maintenance, repair and modernization of the electronic equipment at the IBR-2 spectrometers were carried out.

FLNP local area network.

A new Switch Catalyst 3560E-24TD-E router has been installed in the IBR-2 experimental hall. It should provide switching and transferring data at a rate ranging from 10 Mbit/s to 10 Gbit/s; intrasegment data transfer via twisted pair and fiber-optic cables; connection with the central network segment via a fiber-optic line. At present, in cooperation with the specialists from the Laboratory of Information Technologies the adaptation of the router to the existing FLNP network and the JINR network is carried out. The purchase of the second router is postponed until 2011, since a demand arose for an urgent replacement of a worn-out router Switch Catalyst 5000 in the central segment of the FLNP network (bldg. 119) by Switch Catalyst 2960S-24TD-L l and a mail server Sun Workstation by Server 1U 600W/Xeon E5507.

The disk space of two servers SUN X4200 has been extended up to 1.3 TByte; one of them has been operating as a mail server since August, 2010. New network public domain printers HP LaserJet 2055DN (4 pcs) have been purchased and installed in the main buildings of the

Laboratory. Work is carried out to test and eliminate the mismatch between the crossover joints of fiber-optic cables and the requirements of the 10 Gbit/s interface.

Software.

In 2010 work to develop the software package Sonix+ proceeded as follows:

- *Sonix*+ was adopted for the FSD diffractometer. Tests of the programs with the spectrometer equipment were started.
- A version of *Sonix*+ was prepared for the REFLEX spectrometer (for the equipment available today). Compilation of the library of operations is under way. Development of an adjustment program common to the REFLEX, REMUR and GRAINS reflectometers started.
- Work to improve the Sonix+ software package was continued:
  - change-over to Visual Studio 2008 was completed;
  - a set of drivers was supplemented with the new ones, the exposition server was elaborated;
  - new programs (SCP – Sonix control panel) were included in the graphical interface, as well as the programs developed earlier (SpectraViewer, LogViewer) were significantly improved.
- A new version of the WebSonix site http://sonix.jinr.ru was prepared and put into service (**Fig. 13, 14**). In this version the earlier detected errors were eliminated, the stability in the parallel work of several users was improved, the response time of the slowest operations was reduced, the FSD spectrometer was included into the list of instruments being serviced.
- software support of methodical developments performed in the Department and Laboratory was provided.

Fig. 13. Title page of WebSonix.

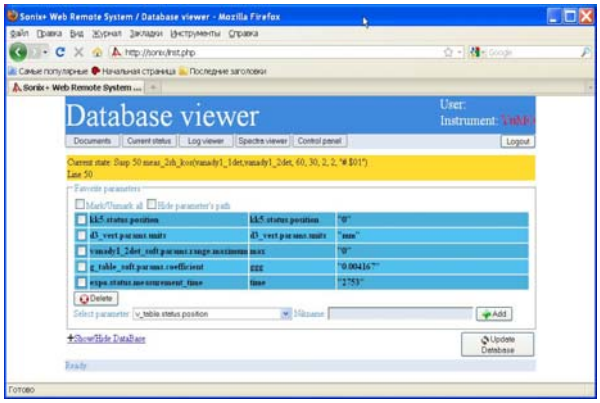

Fig. 14. A page displaying the current status of a spectrometer.

4. EXPERIMENTAL REPORTS

DEPARTMENT OF NEUTRON INVESTIGATION OF CONDENSED MATTER

Theoretical and experimental study of elastic wave propagation in anisotropic texurized rocks
A.N.Nikitin, V.K.Ignatovich, T.I.Ivankina, A.A.Kruglov, T.Lokajicek, L.T.N.Phan and R.N.Vasin

Структурные аномалии pr-содержащих оксидов при низких температурах
А.М. Балагуров, И.А. Бобриков, В.Ю. Помякушин, Е.В. Помякушина, Д.В. Шептяков, И.О.Троянчук

Nucleation theory models for describing kinetics of cluster growth in C60/NMP solutions
T.V. Tropin, M.V. Avdeev, O.A. Kyzyma, V.L. Aksenov

Solvatochromism in fullerene solutions
T.A.Kyrey, O.A.Kyzyma , M.V.Avdeev, V.L.Aksenov, M.V.Korobov, L.A.Bulavin

Sans study of water-based ferrofluids for brain cancer therapy
M.V.Avdeev, A.V.Feoktystov, B.Mucha, V.M.Garamus, R.Willumeit, K.Lamszus, L.Vekas, O.Marinica, R.Turcu

Observation of non-specular neutron reflection from a magnetic film placed in oscillating magnetic field
S.V. Kozhevnikov, V.K. Ignatovich, Yu.V. Nikitenko, F. Radu, A. Rühm and J. Major

Ultrasonic treatment effect on the long-term stability of biogenic ferrihydrite nanoparticles samples in aqueous solution under ambient conditions
M. Balasoiu, L. Anghel, A. V. Rogachev, L.A. Ishchenko, A. Jigounov, G.M. Arzumanian, S.V. Stolyar, R.S. Iskhakov, Yu.L. Raikher

Structural and magnetic phase transitions in multiferroic BiMnO3 at high pressures
D.P.Kozlenko, A.A.Belik, S.E.Kichanov, D.V.Sheptyakov, Th.Straessle and B.N.Savenko

A study of cluster formation in silicon glasses doped by TiO_2/CeO_2 oxides.
S.E.Kichanov, S.A.Samoylenko, D.P.Kozlenko, A.V.Belushkin, L.A.Bulavin, G.P.Shevchenko, V.C.Gurin, V.Haramus and B.N.Savenko

Morphology of the phospholipid transport nanosystem
M.A. Kiselev, E.V. Ermakova, O.M. Ipatova, A.V. Zabelin

Метод след-отображения для решетки пела
Эльмар Аскеров

Results of measurement the residual strains in the WWER-1000 reactor vessel
V.V.Sumin, A.M.Balagurov , I.V.Papushkin , R. Wimpory

The resolution function of a tof reflectometer in the gravity field
I. Bodnarchuk, S.Manoshin, S.Yaradaikin, V.Kazimirov, and V.Bodnarchuk

Aqueous solutions of poly(ethylene glycol): SANS study
G.Lancz, M.V.Avdeev, V.I.Petrenko, V.M.Garamus, M.Koneracká and P.Kopčanský

Contrast variation in small-angle neutron scattering on water-based magnetic fluid with sodium oleate and polyethylene glycol stabilization
M.V.Avdeev, A.V.Feoktystov, P.Kopcansky, G.Lancz, M.Timko, M.Koneracka, V.Zavisova, N.Tomasovicova, A.Jurikova, K.Csach, V.M.Garamus, R.Willumeit, L.A.Bulavin

DEPARTMENT OF IBR-2 SPECTROMETERS COMPLEX

Создание макета технологической системы криогенного замедлителя с электроникой управления и контроля
Ананьев В.Д., Беляков А.А., Богдзель А.А., Булавин М.В., Верхоглядов А.Е., Кулагин Е.Н., Куликов С.А., Кустов А.А., Мухин К.А., Петухова Т.Б., Сиротин А.П., Федоров А.Н., Шабалин Е.П., Шабалин Д.Е., Широков В.К.

NUCLEAR PHYSICS DEPARTMENT

Epithermal neutron activation analysis of the asian herbal plants
Baljinnyam N., Jugder B., Norov N., Frontasyeva M.V.,Ostrovnaya T.M., S.S. Pavlov

Radiometry of ^{137}Cs and ^{210}Pb in moss from belarus
Aleksiayenak Yu. V., Frontasyeva M.V., Florek M., Faanhof A.

THEORETICAL AND EXPERIMENTAL STUDY OF ELASTIC WAVE PROPAGATION IN ANISOTROPIC TEXURIZED ROCKS

A.N.Nikitin[a], V.K.Ignatovich[a], T.I.Ivankina[a], A.A.Kruglov[a], T.Lokajicek[b], L.T.N.Phan[c] and R.N.Vasin[a]

[a] Frank Laboratory of Neutron Physics, Joint Institute for Nuclear Research, DubnaбRussia
[b] Institute of Geology, Academy of Sciences of the Czech Republic, Prague, Czech Republic
[c] Tula State University, Tula, Russia

Theoretical and experimental investigations of elastic wave propagation in a bilayer media have been provided. It was shown that elastic waves of quasi-longitudinal and quasi-transverse polarizations propagate through axial anisotropic media. Wave reflection from a free surface is in general accompanied by triple splitting and all the reflected waves are nonspecular. The quasi-longitudinal and quasi-transverse elastic waves contain the both longitudinal and transverse constituents. This fact may be a reason for the discrepancy which did not observed in the elasticity theory earlier.

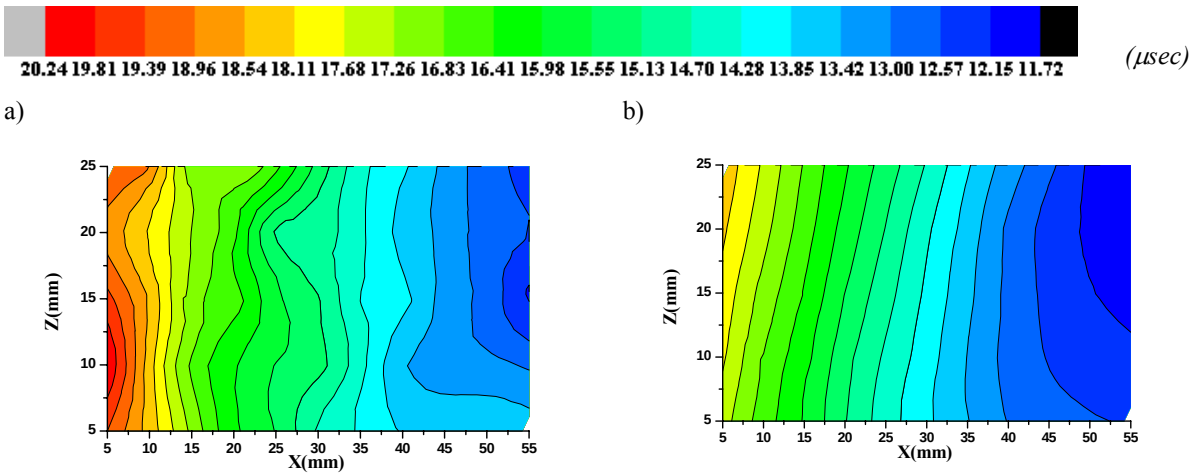

Fig 1. The map of the isoline disctribution of traveltimes of the quasi-longitudinal wave passed through the model – "plexiglas – quartz". The **XZ** plane of the single quartz coincides with the plexiglas surface. The transmitter is fixed on the plexiglas face at the angle of 60° to the horizontal surface. a) ultrasounic frequency - 200 кHz; b) ultrasounic frequency - 5 мHz.

For example, it was found out that even for isotropic medium the reflection of shear wave from an interface having the polarization in the incidence plane can create non Rayleigh longitudinal surface wave which can accumulate devastating amounts of energy at the critical grazing angle. Moreover, the energy density of surface wave may hundred times exceed the energy density of the incident elastic wave. The observed result is very important for seismology.

To improve the considered model and to check the reliability of results we performed the study of elastic wave propagation through model isotropic-anisotropic medium. A set of samples of different compositions were investigated («plexiglas + single quartz oriented parallel to the optical axis», «plexiglas + single quartz oriented perpendicular to the optical axis», «plexiglas + polycrystalline graphite (with certain texture)», «epoxy + biotite»). Crystallographic texture of graphite was determined by means of neutron diffraction.

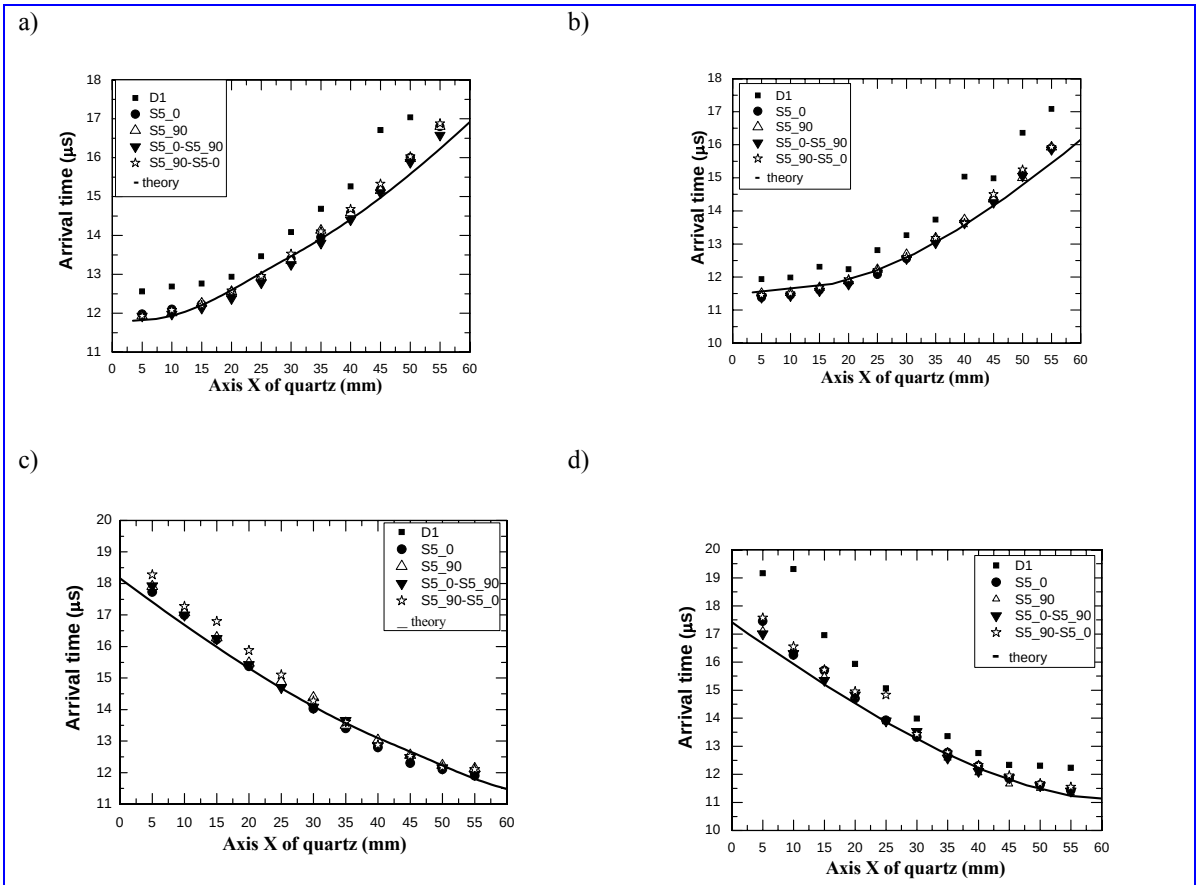

Fig. 2. The comparison of experimental values of arrival time of quasi-longitudinal wave reached the top quartz surface with calculated values. The direction of incident longitudinal wave occurs (a, b) at the angle of 30° to the quartz **XZ** plane; (c, d) at the angle of 60° to the quartz **XY** plane.

Elastic waves were generated by piezoelectric transmitters which are fixed in a certain point of the isotropic part of the sample. The receiver was scanning the surface of the quartz bar (anisotropic part). We registered the wave patterns of the mixed quasi-longitudinal and quasi-transverse elastic waves of different frequencies passing through the investigated samples in depend on grazing angle of the propagating elastic wave in respect to the interface (or to the foliation) **(Figure 1)**.

The comparison between calculated and measured data of quasi-longitudinal waves came to the satisfactory agreement **(Figure 2).**

СТРУКТУРНЫЕ АНОМАЛИИ PR-СОДЕРЖАЩИХ ОКСИДОВ ПРИ НИЗКИХ ТЕМПЕРАТУРАХ

А.М. Балагуров[a], И.А. Бобриков[a], В.Ю. Помякушин[b], Е.В. Помякушина[b], Д.В. Шептяков[b], И.О.Троянчук[c]

[a] Объединенный институт ядерных исследований, Дубна, Россия
[b] Laboratory for Neutron Scattering, Paul Scherrer Institute, Switzerland
[c] Объединенный институт твердого тела и полупроводников, Минск, Белоруссия

В исследованиях сложных оксидов переходных металлов (манганитов и кобальтитов) типа $A_{1-x}A'_xBO_3$, где A - редкоземельный элемент, A′ - щелочноземельный элемент, B = Mn или Co, выбор того или иного редкоземельного элемента или комбинации нескольких разных элементов сводится, как правило, к желанию подобрать необходимую величину среднего радиуса A-катиона, $\langle r_A \rangle$, которая во многом определяет физические свойства соединения. Однако еще в исследованиях ВТСП было замечено, что соединения с празеодимом ведут себя иначе, чем с другими редкоземельными элементами, причем аномальное поведение Pr-содержащих перовскитов, обычно проявляется при сравнительно низких температурах. Для сложных оксидов марганца и кобальта на особые свойства составов с Pr внимание было обращено сравнительно недавно, но уже накоплен необходимый для анализа экспериментальный материал. Так, магнитные исследования состава $Pr_{0.5}Sr_{0.5}CoO_3$, (далее PSCO) показали [**1**], что в нем наблюдаются два фазовых перехода при $T_C \approx 226$ K и $T_A \approx 120$ K, тогда как в соединениях с другими редкоземельными катионами есть только один высокотемпературный переход, при котором возникает ферромагнитное упорядочение. В составе $Pr_{0.5}Ca_{0.5}CoO_3$ в работе [**2**], при $T \approx 75$ K обнаружены аномалии физических свойств (переход метал – изолятор) и заметная перестройка структуры, которые отсутствуют в составе $La_{1/6}Nd_{1/3}Ca_{0.5}CoO_3$, имеющем такой же средний радиус A-катиона. В соединении $PrAlO_3$, в котором нет каких-либо магнитных переходов, обнаружена сходная с PSCO последовательность структурных переходов и аномалия в упругих свойствах при 118 K [**3**].

Таким образом, есть основания считать, что наблюдающиеся в соединениях с Pr низкотемпературные аномалии в физических свойствах связаны с общей причиной, а именно, с формированием новых устойчивых химических связей и следует искать структурные проявления этого эффекта. В принципе, они уже были найдены в нашей недавней работе [**4**], где было показано, что данные, полученные с помощью дифракции синхротронного излучения и особенно нейтронов с очень высоким разрешением, позволяют утверждать, что в PSCO при T_A происходит изменение симметрии кристалла. Экспериментальные результаты, представленные в [**4**], носили предварительный характер и относились только к геометрии кристаллической решетки. В дальнейших более детальных дифракционных экспериментах нам удалось получить информацию об атомной и магнитной структуре PSCO в области низких температур. Анализ всех имеющихся данных позволяет утверждать, что в $Pr_{0.5}Sr_{0.5}CoO_3$ при температурах ниже 170 K происходит расслоение кристалла на две фазы с разной симметрией и разными (хотя и близкими) атомной и магнитной структурами. Основным структурным различием между фазами является конфигурация кубооктаэдра $(Pr,Sr)O_{12}$, а наблюдавшаяся в предыдущих работах при 120 K магнитная аномалия является следствием перестройки кислородного окружения (Pr,Sr) и, в некоторой степени, Co.

Литература

1. И.О. Троянчук и др., Письма в ЖЭТФ **84**, 180 (2006).
2. A.J. Barón-González et al., Phys. Rev. B **81**, 0544427 (2010).
3. M.A. Carpenter et al., Phys. Rev. **B 72**, 024118 (2005).
4. А.М. Балагуров, И.А. Бобриков, Д.В. Карпинский, И.О. Троянчук, В.Ю. Помякушин, Д.В. Шептяков, Письма в ЖЭТФ **88**, 608 (2008).

NUCLEATION THEORY MODELS FOR DESCRIBING KINETICS OF CLUSTER GROWTH IN C_{60}/NMP SOLUTIONS

T.V. Tropin[a], M.V. Avdeev[a], O.A. Kyzyma[a,b], V.L. Aksenov[a,c]

[a] Frank Laboratory of Neutron Physics, Joint Institute for Nuclear Research, Dubna, Russia
[b] Kyiv Taras Shevchenko National University, Kyiv, Ukraine
[c] Russian Research Centre "Kurchatov Institute", Moscow, Russia

In the given report, two kinetic models of cluster growth, based on nucleation theory approach are applied to describe cluster growth in C_{60}/N-methyl-pyrrolidone (NMP) solutions. As compared to low-polarity C_{60} solutions, where fullerenes show a tendency towards aggregation under supersaturation as a result of non-equilibrium dissolution [1], in polar solvents, like NMP, fullerenes C_{60} always form clusters. Particularly, in pyridine [2], NMP [3] and their mixtures with water [1] clusters grow up to 500 nm in size during about one month after fullerene dissolution.

For the spectrum from the initial solution specific features of molecular state of C_{60} can be seen (e.g. peak at λ=330nm). The UV-Vis spectrum from C_{60}/NMP changes with time **(Fig. 1)**, which is known as temporal solvatochromism. The absorption measurements can be used for determination of the free (non-aggregated) fullerene concentration in C_{60}/NMP at different time after the solution preparation. For this purpose fullerene is extracted into a solvent, which dissolves C_{60} and is non-miscible with NMP. The good solvent for such procedure is hexane. The time dependence of free monomer concentration in C_{60}/NMP found in this way is shown in **Fig. 1**. It decreases by more than three orders in comparison with initial solution, which means that fullerene in the "old" NMP solution is mainly in cluster state (free monomer concentration $c_{mon}<10^{-3}$ mg/ml). It is important to note that estimates of cluster density made by SANS at the addition of water to C_{60}/NMP [6] indicate that clusters are fullerene molecular crystallites.

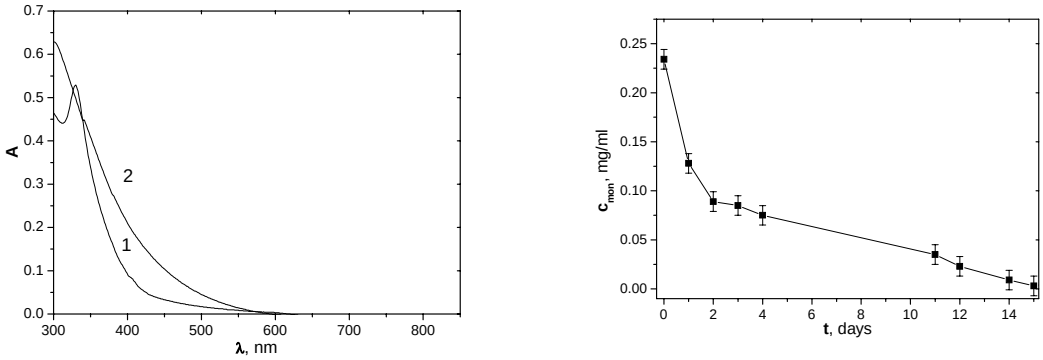

Fig. 1. UV-Vis spectra of fresh and "old" C60/NMP solution (left). Time-dependence of free monomer concentration in C_{60}/NMP solution obtained by following concentration of C_{60} extracted into hexane (right) [9].

Basics of aapplication of nucleation theory for describing fullerene cluster formation are described elsewhere [1,4]. Evolution of a system in frame of classical nucleation theory, described by liquid drop model, results in phase separation, when all but c_{eq} of free molecules, transfer finally to the solid phase (infinite cluster). Because this is not the case for fullerene polar solutions, where clusters stay stable for long periods of time, one should consider new models. Taking into account a possible appearance of some new chemical bonds, which stabilize clusters in this type of solutions, the corresponding modifications of kinetic equations can be done in two ways.

In the first case (model I), we introduce an additional function $f^{*}(n,t)$, which describes clusters excluded at the moment t from the nucleation process (segregating phase). The size of these clusters is strongly stabilized and does not change furthermore. It is clear that finally the segregating phase transfers completely into the stabilized phase. The basic equations for this model take the form:

$$\frac{\partial f(n,t)}{\partial t} = w^{(+)}_{n-1,n} f(n-1,t) + w^{(-)}_{n+1,n} f(n+1,t) - w^{(+)}_{n,n+1} f(n,t) - (w^{(-)}_{n,n-1} + \frac{1-e^{t/\tau}}{\tau}) f(n,t),$$

$$\frac{\partial f'(n,t)}{\partial t} = \frac{1-e^{t/\tau}}{\tau} f(n,t), \quad \sum_{n=1}^{\infty} n(f(n,t) + f'(n,t)) = c, \qquad (1)$$

$$f(n,t=0) = \begin{cases} 0, & n>1, \\ c, & n=1. \end{cases} \quad f'(n,t=0) = 0.$$

Where the additional term in the kinetic equations for $f(n,t)$ corresponds to exponential depletion of the segregating phase. The new model parameter, τ, is the characteristic time of cluster stabilization.

In the other case (model II), kinetic equations keep the classical form [1,4], but probabilities of cluster growth / depletion $w^{(\pm)}_{m,n}$ are the functions of time:

$$w^{(\pm)}_{m,n}(t) = w^{(\pm)}_{m,n} e^{-t/\tau}, \qquad (2)$$

where the characteristic time τ reflects a decrease in the nucleation rate.

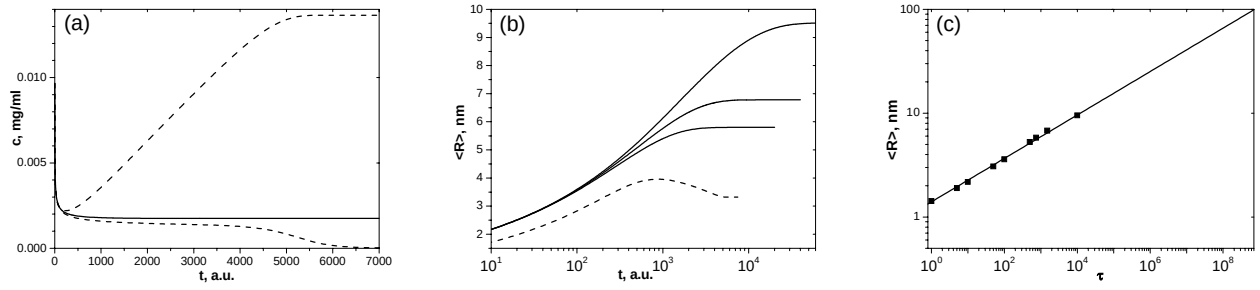

Fig. 2. (*a*) time evolution of monomer concentration for both models I (dashed lines) and II (solid line). For model I the upper curve shows the sum $f(1,t)+f'(1,t)$; and the lower curve shows $f(1,t)$; (*b*) evolution of mean cluster size for models I (dashed line) and II (solid lines); curves for model II correspond to different $\tau=10^4$; $1.5*10^3$; 750 from up to bottom; (*c*) dependence of model limiting $<R>$ values on τ (points) with corresponding power-law fit (solid line).

The proposed models are qualitatively compared **(Fig. 2a)** with respect to the time dependence of free monomer concentration, c_{mon}, whose experimentally found behaviour is proportional to the graph given in **Fig. 1**. As one can see, model I shows a significant increase in c_{mon} at a certain stage, which is in disagreement with the experiment. In contrast, for model II the time evolution of both free monomer concentration **(Fig. 2a)** and mean cluster size **(Fig. 2b)** has a monotonous character, which is close to the experimental one. This means that this model is a reasonable approach for describing cluster growth in fullerene polar solutions.

The change in the time dependence of mean cluster size, $<R>$, with varying τ is illustrated in Fig. 2b, where one can see that its limit is determined by τ. The found limits of $<R>$ in **Fig. 2b** are far from the real one, which means that significantly larger τ-values should be used in calculations. However, the corresponding numerical solution requires too much time resources, which are hardly available for the moment. The τ-value which fits experiment can be estimated from dependence $<R>$ vs. τ obtained at smaller cluster sizes **(Fig. 2c)**. It is of the power-law type, and the corresponding extrapolation for $<R>\sim100$ nm gives $\tau\sim10^8$ a.u.. Taking into account that initial supersaturation $c_{mon}(0)/c_{eq}$ can be higher, one can conclude that to fit the experimentally observed cluster size, the approximate τ estimate is within 10^6-10^8 a.u. for supersaturations of 10^4-10^6. Further work on the proposed models and their development is in progress.

References

[1] M. V. Avdeev, V. L. Aksenov, T. V. Tropin, Russ. J. Phys. Chem. A Vol. 84 No. 8, 1274 (2010).
[2] A. Mrzel, A. Mertelj, A. Omerzu, et al., J. Phys. Chem. **103**, 11256 (1999).
[3] V. L. Aksenov, M. V. Avdeev, T. V. Tropin, M. V. Korobov, N. V. Kozhemyakina, N. V. Avramenko, L. Rosta, Physica B **385**, 795 (2006).
[4] V. L. Aksenov, T. V. Tropin, M. V. Avdeev, V. B. Priezzhev, J. W. P. Schmelzer, Physics of Particles and Nuclei, **36**, S52 (2005).

SOLVATOCHROMISM IN FULLERENE SOLUTIONS

T.A.Kyrey[a,b], O.A.Kyzyma[a,b], M.V.Avdeev[a], V.L.Aksenov[a,c], M.V.Korobov[d], L.A.Bulavin[b]

[a]Joint Institute for Nuclear Research, Dubna, Moscow reg., Russia
[b]Kyiv Taras Shevchenko National University, Kyiv, Ukraine
[c]Russian Research Center Kurchatov Institute, Moscow, Russia
[d]Moscow State University, Moscow, Russia

Solutions of fullerene C_{60} in nitrogen-containing solvents (pyridine, N-methyl-2-pyrrolidone (NMP), benzonitrile and acetonitrile) and its mixtures are of current interest due to the time evolution of the electrooptical constant [1], as well as photoluminescence [2], IR [3], Raman [2] and UV-Vis spectra [4] which correlate with cluster formation.

In the given experiments we study solvatochromic effects after dissolution of C_{60}/NMP system. Previously, time-dependent solvatochromic effect (temporal solvatochromism) was observed in C_{60}/NMP solution [2]. Addition of polar solvent (water, miscible with NMP) to this system leads to sharp solvatochromic effect (at negligible changes of system's composition) and increasing of absorbance at 450-550 nm [5,6]. Here, the changes in UV-Vis spectra of fullerene C_{60} in mixture NMP/toluene at the solution polarity variation (ε = 3,8 ÷ 26,6) were investigated. Time-dependent study at increasing as well as decreasing of solvent polarity was done. Smearing of absorbance spectra for fullerene solutions in different polarity mixtures was observed. These solvatochromic effects are analyzed with respect to solvation processes.

Fullerenes (Fullerenovye Tekhnologii, purity > 99.5%) and solvents of different polarity: polar NMP (ε=32) (Merck, purity > 99.5%) and low-polar toluene (ε=2,4) (Merck, purity >99.5%) were used for samples preparation. The C_{60}/NMP solution was prepared by adding 20 mg fullerene in 34 ml NMP with stirring for one hour at room temperature The solution was stored in darkness at room temperature. To obtain the C_{60}/toluene solution the fullerene was dissolved in toluene and stirred for ten minutes. Ternary solutions C_{60}/NMP/toluene and C_{60}/toluene/NMP were obtained in two ways: by addition of toluene or NMP to initial C_{60}/NMP or C_{60}/toluene solution, respectively. The volume fraction of toluene or NMP in the final mixture was varied in the range of 20-95 % (ε = 3,8 ÷ 26,6). Absorption spectra were obtained using Hitachi U-2000 (wavelength range 200-1000 nm) UV-Vis spectrophotometer. Quartz cells with 2 mm path length were used. The spectra were obtained right after the solution preparation, several days after preparation and one month later.

The UV-Vis spectra of fresh C_{60}/NMP and C_{60}/toluene solutions are compared in fig.1. They both exhibit characteristic peaks of molecular C_{60} at about 330 and 410 nm with slight shifts, when comparing the two solutions, determined by a difference in the fullerene-solvent interaction. Changes in UV-Vis absorption spectra of C_{60}/toluene system at NMP addition are presented in Fig. 2. It is clearly seen that the addition of NMP to the C_{60}/toluene system leads to a smearing of specific peaks at λ = 330 nm and λ = 410 nm and also an increase in absorption at λ = 400 ÷ 550 nm.

The cluster formation [4] and fullerene salvation by NMP molecules take place after addition of polar components to solution (increase permittivity up to 26,6). New solvate C_{60}/NMP are formed and therefore absorbance spectra are changed. It should be noted that change of solution color from purple specific for the system C_{60}/toluene to yellow-brown specific for the system C_{60}/NMP and hypsochromic effect (the shift of the absorption peak towards higher energy) are observed (Fig. 3). There is indication about formation of donor-acceptor complexes between fullerene and solvent molecules [2].

Addition of toluene to C_{60}/NMP leads to decrease of solution polarity from 32 (C_{60}/NMP) to 3,8 (C_{60}/NMP/toluene with 95 vol. % of toluene). The sharp solvatochromic effect was observed when volume fraction of toluene in the ternary solution more than 80 vol. % (Fig. 4). In this case the spectrum of the system takes the form specific to the fullerene solution in toluene. It should be noted, that increase of low-polar component in the C_{60}/NMP/toluene solution leads to increase of selective salvation (considerable difference between composition of salvation shell and bulk solution) due to greater salvation power of NMP in compare to toluene. When volume fraction of toluene in solution up to 80% fullerene clusters are dissolve (transition from colloidal to molecular solutions) and UV-Vis spectrum takes form of molecular C_{60}/toluene solution.

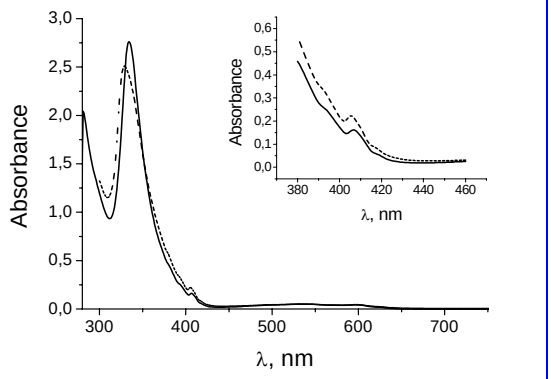

Fig. 1. UV-Vis spectra of fresh C_{60}/NMP (dash), and C_{60}/toluene (solid) solutions. Absorbance normalized to fullerene concentration. Inset shows peak shift at 410 nm

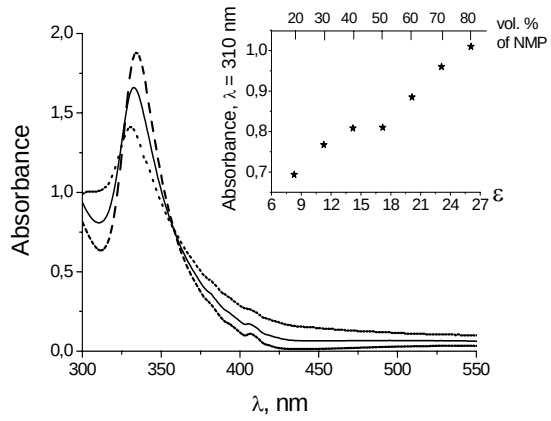

Fig. 2. UV-Vis spectra of C_{60}/toluene solution (dash) and C_{60}/toluene/NMP solutions at 50 vol. % (solid) and 80 vol. % (dot) of NMP. Inset: absorbance at wavelength of 310 nm versus dielectric constant (ε) and NMP vol. fraction (20-90%). Absorbance normalized to fullerene concentration

It should be noted that the addition of toluene to an old C_{60}/NMP system (with a smoothed spectrum) did not lead to any changes in the absorption spectra. In this case considerable amount of added toluene leads to partial cluster decomposition without complete transition to molecular solution. Similar effects were observed in C_{60}/NMP solution at water addition [7, 8].

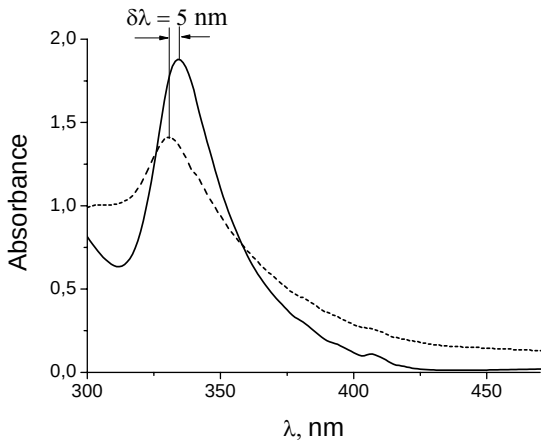

Fig. 3. Hypsochromic effect for C_{60}/toluene (solid) and C_{60}/toluene/NMP (dash – 80 vol. % of NMP) solutions. Absorbance normalized to fullerene concentration

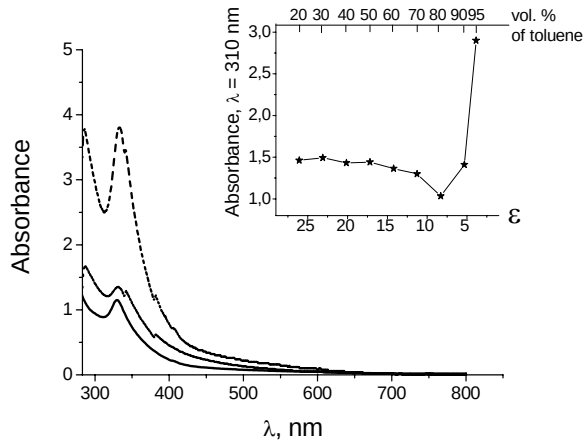

Fig. 4. UV-Vis spectra of C_{60}/NMP solution (solid) and C_{60}/NMP/toluene at 90 vol. % (dot) and 95 vol. % (dash) of toluene. Inset: absorbance at wavelength of 310 nm versus dielectric constant (ε) and toluene vol. fraction (20-95%). Absorbance normalized to fullerene concentration

It was shown [8], that C_{60}/NMP characterized by temporal solvatochromism (spectrum smearing with time). Similar temporal smearing (during one month) was observed for all samples of both systems (C_{60}/NMP/toluene and C_{60}/toluene/NMP) regardless the ratio NMP/toluene. The reason of temporal solvatochromism is formation of donor-acceptor complexes C_{60}/NMP due to high salvation power of NMP. Namely, selective salvation in ternary fullerene solutions with low NMP content takes place.

Sharp (change mixture composition) and temporal (with time) solvatochromism of fullerene solution in mixture N-methyl-2-pyrrolidone (NMP)/toluene at the solution polarity variation (ε = 3,8 ÷ 26,6) were observed. Addition of polar NMP to C_{60}/toluene solution leads to clusterization and formation of donor-acceptor complexes between C_{60} (acceptor) and NMP molecules (donor), which accompanied by hypsochromic effect and smearing of specific peaks at 330 and 410 nm. Decrease of fullerene solution polarity (toluene addition) leads to increase of selective salvation due to greater salvation power of NMP in compare to toluene. When volume fraction of toluene in solution up to 80% fullerene clusters in ternary solution are dissolve (transition from colloidal to molecular solution) and sharp solvatochromic effect are observed. In this case the spectrum of the system takes the form specific to the fullerene solution in toluene. The temporal solvatochromism occurred for all ternary fullerene solutions regardless the ratio NMP/toluene in mixtures. The reason of this effect is high salvation power of NMP, which leads to formation of donor-acceptor complexes C_{60}/NMP with time in all samples.

References

[1] Baltog I., Baibarac M., Mihut L., et al. // Romanian Rep. Physics. 57 (2005) 837.
[2] N.P. Yevlampieva, Yu.F. Biryulin, et al. // Coll. and Surf. A 209 (2002) 167.
[3] O.A. Kyzyma, M.V. Korobov, M.V. Avdeev et al. // Fullerenes, Nanotubes and Carbon Nanostructures.18 (2010) 458.
[4] Nath S., Pal H., Palit D.K., et al. // J. Phys. Chem. B. 102 (1998) 10158.
[5] Mrzel A., Mertelj A., Omerzu A., Copia M., Mihailovic D // J. Phys. Chem. B 103 (1999) 11256.
[6] Kyzyma O.A., Avdeev M.V., Aksenov V.L., Bulavin L.A., Snegir S.V. // FLNP Annual report 2007 123.
[7] L. Aksenov, M.V. Avdeev, T.V. Tropin, et al. // Physica B 385-386 (2006) 795.
[8] V.L. Aksenov, M.V. Avdeev, O.A. Kyzyma, L. Rosta, M.V. Korobov. // Cryst. Rep. 52 (2007) 479.

SANS STUDY OF WATER-BASED FERROFLUIDS FOR BRAIN CANCER THERAPY

M.V.Avdeev[a], A.V.Feoktystov[a,b], B.Mucha[c], V.M.Garamus[c], R.Willumeit[c], K.Lamszus[d], L.Vekas[e], O.Marinica[f], R.Turcu[g]

[a]*Frank Laboratory of Neutron Physics, Joint Institute for Nuclear Research, Dubna, Russia*
[b]*Kyiv Taras Shevchenko National University, Kyiv, Ukraine*
[c]*Helmholtz-Zentrum Geesthacht, Geesthacht, Germany*
[d]*University Medical Centre Hamburg Eppendorf, Hamburg, Germany*
[e]*Center for Fundamental and Advanced Technical Research, Romanian Academy, Timisoara Division, Timisoara, Romania*
[f]*University Politehnica Timisoara, Timisoara, Romania*
[g]*National Institute R&D of Isotopic & Molecular Technologies, Cluj-Napoca, Romania*

Applications of magnetic nanoparticles for biomedical purposes were actively developed in the last decade [1]. As an example, cancer treatment in what concerns controllable drug delivery [2], diagnostics (magnetic resonance imaging [3]), and therapy (magnetic hyperthermia [4]) can be mentioned. This raises the problem of synthesizing biocompatible ferrofluids or magnetic fluids (fine liquid suspensions of magnetic nanoparticles), which are stable and controllable in biological media under different conditions.

Recently, some progress in the synthesis of concentrated water-based magnetic fluids (φ_m >10%) has been achieved [5] for the double stabilization of nanomagnetite by saturated monocarboxylic acids with short carbon chains, such as lauric acid (LA, $C_{12}H_{24}O_2$) and myristic acid (MA, $C_{14}H_{28}O_2$). In the present experiments, we study the concentrated samples with one of the highest φ_m values among those for available water-based ferrofluids with long-term stability (at least 1 year). The key point is that a significant increase in the stabilized fraction of magnetite when using LA and MA indicates that there should be specific structural peculiarities in these fluids as compared to other stabilization schemes.

The measurements were made on the SANS-1 instrument [6] at the GKSS Research Centre. A differential cross section per sample volume (scattering intensity) that is isotropic over the momentum transfer vector q was obtained as a function of modulus $q=(4\pi/\lambda)\sin(\theta/2)$, where λ is the neutron wave length and θ is the scattering angle. Experiments were carried out in a standard way to cover a q interval of 0.06-2.5 nm^{-1}. The contrast variation was achieved by diluting the initial samples with different mixtures of light water (H_2O) and heavy water (D_2O) in a way, in which the D_2O content, η, in the final sample is varied from 0 to 90%.

The presence of aggregates in bulk ferrofluids is clearly observed in the SANS curves corresponding to different contents of D_2O in the carrier (Figure 1). The SLDs of the surfactants (about 0.10×10^{10} cm^{-2}) do not differ much from the SLD of water (-0.56×10^{10} cm^{-2}), which means that in pure H_2O the surfactant component in the fluid structures is almost matched and the scattering comes mainly from magnetite with an SLD of about 6.90×10^{10} cm^{-2}. The addition of D_2O with an SLD of 6.34×10^{10} cm^{-2} increases the contrast from surfactants against the carrier, so specific features appear in the scattering curves as compared to the H_2O case. We fail in fitting the experimental curves to the model of separate core-shell particles imitating spherical magnetite cores coated with a surfactant shell. Hence, the data in **Figure 1** are treated in terms of the approach of modified basic functions [7], which was recently applied well [8] to aqueous magnetic fluids with charge stabilization.

Resulting basic functions $I_c(q)$ for the two ferrofluids are given in **Figure 2**, together with their indirect Fourier transform (IFT) [9] in the form of the $p(r)$ function. Because shape scattering function $I_c(q)$ describes the effective homogeneous particles, the $p(r)$ function is the pair distance distribution (PDD) averaged over the particle shapes. The maximal values, where the $p(r)$ functions approach zero, correspond to the maximal aggregate sizes, which are 49 and 33 nm for samples LA+LA and MA+MA, respectively. The obtained values are in agreement with the dynamic light scattering data for similar samples [10] with reported average hydrodynamic sizes of 77 and 48 nm for fluids LA+LA and MA+MA, respectively. In particular, the average size ratios between the two fluids are similar:1.5 (SANS) and 1.6 (DLS). The radius of gyration, R_g, calculated from the $p(r)$ functions (15.2 ± 0.2 nm (LA) and 10.2 ± 0.1 nm (MA)) is connected to the radius of gyration of the particle shape, R_c, and volume, V_c, as $R_g^2 = \langle R_c^2 V_c^2 \rangle / \langle V_c^2 \rangle$, where the brackets denote the averaging over the particle radius distribution $D_n(R)$. Assuming the quasi-spherical shape of the aggregates, which allows one to use the relation $R_c^2 = (3/5)R^2$, one obtains the characteristic radii of the particles $(\langle R^2 V_c^2 \rangle / \langle V_c^2 \rangle)^{1/2}$ to be equal to 19.5 ± 0.3 and 13.8 ± 0.1 nm for fluids LA+LA and MA+MA, respectively. For comparison, the PDD functions calculated from the TEM data of separate particles are also given in **Figure 2b**.

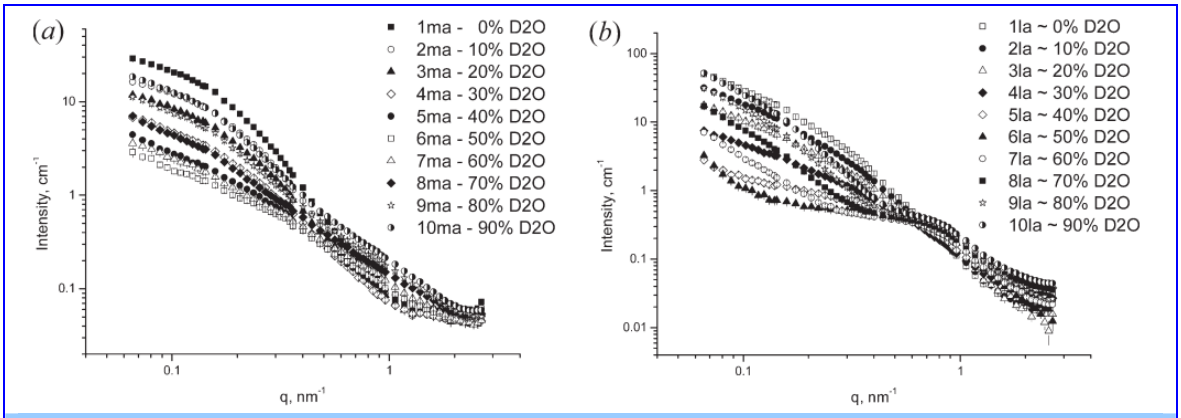

Fig. 1. SANS contrast variation for samples (a) MA+MA and (b) LA+LA. Sample labels correspond to the content of D_2O in the carrier.

Taking into account the mentioned difference in the $I_c(q)$ function and the scattering intensity in the case of pure H_2O (η =0), we compare the corresponding PDD functions in **Figure 2b**. It is interesting that such a difference is clearly seen only in the LA+LA sample. The maximal size from the $I_c(q)$ function is shifted up to about 7 nm from that of the magnetite component, which can be related well to the effective thickness (about 3.5 nm) of the surfactant shell around magnetite nanoparticles. The obtained thickness exceeds the doubled length of the LA molecule, 1.4 nm, which points to the bulky (nonoverlapped) structure of the stabilizing shell. In the MA+MA sample, both kinds of PDD functions are very similar, so the surfactant shell does not have any effect.

The incorporation of magnetite particles into cancer cells as a result of endocytosis were observed in optical microscope images of the samples stained with Berliner blue. The intensity of the absorbed magnetite correlates with the amount of ferrofluids initially added to the cancer medium. The toxicity rate depends on the cancer cell line. In some cases, the incorporation of magnetic particles slows the culture growth to 50-60%, but in other cases, such incorporation is almost nontoxic. At the same time, on average one can conclude that the magnetic particles that are used have some selective toxic effect with respect to the cancer cells. This follows from the fact that the cytotoxicity of the studied particles for astrocytes is low and does not depend on the initial particle concentration.

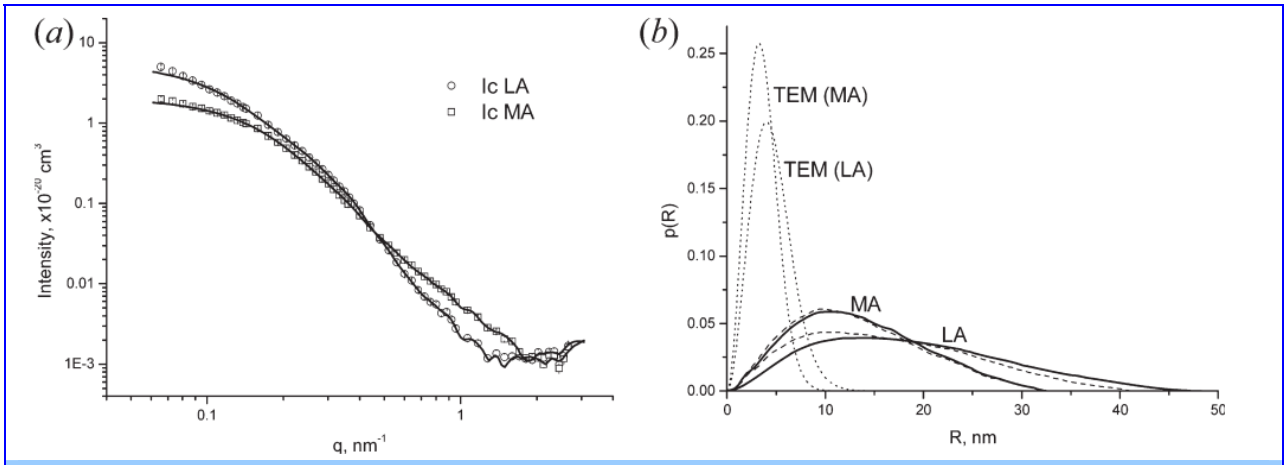

Fig. 2. (a) Experimentally obtained $I_c(q)$ basic functions for the two ferrofluids. The line shows IFT fits of the curves with parameters of R_g=15.1 ± 0.2 nm, $I(0) = (5.8 \pm 0.1) \times 10^{-20}$ cm^3 (LA+LA) and R_g = 10.7 ± 0.1 nm, $I(0) = (2.1 \pm 0.1) \times 10^{-20}$ cm^3 (MA+MA). (b) Pair distance distribution functions of particles found from $I_c(q)$ basic functions (−) are compared with the pair distance distribution functions from curves with 0% D_2O content (---) and from the TEM measurements of the individual particles (···).

So, the structure of water-based ferrofluids with double-layer sterical stabilization by short monocarboxylic acids (lauric and myristic acids) is described relative to their possible biomedical applications, in particular for cancer treatment. It is shown that besides discrete particles coated with a surfactant shell, a significant part of the particles are bound into aggregates. The inner structure of the aggregates differs for the two ferrofluids with respect to the relative content of

magnetite and surfactant, showing that in the case of myristic acid stabilization the magnetite particles are not fully coated with surfactant. Nevertheless, this factor does not have any significant effect on fluid stability in the absence of an external magnetic field. Both fluids can be used well in cancer (glioblastoma) treatment. As a source of magnetic nanoparticles, they show high stability in the cancer cell medium and provide a high incorporation of magnetic nanoparticles into cancer cells, which is strongly dependent on the cancer cell line. The magnetic particles from the probed ferrofluids are characterized by very low toxicity in human brain cells.

References

[1] Proceedings of the 7th International Conference on the Scientific and Clinical Applications of Magnetic Carriers, Vancouver, Canada, May21-24, 2008; Haeafeli, U., Zborowski, M., Eds.; J. Magn. Magn. Mater. 2009, Vol. 321.

[2] Berry, C.C.; Curtis, A.S.G. J. Phys. Appl. Phys. 2003, 36, R198–R206.

[3] Arbab, A.S.; Liu, W.; Frank, J.A. Expert Rev. Med. Dev. 2006, 3, 427–439.

[4] Brusentsov, N.A.; Nikitin, L.V.; Brusentsova, T.N.; Kuznetsov, A.A.; Bayburtskiy, F.S.; Shumakov, L.I.; Jurchenko, N.Y. J. Magn. Magn. Mater. 2002, 252, 378–380.

[5] Bica, D.; Vekas, L.; Avdeev, M.V.; Marinica, O.; Socoliuc, V.;Balasoiu, M.; Garamus, V.M. J. Magn. Magn. Mater. 2007, 311, 17–21.

[6] Zhao, J.; Meerwinck, W.; Niinkoski, T.; Rijllart, A.; Schmitt, M.; Willumeit, R.; Stuhrmann, H. Nucl. Instrum. Methods A 1995, 356, 133–137.

[7] Avdeev, M.V. J. Appl. Crystallogr. 2007, 40, 56–70.

[8] Avdeev, M.V.; Dubois, E.; Meriguet, G.; Wandersman, E.; Garamus, V.M.; Feoktystov, A.V.; Perzynski, R. J. Appl. Crystallogr. 2009, 42, 1009–1019.

[9] Pedersen, J.S. Adv. Colloid Interface Sci. 1997, 70, 171–210.

[10] Tombacz, E.; Bica, D.; Hajdu, A.; Illes, E.; Majzik, A.; Vekas, L. J. Phys. Cond. Mater. 2008, 20, 204103.

OBSERVATION OF NON-SPECULAR NEUTRON REFLECTION FROM A MAGNETIC FILM PLACED IN OSCILLATING MAGNETIC FIELD

S.V. Kozhevnikov[a], V.K. Ignatovich[a], Yu.V. Nikitenko[a], F. Radu[b], A. Rühm[c] and J. Major[c]

[a]Frank Laboratory of Neutron Physics, JINR, 141980 Dubna, Moscow Region, Russia
[b]Helmholtz-Zentrum Berlin für Materialien und Energie, Albert Einstein Strasse 15, D-12489 Berlin, Germany
[c]Max Planck Institut für Metallforschung, Heisenbergstr. 3, D-70569, Stuttgart, Germany

When the oscillating high frequency magnetic field is applied to the uniformly magnetized film, the neutron spin-flip takes place inside the film at the resonance condition. This leads to non-specular reflection in glancing geometry. We carried out an experiment to proof this phenomenon theoretically predicted in the articles [1-5].

The measurements were done at NReX$^+$ reflectometer (reactor FRM II, Garching, Germany). Fixed neutron wavelength 0.426 nm (1% FWHM) is used. The sample is the film of permalloy (500 nm) on the Si substrate. The sample sizes are 25×25×1 mm^3. The geometry of the experiment is shown in Fig. 1. The glancing angle of the incident beam is 0.4° and the angular divergence is 0.006°. The permanent magnetic field $H_0 = 20$ Oe is applied in the sample plane along the guide field. The oscillating magnetic filed with the amplitude $H_1 = 10$ Oe and the frequency about 30 MHz is applied in the sample plane along the beam path.

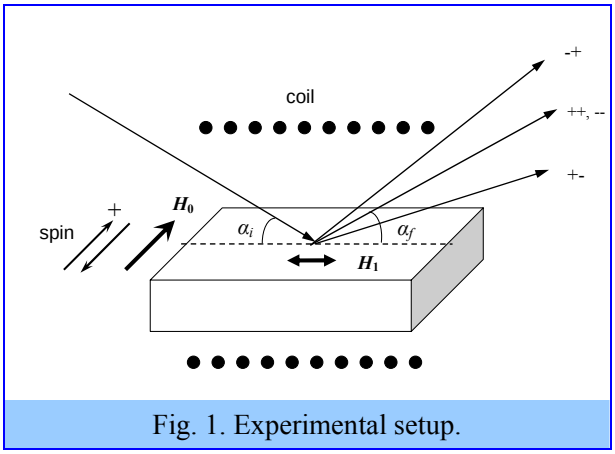

Fig. 1. Experimental setup.

At the resonant frequency non-specular reflection at 0.26° and 0.50° outgoing angles has been observed for both incident polarization up and down (Fig. 2).

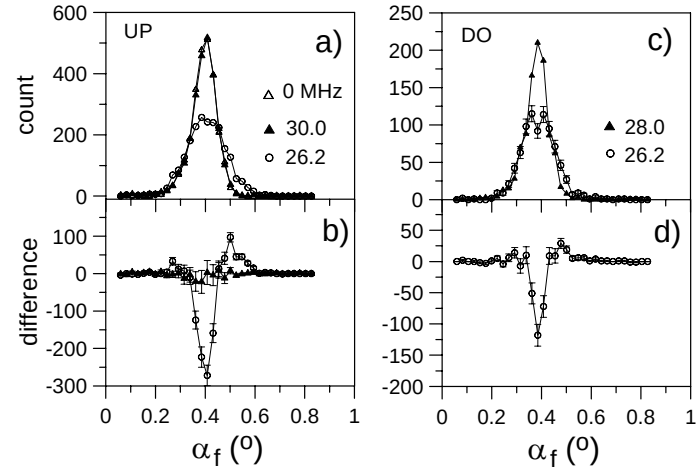

Fig. 2. Neutron count of reflected beam in dependence on outgoing angle.

Such big angular effect of beam-splitting corresponds to the energy changing in the internal magnetic induction 8.7 kG but not in the small external magnetic field 20 Oe. In Fig. 2 b one can see that there is no difference in reflected intensity in the cases of out-of-resonance frequency 30.0 MHz and switched-off frequency f=0 MHz.

In Fig. 3 the count of specularly reflected beam is shown in dependence on the frequency of the oscillating field (upper panels are integrated intensity, bottom panels are maximum of the intensity). One can see the resonance at 26.2 MHz (FWHM=1.2 MHz).

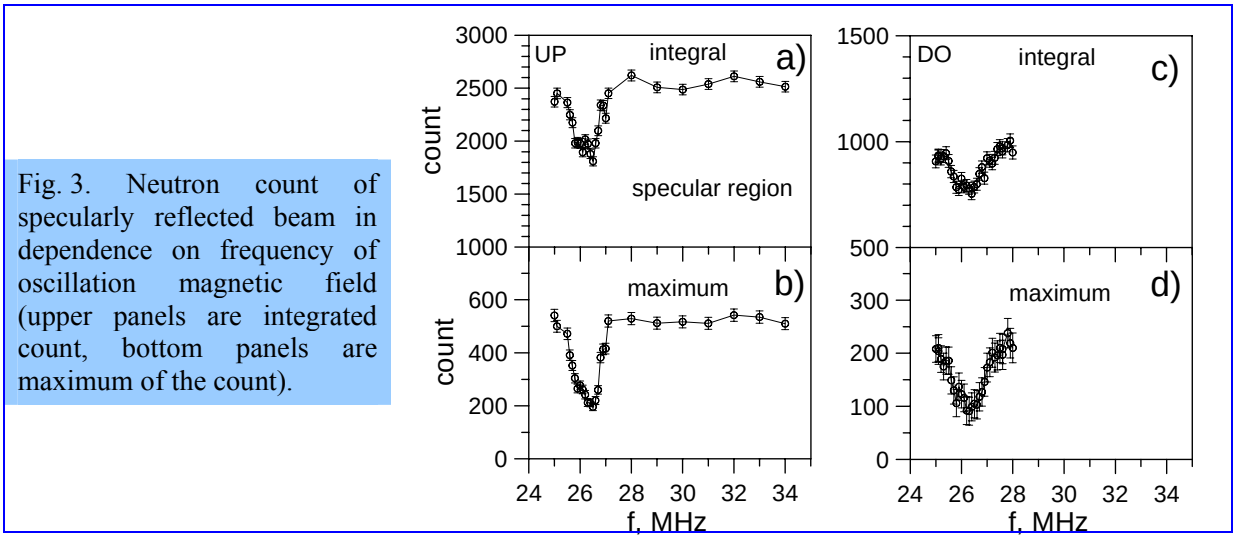

Fig. 3. Neutron count of specularly reflected beam in dependence on frequency of oscillation magnetic field (upper panels are integrated count, bottom panels are maximum of the count).

The effect of the specular intensity decreasing in the resonance consists of about 25 % for the integral and 50 % for the maximum. To define non-specular intensity effect we integrated intensity in two non-specular regions with frequency and extracted the intensity in the same regions with switched-off frequency for spin UP (see Fig. 4 a) or out-of-resonance frequency 28.0 MHz for spin DO (see Fig. 4 c). We define non-specular reflection probability (see Fig. 4 b,d) as the difference of non-specular intensity in Fig. 4 a normalized on out-of-resonance specular intensity integral in Fig. 3 (upper panels). The effect of non-specular intensity consists of 12% for the interval of $\alpha_f = 0.455° \div 0.641°$ and 3% for the outgoing angles $\alpha_f = 0.199° \div 0.338°$.

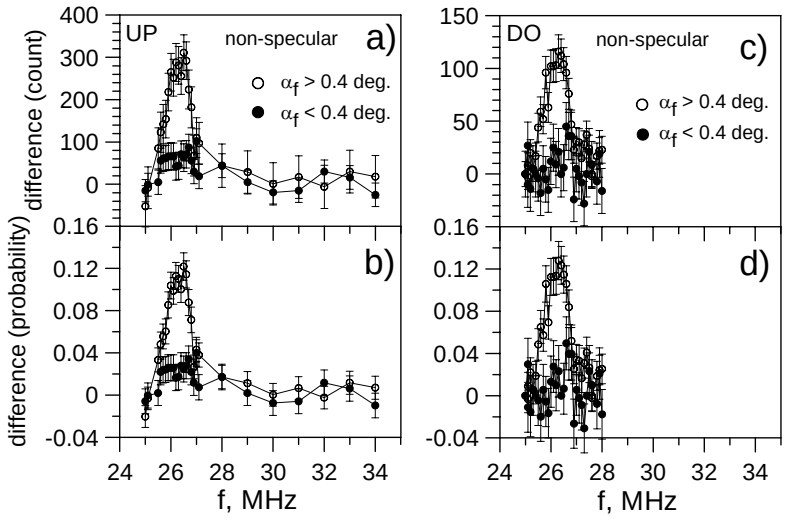

Fig. 4. Neutron count of non-specularly reflected beam in dependence on frequency of oscillation magnetic field. Upper panels are difference of count in- and out-of-resonance. Bottom panels are probability (difference of counts divided by the integrated intensity of the specularly reflected beam out-of-resonance).

In conclusion, we have observed experimentally non-specular neutron reflection from a uniformly magnetized film in an applied high-frequency oscillating magnetic field. The non-specular reflection takes place at resonance frequency. The resonance frequency corresponds to Larmor precession in the magnetic induction of the film. The value of angular beam-

splitting is big and cannot be explained by spin-flip in the external small magnetic field. For correct determination of the sign of spin-flip transitions, the following experiments with analyzer will be done.

The support of the management and staff at the FRM II, Garching, is gratefully acknowledged. This work was supported by a Focused Neutron Research Funding of the Max Planck Society, Munich. One of the authors (S.K.) is grateful to A.I. Frank for the interest to this subject and J. Franke for the technical help during the experiment.

References

[1] V.K. Ignatovich, F.V. Ignatovich, Am.J.Phys., 71 (2003) 1013.
[2] A.V. Kozlov, A.I. Frank, Physics of Atomic Nuclei, V.68, No.4 (2005) 1104-1119.
Yadernaya Fizika, V.68, No.4 (2005) 1149-1164.
[3] V.K. Ignatovich, Neutron optics, Moscow, Physmatlit, 2006, 335p.
[4] A.V. Kozlov, A.I. Frank, Physica B 404 (2009) 2550-2552.
[5] V.K. Ignatovich, Yu.V. Nikitenko, F. Radu, Nucl. Instr. and Meth. A 604 (2009) 653-661.

ULTRASONIC TREATMENT EFFECT ON THE LONG-TERM STABILITY OF BIOGENIC FERRIHYDRITE NANOPARTICLES SAMPLES IN AQUEOUS SOLUTION UNDER AMBIENT CONDITIONS

M. Balasoiu[a,b], L. Anghel[a,c], A. V. Rogachev[a], L.A. Ishchenko[d,e], A. Jigounov[f], G.M. Arzumanian[a], S.V. Stolyar[d,e], R.S. Iskhakov[d,e], Yu.L. Raikher[g]

[a]Joint Institute of Nuclear Research, Dubna, 141980, Russia
[b]Horia Hulubei National Institute of Physics and Nuclear Engineering, Bucharest, Romania
[c]Institute of Chemistry of ASM, Kisinau, Moldova
[d]Siberian Federal University, 660041, Krasnoyarsk, Russia
[e]Institute of Physics, Siberian Branch of RAS, 660036, Krasnoyarsk, Russia
[f]Institute of Macromolecular Chemistry, ASCzR Prague
[g]Institute of Continuum Media Mechanics, Ural Branch of RAS, 614013, Perm, Russia

Introduction

Ferrihydrite is an iron oxyhydroxide given the molecular formula $Fe_5HO_8 \cdot 4H_2O$, although $5Fe_2O_3 \cdot 9H_2O$ and others have been accepted. Ferrihydrite can show from two to six X-ray diffraction lines and nanoparticles are typically 2-10 nm in size. Structurally, ferrihydrite is believed to be based on simple chains of iron octahedral, although tetrahedrally coordinated iron has also been proposed. Ferrihydrite large surface area to volume ratio gives it high sorptive capabilities especially towards the heavy and transition metals, which are of environmental and industrial importance [1].

The literature [2] gives several methods for synthesis and purification of ferrihydrite. Although ferrihydrite occurs mainly in situations where Fe^{2+} is oxidized rapidly and/or where crystallization inhibitors are present. Oxidation can proceed via an inorganic pathway, but may also be assisted by micro-organisms.

In the present work methods to improve long-term stability of biogenic ferrihydrite nanoparticles produced by *Klebsiella oxytoca* are investigated. Earlier, it was shown that ferrihydrite nanoparticles produced by bacteria *Klebsiella oxytoca* in the course of biomineralization of iron salt solutions from natural medium [3] exhibit unique magnetic properties: they are characterized by both the antiferromagnetic order inherent to a bulk ferrihydrite and spontaneous magnetic moment due to the decompensation of spins in sublattices of nanoparticles [4]. Also, it was established that bacterium *Klebsiella oxytoca* creates two types of ferrihydrite nanoparticles as a result of variation of the growth conditions for the microorganisms, whose differences are accurately identified by means of Mossbauer spectroscopy [5, 6] static magnetic measurements analysis [6, 7] scanning electron microscopy and small angle X-ray scattering methods [8] on dry powder samples. The investigations in the direction of biomedical applications have revealed that the particles do not present cytotoxity and when attached to specific drugs present a weak antitumor activity against Ehrlich ascites carcinoma in mice [9].

Microstructure investigations of these biogenic nanoparticles by means of SAXS and SANS need special prepared samples: ferrihydrite nanoparticles dispersed in aqueous solution. Preliminary particle size analysis using high-resolution transmission electron microscopy images (HRTEM) combined with small angle X-ray scattering structure investigation of biogenic ferrihydrite aqueous suspensions are reported in [10]. Characteristic size of the particles (1-2 nm) (**Figure 1a**) estimated from HRTEM observations agrees with the height value of the objects identified by the small angle X- ray scattering data fit. Also the presence of organic material is detected by means of HRTEM. The nanoparticles or clusters of nanoparticles are withheld in the organic network (**Figure 1b**).

The low stability of the aqueous dispersions of the samples obtained from bacterial metabolism up to now made difficult detailed methodological SAXS and SANS studies.

Thus, effective methods to improve the stability of the biogenic ferrihydrite liquid dispersions are needed. Here results on the influence of ultrasonic treatment on the stability of before mentioned aqueous dispersions are reported.

Materials

Aqueous samples of biogenic particles of ferrihydrite were provided by Siberian Federal University, Krasnoyarsk, Russia. Ferrihydrite particles were obtained from microorganism isolated from Lake Borove (Krasnoyarsk krai). Initial concentration of magnetic nanoparticles in aqueous solution was 12.5g/l (5g of ferrihydrite powder dissolved in 400 ml double distilled water). From initial solution were prepared 4 samples of different concentration: $7.41 \cdot 10^{-3}$M, $5.54 \cdot 10^{-3}$M, $3.70 \cdot 10^{-3}$M, $1{,}85 \cdot 10^{-3}$M.

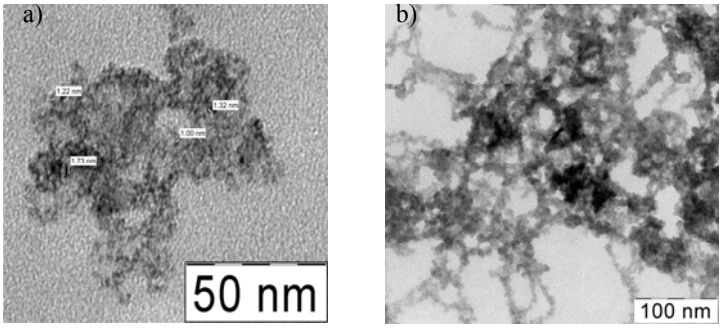

Fig. 1. HRTEM images of a sample of ferrihydrite nanoparticles dispersion in water: (a) and (b).

Prepared samples of different concentration of ferrihydrite were treated for two hours using a TRANSSONIC 310/H ultrasonic bath. Characterization of ultrasonic ferrihydrite samples in time consisted monitoring of visible spectra analysis on spectrophotometer. The absorbtion spectra of the samples with different ferrihydrite concentrations are presented in **Figure 2**.

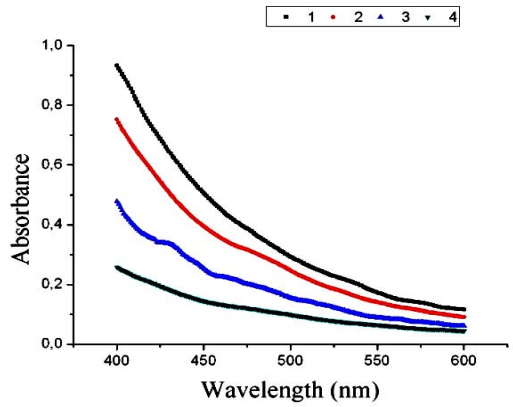

Fig. 2. Absorption spectrum vs concentration of ferrihydrite: (1) concentration of ferrihydrite $7.41 \cdot 10^{-3}$M; (2) concentration of ferrihydrite $5.54 \cdot 10^{-3}$M; (3) concentration of ferrihydrite $3.70 \cdot 10^{-3}$M; (4) concentration of ferrihydrite $1{,}85 \cdot 10^{-3}$M

Results and discussion

Due to its high sorptive properties, it is difficult to purify the biogenic ferrihydrite from organic matter and to maintain it dispersed in aqueous solution for a long time. We attempted the ultrasonic treatment as a physical method to disperse particle agglomerates without causing changes in chemical composition of the sample. The ferrihydrite concentration varied in each sample ultrasonic treated. A spectrum of ferrihydrite solution before ultrasonic treatment is shown in **Figure 2.1.** The spectrum is rather nondescript with gradual absorbance decline from 400 to 650 nm. For comparison purposes, the spectrum of the same ferrihydrite sample after ultrasonic treatment is shown in **Figure 2.2**.

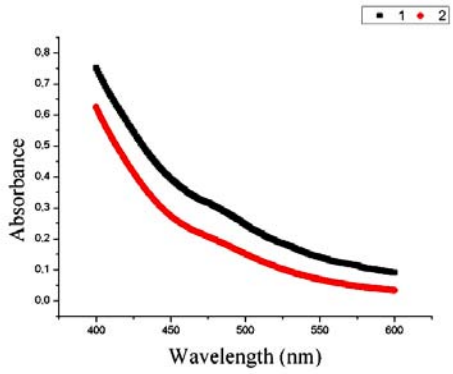

Fig. 3. Absorption spectrum of ferrihydrite sample of concentration $5.54 \cdot 10^{-3}$M: (1) before ultrasonic treatment; (2) after ultrasonic treatment

Visible spectra of ferrihydrite samples have shown changes after ultrasonic treatment. Decrease of absorbance values might be related to the reduction of the particles size. We also attempted to monitor the visible spectra of ultrasonic treated samples of ferrihydrite after 24h, 36h, 72h, and one week. The obtained data show that the samples remain stable during one week after ultrasonic treatment.

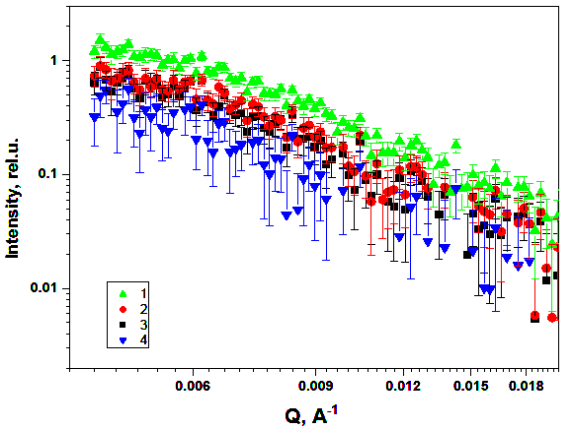

Fig. 4. SAXS experimental curves from biogenic ferrihydrite aqueous dispersions of following particle concentrations obtained at Rigaku spectrometer in function at IMC (Prague): (1) concentration of ferrihydrite $7.41 \cdot 10^{-3}$M; (2) concentration of ferrihydrite $5.54 \cdot 10^{-3}$M; (3) concentration of ferrihydrite $3.70 \cdot 10^{-3}$M; (4) concentration of ferrihydrite $1.85 \cdot 10^{-3}$M.

In **Figure 4** are presented SAXS experimental curves from biogenic ferrihydrite aqueous dispersions of four particle concentrations (after ultrasonic treatment) measured at Rigaku spectrometer in function at IMC (Prague): (1) $7.41 \cdot 10^{-3}$M; (2) $5.54 \cdot 10^{-3}$M; (3) $3.70 \cdot 10^{-3}$M; (4) $1{,}85 \cdot 10^{-3}$M. Further experimental data treatment is in progress.

References

1. Mabe D.R., Khasanov A.M., Stevens J.G., Hyperfine Interact (2005) 165: 209–213.
2. Schwertmann U., Cornell R.M., *Iron oxides in the laboratory. Preparation and characterization,* Wiley-VCH Publishing House Second Edition 2000, 8:103-113.
3. S. V. Stolyar, O. A. Bayukov, Yu. L. Gurevich, E. A. Denisova, R. S. Iskhakov, V. P. Ladygina, A. P. Puzyr', P. P. Pustoshilov, M. A. Bitekhtina, Inorganic Materials Vol.42, 763 (2006).
4. Yu. L. Raikher, V.I. Stepanov, S.V. Stolyar, V.P.Ladygina, D.A.Balaev, L.A. Ishchenko, M.Balasoiu, Phys. of Solid State, Vol.52, No.2, 277 (2010).
5. S.V. Stolyar, O.A. Bayukov, Yu.L. Gurevich, E.A. Denisova, R.S. Iskhakov, V.P. Ladygina, A.P. Puzyr', P. P. Pustoshilov, L.A. Cekanova M. A. Bitekhtina, Materialovedenie, No.7, 34 (2006) (Rus).
6. S. V. Stolyar, O. A. Bayukov, Yu. L. Gurevich, V. P. Ladygina, R. S. Iskhakov, P. P. Pustoshilov, Inorganic Materials Vol.43, 638 (2007).
7. Yu.L. Raikher and V.I. Stepanov, Journ. Exp. Theor. Phys., Vol.107, No.3, 435 (2008).
8. M. Balasoiu, S. V. Stolyar, R.S. Iskhakov, L.A. Ishchenko, Y.L. Raikher, A. I. Kuklin, O. L. Orelovich, Y. S. Kovalev, T. S. Kurkin, G.M. Arzumanian, Rom. Journ. Phys. Vol 55, No.7-8, 782 (2010).
9. L.A. Ishchenko, S.V. Stolyar , V. P. Ladygina, Y. L. Raikher, M. Balasoiu, O. A. Bayukov, R., S. Iskhakov, E. V. Inzhevatkin, International Conference on Magnetic Fluids ICMF12, 1-4 August 2010, Senday, Japan.
10. M. Balasoiu, L.A. Ischenko, S.V. Stolyar, R.S. Iskhakov, Yu.L. Raikher, A.I. Kuklin, D.V. Soloviov, T.S. Kurkin, D. Aranghel, G.M. Arzumanian, Optoelectronics and Advanced Materials –Rapid Communications, Vol. 4, No. 12, 2136 (2010).

STRUCTURAL AND MAGNETIC PHASE TRANSITIONS IN MULTIFERROIC $BiMnO_3$ AT HIGH PRESSURES

D.P.Kozlenko[a], A.A.Belik[b], S.E.Kichanov[a], D.V.Sheptyakov[c], Th.Straessle[c] and B.N.Savenko[a]

[a]Frank Laboratory of Neutron Physics, JINR, Dubna, Russia
[b]International Center for Materials Nanoarchitectonics, National Institute for Materials Science), Japan
[c]Laboratory for Neutron Scattering, ETH Zurich and Paul Scherrer Institut, Villigen, Switzerland

A great attention has been given to multiferroic effects, observed in $RMnO_3$ (R = Tb, Dy, Gd, Bi) compounds. In these materials ferroelectricity coexists with long range magnetically ordered ground state of incommensurate or commensurate nature. This leads to quite interesting novel physics, such as possibility of switching of electric polarization by magnetic field, very prospective for electronic devices, possible composite excitation of electromagnon, and promising many more surprises awaiting to be unearthed. The multiferroic $BiMnO_3$ is a rare example of the compound with collinear ferromagnetic ground state (T_{FM} = 100 K), possessing orbital order at T_{FE} = 500 K [1].

Our results [2] demonstrate that application of relatively moderate pressure ($P \sim 1$ GPa) leads to suppression of the initial FM ground state and appearance of the AFM ground state with the propagation vector k = (1/2 1/2 1/2) in $BiMnO_3$. The modification of the balance between FM and AFM superexchange interactions due to structural transformation is the possible reason for the observed magnetic phase transition. However, the structural details of high pressure phase of $BiMnO_3$, important for further elucidation of the nature of its multiferroic properties, remain unexplored.

The crystal structure of $BiMnO_3$ was investigated using the HRPT diffractometer [3] at the SINQ neutron spallation source (Paul Scherer Institute, Switzerland) at high pressures up to 10 GPa and ambient temperature. The incident neutron wavelength was 1.494 Å. The Paris-Edinburgh high pressure cell was used with a 4:1 volume mixture of fully deuterated methanol-ethanol as a pressure transmitting medium. For the pressure determination, an equation of state of NaCl, admixed to the sample in 1:2 volume proportions, was used.

The characteristic neutron diffraction patterns of $BiMnO_3$ measured at selected pressures up to 10 GPa and ambient temperature are shown in fig. 1. At ambient conditions the monoclinic structure of *C2/c* symmetry was detected. At pressures above 1 GPa, noticeable changes in diffraction data were observed, evidencing the structural phase transition. From the data analysis it was found that the structure of the high pressure phase of $BiMnO_3$ can be also described as monoclinic one with *C2/c* symmetry, but with different ratio of lattice parameters with respect to ambient pressure phase. The pressure-induced structural phase transition causes an increase of the *a* lattice parameter and decrease of *b* and *c* lattice parameters, while the unit cell volume decreases. The monoclinic angle β value is weakly affected.

At pressures above 8.5 GPa, appearance of another structural phase transition was observed in diffraction data (fig. 1). From the data treatment it was found that the crystal structure of the second high pressure phase has the *Pbnm* orthorhombic symmetry. Comparison between structural parameters of $BiMnO_3$ and those of related orthorhombic $RMnO_3$ compounds implies that a magnetic state modification from commensurate to incommensurate AFM one is expected at monoclinic-orthorhombic phase transition.

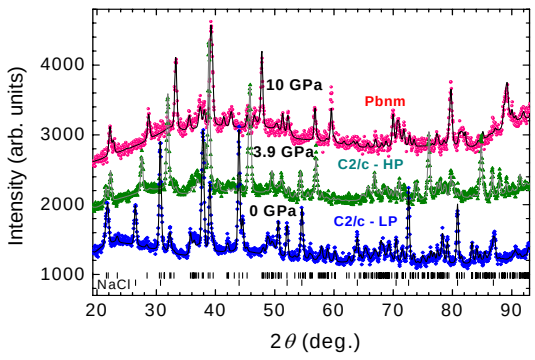

Fig. 1. Neutron diffraction patterns of $BiMnO_3$ measured at selected pressures and ambient temperature for two monoclinic (C2/c-LP and C2/c-HP) and orthorhombic structural phases and processed by the Rietveld method. Experimental points and calculated profiles are shown. Ticks below represent calculated positions of nuclear peaks of ambient pressure monoclinic phase (C2/c-LP) and NaCl, used for pressure calibration.

Our results demonstrate that suppression of the initial FM ground state and appearance of the AFM ground state accompanied by the structural phase transition between ambient pressure and high pressure monoclinic phases. The highly competing character of these magnetic interactions, resulting in a coexistence of FM and AFM phases under pressure, supports the mechanism of multiferroic phenomena in $BiMnO_3$ due to inversion symmetry breaking [2].

References

[1] T. Kimura, S. Kawamoto, I. Yamada, M. Azuma, M. Takano, and Y. Tokura, Phys. Rev. B 67, 180401(R) (2003).
[2] D. P. Kozlenko, A. A. Belik, S. E. Kichanov, I. Mirebeau, D. V. Sheptyakov, Th. Strässle, O. L. Makarova, A. V. Belushkin, B. N. Savenko, and E. Takayama-Muromachi, Phys. Rev. B 82, 014401 (2010).
[3] S.Klotz, Th.Strässle, G.Rousse, G. Hamel, and V. Pomjakushin, Appl. Phys. Lett. **86**, 031917 (2005).

A STUDY OF CLUSTER FORMATION IN SILICON GLASSES DOPED BY TiO_2/CeO_2 OXIDES.

S.E.Kichanov[a], S.A.Samoylenko[a,b], D.P.Kozlenko[a], A.V.Belushkin[a] L.A.Bulavin[b], G.P.Shevchenko[c], V.C.Gurin[c], V.Haramus[d] and B.N.Savenko[a]

[a]Frank Laboratory of Neutron Physics, JINR, Dubna, Russia
[b]Taras Shevchenko National University of Kiev, Kiev, Ukraine
[c]Research Institute for Physical Chemical Problems of the BSU, Minsk, Belarus
[d]GKSS, Geesthacht, Germany

The prospective material for optical filters is silicon glasses with doped oxides of the transition and rare earth elements [1]. Such glasses are characterized by high ultraviolet radiation protection and thermal stability, and they are suitable for numerous technological applications, including the development of novel modifications of laser glasses, light filters and the imitation of gem production [2].

The glasses doped by cerium and titanium oxides are yellow–orange and the optical absorption edge can be shifted significantly by varying the CeO2/TiO2 concentrations ratio [3]. It was assumed that the thermal stability of the yellow–orange color in silicon glasses is a result of the formation of complex clusters Ce–Ti–O [3].

In order to study the structural characteristics of silicon glasses containing CeO2 and TiO2 oxides with different concentration ratios, small-angle neutron scattering experiments were carried out with the spectrometer SANS-1 [4] on the research reactor FRG-1 (GKSS, Germany).

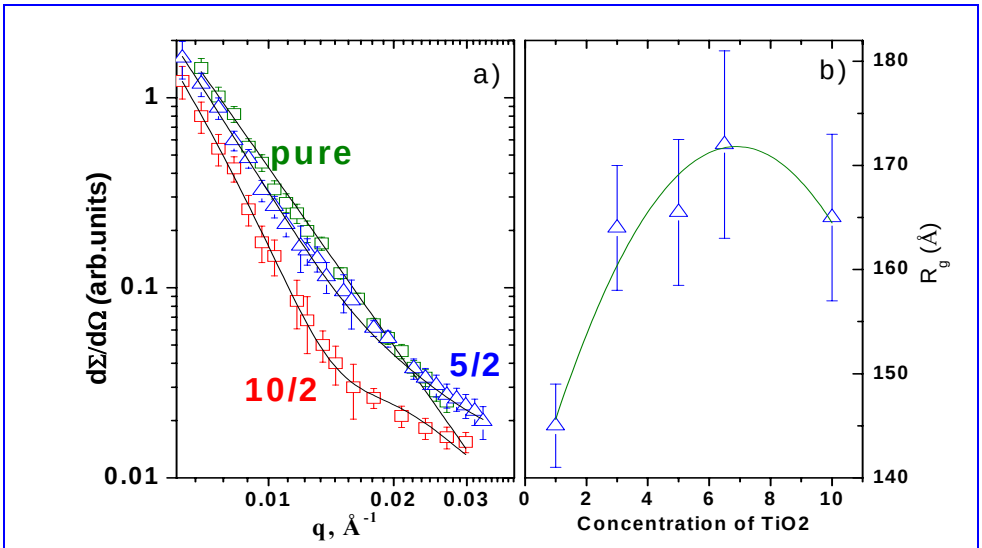

Fig 1. a) The small angle neutron scattering curves for pure silicon glass and glasses with a concentration ratio of TiO2/CeO2 oxides 5.0/2.0 and 10.0/2.0. The solid lines are calculated profiles. b) The calculated values of a gyration radius of the Ti-Ce-O clusters as function of TiO2 relative concentration (the concentration x (CeO2)=2.0). The solid line is polynomial fit.

The scattering curves for pure silicon glass and glasses with a molar concentration ratio of CeO2/TiO2 oxides 2.0/5.0 and 2.0/10.0 are shown in figure 1a. The curve for the pure glass indicates scattering from large objects - microscopic air bubbles, which appeared in the manufacture of glass material. The SANS curves of silicon oxides doped with CeO2/TiO2 exhibit somewhat different behavior. This corresponds to scattering from two different types of object, one related to larger air bubbles in the glass matrix and the other to smaller aggregates formed by Ce, Ti and O atoms. The experimental data were fitted by a function [5]:

$$d\Sigma(q)/d\Omega = Aq^{-\alpha} + C\exp(-\frac{1}{3}q^2R_g^2) + D$$

The calculated values of the gyration radius of those oxide clusters indicate weak nonlinear dependence of the cluster size on titanium oxide concentration (fig. 1b).

References

[1] G.S.Bogdanova, S.L.Antonova, and B.F.Dzhurinskii, Izv. Akad. Nauk SSSR, Neorg. Mater., 6, 943–948 (1970).
[2] W.Xu, S.Tang and W.Huang, "Fusion of glasses containing ceria and titania," J. Non-Cryst. Solids, 112, 186 – 189 (1989).
[3] E.E. Trusova, N.M. Bobkova, V.S. Gurin, and E.A. Tyavlovskaya, Glass and Ceramics Vol.66, Nos.7–8, 2009.
[4] H. B. Stuhrmann, N. Burkhardt, G. Dietrich, R. Jünemann, W. Meerwinck, M. Schmitt, J. Wadzack, R. Willumeit, J. Zhao, K. H. Nierhaus. Nucl. Instr. & Meth. A, **356** 133 (1995)]
[5] Brumberger H (ed) 1995 Modern Aspects of Small Angle Scattering (Dordrecht: Kluwer), p. 53.

MORPHOLOGY OF THE PHOSPHOLIPID TRANSPORT NANOSYSTEM

M.A. Kiselev[1], E.V. Ermakova[1], O.M. Ipatova[2], A.V. Zabelin[3]

[1] *Frank Laboratory of Neutron Physics, JINR, Dubna*
[2] *Institute of Biomedical Chemistry RAMS, Moscow*
[3] *Federal Scientific Center «Kurchatov Institute», Moscow*

Phospholipid transport nanosystem (FTNS) has different applications. First, FTNS is nanodrug with application at acute toxic exposure and at precomatose state. Second, FTNS is drug delivery system for 6 different antitumoral, antiphlogistic, and antioxidant drugs. Third, FTNS could be used as carrier for chlorin E6 in the photodynamic therapy and diagnostic. More important application of FTNS is drug delivery. A lot of studies have been carried out at the time of the design and medical test of FTNS. Nevertheless, the morphology of FTNS nanopartricle is not clear (vesicles or micelles?). Fig. 1 presents the vesicular morphology of FTNS with incorporated hydrophilic and hydrophobic drugs. Molecules of the hydrophobic (nonsoluble in water) drugs localized in the phospholipids bilayer. Molecules of the hydrophilic (water soluble) drugs locates inside of the vesicle.

The purpose of the presented experimental study was characterization of the FTNS morphology via small-angle X-ray scattering at the station DIKSI of synchrotron ring «Sibirea 2». Methodological purpose of the experiment was the development of the small-angle mode at the DIKSI beam line for the nanodiagnostic of nanodrugs. Data acquisition was carried out at sample to detector distance L_{sd}=30cm and 243.5cm, wavelength of the photons was λ=1.625Å. Samples were prepared as 25% and 50% dilution in water (w/w) of lyophilizated drug. At 25% of delution the sample consist of (w/w) 75% of water, 20% of maltose, and 5% of phospholipids as shown at Fig. 2. From the medical point of view, 25% concentration of drug corresponds to medical recipe for the intravenous injection. From physical point of view, 5% of phospholipids and 20% of maltose in water corresponds to the good X-ray contrast between maltose solution in water and phospholipids bilayer and not so strong intervesicle interaction [1-3]. It was shown in our previous study [1-3] that water solutions of disaccharides (sucrose, trehalose, maltose) create best experimental conditions for the characterization of phospholipid vesicular systems via X-ray small-angle scattering and allows to acquire the small-angle scattering curve in the broad q range.

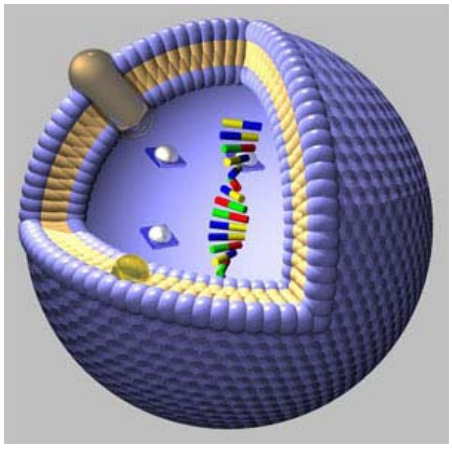

Fig. 1. Vesicular phospholipids based drug delivery system with incorporated hydrophilic and hydrophobic drugs.

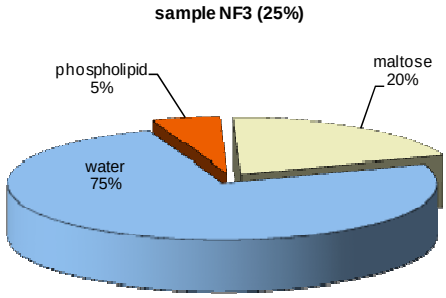

Fig. 2. Component distribution (w/w) in the sample under investigation (25% of FTNS).

The small-angle scattering curve from the sample 25% of FTNS is presented at Fig. 3. The small-angle scattering curve from extruded DMPC vesicles in 40% sucrose solution is presented for the comparison. This curve was obtained at beam-line D24 of synchrotron DCI, LURE, France. The line $1/q^2$ describes common law of scattering from the unilamellar vesicles with high value of polydispersity. Common direction of scattering curve from FTNS corresponds to the $1/q^2$, which is evidence of the vesicular morphology of FTNS nanoparticles after hydration. Comparison of scattering from extruded DMPC vesicles in 40% sucrose solution shows that FTNS vesicles in 20% maltose solution have low polydispersity. The polydispersity of FTNS vesicles is about 20-30%. The average vesicle radius 160Å for FTNS was calculated from the

position of first minimum in the form factor of the vesicle shape. DMPC vesicles after extrusion has larger radius - 210Å. FTNS consists from the unsaturated phospholipids – lecithin. Position of the first minimum in the form-factor of the bilayer at Fig. 3 shows that thickness of the bilayer from the lecithin is different from the thickness of fully saturated DMPC bilayer.

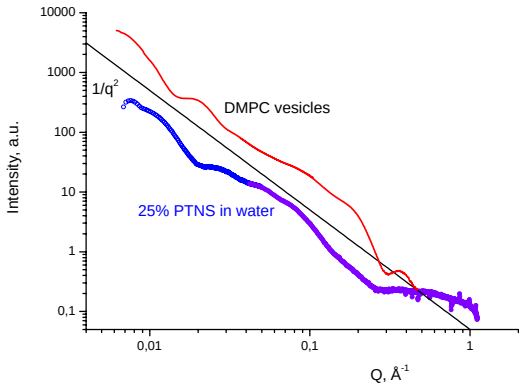

Fig. 3. Small-angle X-ray scattering curves: DMPC vesicles in 40% sucrose solution – red (LURE, France), 25% solution of phospholipid transport nanosystem (FTNS) in water – blue, law $1/q^2$ - black.

Presented result was first experiment at DIKSI beam line in the small-angle mode. Creation of the best experimental conditions for the investigation of lyophilizated nanodrugs has two contradictory requirements. Increasing of nanodrug concentration (low value of dilution in water) increase the interparticle interaction and create problem of artifact (form factor separation from the structure factor influence). Decreasing of nanodrug concentration decrease signal from phospholipids, but increase contrast from maltose. Comparison of experimental results from samples with different FTNS concentration shows that 25% FTNS in water (5% of lipid and 25% of maltose) create best experimental conditions for the investigation of lyophilizated nanodrugs in maltose without essential distortion and with good contrast.

Our previous study of disaccharides application for contrast variation in the SAXS experiment [1-3] allows one to start investigation the nanostructure of real drugs developed in the Institute of Biomedical Chemistry.

References

1. M.A. Kiselev, P. Lesieur, A.M. Kisselev, D. Lombardo, M. Killany, S. Lesieur, M. Ollivon. A sucrose solutions application to the study of model biological membranes. *Nuclr. Inst&Method A* 470 (2001) 409-416.
2. M.A. Kiselev, P. Lesieur, A.M. Kisselev, D. Lombardo, M. Killany, S. Lesieur. Sucrose solutions as prospective medium to study the vesicle structure: SAXS and SANS study. *J. Alloys and Compounds* 328 (2001) 71-76.
3. M.A. Kiselev, S. Wartewig, M. Janich, P. Lesieur, A.M. Kiselev, M. Ollivon, R. Neubert. Does sucrose influence the properties of DMPC vesicles? *Chemistry and Physics of Lipids* 123 (2003) 31-44.

МЕТОД СЛЕД-ОТОБРАЖЕНИЯ ДЛЯ РЕШЕТКИ ПЕЛЛА

Эльмар Аскеров

Лаборатория Нейтронографии им.Франка, ОИЯИ, Дубна, Российская Федерация
Институт Радиационных Проблем НАНА, Баку, Азербайджан

После экспериментального открытия квазикристаллов [1], эти новые объекты стали одной из перспективных направлений физики конденсированного состояния [2]. Существует большой интерес к одномерным квазикристаллам, так как имеется ряд нерешенных проблем в этой области, в числе которых и одна из существенных задач математики - классификация одномерных квазикристаллов.

Рассмотрим одномерную квазипериодическую решетку Пелла [3]. Одномерные квазикристаллы обычно описываются дискретным одномерным уравнением Шредингера, так как гамильтониан уравнения достаточно хорошо характеризует особенности квазипериодической структуры:

$$\sum\nolimits_j t_{ij}\psi_j = E\psi_i \ ,$$

где t_{ij} интегралы переноса, Ψ_j - волновая функция на *i*-ом узле.

Следуя [4] перепишем уравнение Шредингера в терминах трансфер-матриц. Нахождение волновых функций сводится к нахождению рекуррентной формулы для следа произведения матриц. Данный метод называют след-отображением.

В случае $t_{n,n+1} = t_{n,n-1} = 1$ мы получили рекуррентное соотношение для следа произведения матриц для решетки Пелла:

$$TrM_{n+1} = TrM_{n-1}\left(TrM_n\right)^2 - \frac{\left(TrM_n\right)^2 + TrM_{n-2}TrM_n}{TrM_{n-1}} - TrM_{n-1},$$

где M_n - так называемая трансфер-матрица для решетки длиной n. В этом случае данное след-отображение имеет интеграл движения (инвариант):

$$I = -xz + \left(\frac{x+z}{y}\right)^2 + y^2 \ , \text{ где}$$

$$x = TrM_{n+1}, y = TrM_n, z = TrM_{n-1} .$$

Полученная формула для следа произведения трансфер-матриц может быть использована для расчетов многих физических величин, таких как плотность уровней энергии, коэффициент трансмиссии и т.д.

Литература

[1] Shechtman D et al. Phys. Rev. Lett. 53 1951 (1984);
[2] Ю. Х. Векилов, М. А. Черников, УФН Т. 180 561—586 (2010);
[3] Gahramanov. I, Asgerov E., arXiv cond-mat.dis-nn:1010.24 (2010);
[4] M. Kohmoto, L. P. Kadanoff, and C. Tang, Phys. Rev. Lett. 50, 1870 (1983).

RESULTS OF MEASUREMENT THE RESIDUAL STRAINS IN THE WWER-1000 REACTOR VESSEL

V.V.Sumin[a], A.M.Balagurov[a] , I.V.Papushkin[a] , R. Wimpory[b]

[a] Frank Laboratory of Neutron Physics, Joint Institute for Nuclear Research, 141980, Dubna, Russia
[b] Helmholtz-Centrum Berlin for Material and Energy, D-14109, Berlin, Germany

Introduction

Owing to a high penetrability of thermal neutrons, neutron diffraction can be used to measure the distributions of residual stresses in a bulk of crystalline materials to depths of the order of several centimeters. The principle of the method is the measurement of the shift of the position of the diffraction peaks from the positions determined by the unit cell parameters of the undeformed material [1, 2]. Internal stresses existing in a material cause corresponding deformation of the crystal lattice, which, in turn, is manifested in the shift of the Bragg peaks in the diffraction pattern. This gives direct information on changes in the interplanar distances, from which the internal stresses can be easily calculated. At the present time, the method is widely used to determine residual stresses in bulk products and composites, to test welds, and to study complicatedly deformed products and behavior of materials during fatigue tests.

The strains due to internal stresses are usually of the order of 10^{-3}–10^{-4}; because of this, in order to measure such strains, a high resolution neutron diffractometer with $\Delta d/d = (3–5) \times 10^{-3}$ is used. In this case, the accuracy of determination of residual stresses in steels is 20–40 MPa. In this work, we studied the residual stresses in the natural WWER-1000 reactor vessel under stainless steel facing inside the vessel. The vessel base metal is the Grade 15KhGMFAA ferrite. The sign of the residual stresses in the direction parallel to the facing ferrite interface (tangential stress) is of great importance for the vessel corrosion resistance. As the tangential stresses are positive (tensile stresses), any crack in the stainless steel facing brings about cracking also in the ferrite. And vice versa, negative tangential stresses prevent the cracking.

Results

The view and scheme of measurements on the thick template are shown in **Fig. 1.** From the symmetry considerations, one can assume that the strains in both the tangential directions are equal, i.e., $\varepsilon_z = \varepsilon_y$. Because of this, we measured only one tangential component and also the normal component of the residual strains. The measurements were performed on a E3 stress diffractometer of the Hahn–Meitner Institute. The results of the measurements are presented in

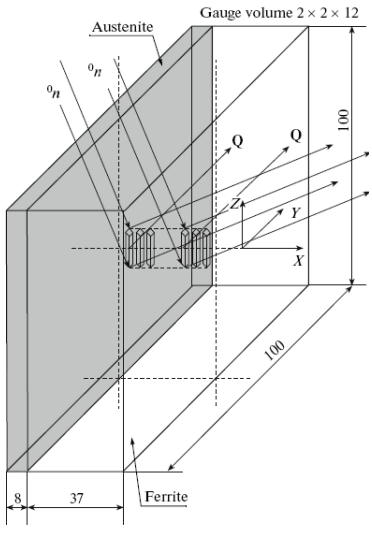

Fig. 1 Sizes and scheme of measurement of the tangential residual strains in the templet. Q is the scattering vector of neutrons.

Fig. 2. The measurements were performed in the normal direction from two sides of the specimen: on the side of the facing, to a depth of 5 mm in the ferrite phase and, on the side opposite to the facing, from the coordinate 34 to 17 mm inside the ferrite. We failed to measure the residual strains in the middle of the template because of the limitations in aperture ratio.

The residual stresses in the thick template were calculated by known relationships [1, 2] with the assumption $\varepsilon_z = \varepsilon_y$. As in the case of the thin template, the residual stresses under the facing in the ferrite phase remain negative, i.e., as aforementioned, favorable regarding the corrosion cracking, and they are somewhat lower (–140 MPa) in the thick template as compared to the thin template (–220 MPa). A reason of such a disagreement is the underestimate of the normal residual stresses ($\varepsilon x = 0$) for the thin template which are not really small: in the thick template, studied early on FSD-spectrometer the residual stresses are positive and are equal to 70 MPa .

The partial discrepancy between obtained neutron and cutting experimental results can be explained by the methodological differences of applied experimental techniques. But all methods showed qualitative consent.

Fig. 2. Residual stresses in studied template along phase interface. Vertical line indicates austenite-ferrite interface position at Z = 8 mm. Points represent residual stresses measured by neutron diffraction parallel to phase interface (♦ - σ_y, ■ - $\sigma_x \approx \sigma_z$). Dash curve represents stress kinetic intensity value obtained using crack propagation method while solid curve corresponds to the residual stress value estimated by cutting method.

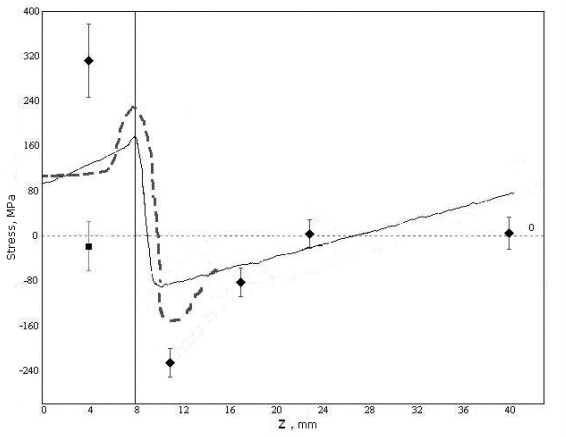

Acknowledgments

This study was supported by the International Scientific and Technical Centre (project no. 3074.2).

References

1. A. J. Allen, M. T. Hutchings, C. G. Windsor, and C. Andreani, Adv. Phys. **34**, 445 (1985).
2. V. L. Aksenov, A. M. Balagurov, G. D. Bokuchava, V. V. Zhuravlev, E. S. Kuz'min, A. P.Bulkin, V. A. Kudryashev, and V. A. Trunov, Soobshch. Ob'edin. Inst. Yad. Issled. P13_2001_30 (2001).

THE RESOLUTION FUNCTION OF A TOF REFLECTOMETER IN THE GRAVITY FIELD

I. Bodnarchuk[a], S.Manoshin[b], S.Yaradaikin[b], V.Kazimirov[b], and V.Bodnarchuk[b]

[a] Lomonosov Moscow State University, Skobeltsyn Institute of Nuclear Physics, Moscow, Russia
[b] Joint Institute for Nuclear Research, Frank Laboratory of Neutron Physics, Dubna, Russia

The effect of gravity on neutron scattering is negligible if a thermal spectrum up of to 10 Å is used. Modern cold sources produce spectra with an ample quantity of cold neutrons. Gravity may have a crucial role for the cold part of the spectrum in neutron scattering experiments demanding high angle resolution. It mainly concerns the reflectometry method where a small deviation in the angle distribution may lead to visible effects.

Presently, the new multifunctional time-of-flight (TOF) reflectometer, GRAINS, is under construction at the modernized high flux pulsed reactor with the new cold moderator, IBR-2M, in Dubna (Russia) [1]. It is necessary to study the influence of gravity on the resolution function because the principal feature of this reflectometer is the horizontal sample plane.

We consider the general configuration of elements, which defines the reflectometry mode including the source *M*, two slits *D1* and *D2*, sample *S* and a detector. The centers of the slits and the sample are on the line inclined at an angle $\theta = 15$ mrad to the horizontal plane. The angular resolution function for such reflectometer with parameters based on the real beam line characteristics of the reflectometer GRAINS was deduced by extending the analytical beam-analysis method [2], which took into account the influence of gravity. This function was obtained for the fixed neutron wavelength and then convoluted with the wavelength resolution function.

To test the approach, reflectivity curves smeared by the derived resolution function were compared with the reflectivity curves simulated by the VITESS Monte-Carlo software package [3]. A thin monolayer with a critical angle of 5.56×10^{-4} rad/Å and thickness of 1500 Å on a substrate with a critical angle of 4.17×10^{-4} rad/Å was used as an idealized sample. The wavelength dependence of reflectivity from such a monolayer consists of a sequence of narrow oscillations whose positions and shapes are very sensitive to the resolution factor. An incident spectrum of constant intensity for all wavelengths was used to exclude the factor of spectrum shape from consideration.

The dependence of the gravity effect on the distance between the second slit and the sample S_{D2S} and on the sample size L_S was analyzed. The reflectivities for two sample lengths, $L_S = 20$ mm and $L_S = 100$ mm, and three sample positions, $S_{D2S} = 0.033$ m or $S_{D2S} = 0.05$ m (the sample position right after the second slit for two sample lengths correspondingly), $S_{D2S} = 0.5$ m and $S_{D2S} = 1$ m are shown on Fig. 1.

It can be seen that the agreement between the theoretical calculations in the frame of proposed approach and the Monte-Carlo simulations by means of the VITESS package is very good. In all cases, the deviations of reflectivity with zero and non-zero gravity can be observed. An increase in the distance between the second slit and the sample leads to higher deviation. Two factors, both of which are due to the bending of neutron trajectories in the gravity field, contribute to the deviation. The first factor is the increase in the grazing incidence angle, which leads to the shift of reflectivity fringes to higher wavelengths. If the angular divergence increases, the fringes broaden, and the gravity shift becomes less distinguishable. The second factor is that neutrons fall before the sample, which leads to the flux deficiency for longer wavelengths. This effect is greater for a smaller sample length. In the case of non-zero gravity, each element of the reflectometer acts as a wavelength and angular filter while in the case of zero gravity, each element only selects angles.

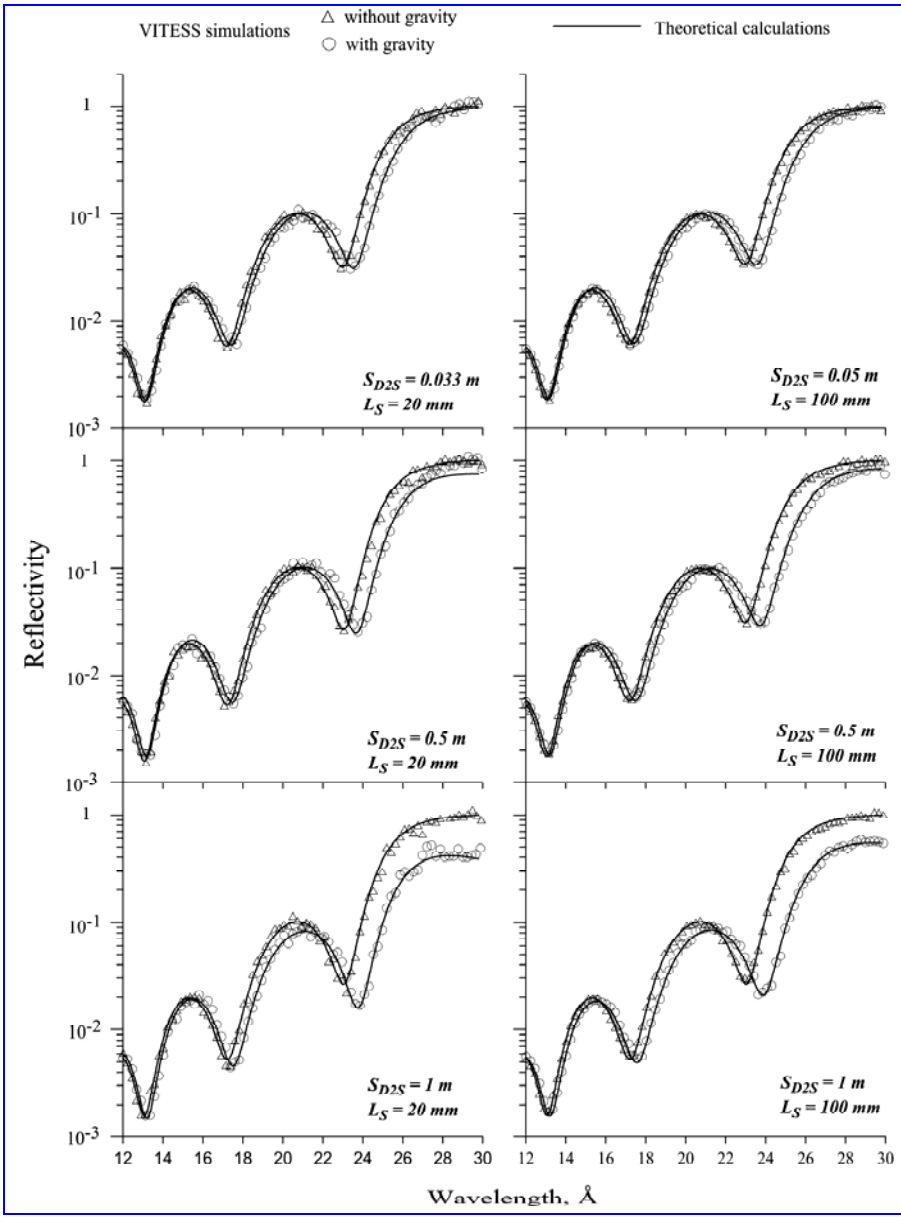

Fig. 1. The reflectivities for two sample lengths and three sample positions with respect to the second slit. The solid lines are the theoretical calculations, and the triangles and circles are the Monte-Carlo simulations prepared by the VITESS package with zero and non-zero gravity respectively. All plots are represented from 12 Å where all curves are distinguishable.

Conclusions

The analytical beam-line analysis method for deriving of the resolution function for the neutron TOF reflectometer accounting for effect of gravity was applied. The theoretical calculations are in good agreement with Monte-Carlo simulations, which mimic the real measurements with idealized samples. The proposed theoretical approach makes it possible to take the resolution into account correctly and allows one to carry out real measurements with a broad wavelength band.

References

[1] M.V. Avdeev, V.I. Bodnarchuk, et al., J. Phys.: Conf. Ser. 251 (2010) 012060;
[2] J.S. Pedersen, C. Riekel, J. Appl. Cryst. 24 (1991) 893;
[3] VITESS web site: <http://www.hmi.de/projects/ess/vitess>.

AQUEOUS SOLUTIONS OF POLY(ETHYLENE GLYCOL): SANS STUDY

G.Lancz[a], M.V.Avdeev[b], V.I.Petrenko[b,c], V.M.Garamus[d], M.Koneracká[a] and P.Kopčanský[a]

[a]Institute of Experimental Physics, Slovak Academy of Sciences, Košice, Slovakia
[b]Frank Laboratory of Neutron Physics, Joint Institute for Nuclear Research, Dubna, Moscow region, Russia
[c]Physics Department, Taras Shevchenko Kyiv National University, Kyiv, Ukraine
[d]GKSS Research Centre, Geesthacht, Germany

Hydrophilic poly(ethylene glycol) (PEG) is used for coating of colloidal particles for gaining biocompatibility. Its introduction into magnetic fluids (liquid dispersions of magnetic nanoparticles) may increase the circulation time of magnetic particles in organisms by hindering the action of the mononuclear phagocyte system (reticuloendothelial system), which is a part of the immune system. This is because nanoparticles, or surfaces in general, coated with PEG show enhanced resistance against protein adsorption, see e. g. [1] and references therein. An increase in biocompatibility of a given magnetic fluid is expected even by the simple addition of PEG, i.e. without a covalent bond between PEG and the magnetic particle. The goal of this study was to understand the structural characteristics of PEG molecules in water, which give some basic knowledge useful for further investigations of complex systems comprising PEG. In the given work the solutions of PEG in deuterated water (D_2O) with different molecular weights in a range of M_n = 400 – 20000 were investigated using small-angle neutron scattering (SANS) technique. Recently [2, 3], SANS was successfully applied for PEG in D_2O within a narrow range of M_n = 2000 – 8000 at different solution ion strength. Together with the compressibility and intermolecular distance as a function of PEG concentration [2], two possible structures (Gaussian coils and flat 'plates') of PEG were discussed [3] with respect to the scaling in the scattering as a function of M_n. Here, SANS characterization of PEG covers wider M_n-interval. Additionally, the measurements were performed at the physiological temperature of 37°C taking into account a specific interest for using PEG in biocompatible ferrofluids.

PEG with four different molar masses was purchased from Sigma-Aldrich ('average mol wt 400', 'typical M_n 1000', and '16000 - 24000') and Merck ('9000 - 11250 g/mol'). PEG with M_n = 400, 1000, 10000, 20000 was dissolved in pure D_2O (D-content 99.9%) with the mass fractions within an interval of 0.5–10%. D_2O was used to achieve a sufficient scattering contrast between PEG and the liquid carrier, as well as for reduction of the incoherent scattering background from hydrogen. SANS experiments were performed using the SANS-1 instrument located at the Neutron Facility at GKSS Research Centre, Geesthacht, Germany. Measurements were done at the temperature of 37 °C. For solutions of PEG with M_n = 400, the 5 mm thick quartz cells were used. In other cases the thickness of the cells was 2 mm. In all cases pure D_2O was used as a buffer (blank, background sample). To obtain the differential cross-section per sample volume (hereafter referred to as scattered intensity) in the absolute scale (cm^{-1}) the standard calibration [4] using the scattering from 1-mm water sample was made after the background, buffer (D_2O) and empty cell corrections.

Changes in the experimental SANS intensities are followed in **Fig.1** (examples are given for PEG 1000 and PEG 10000). One can see that at the PEG concentrations of less than 3% the scattering shows a pronounced Guinier-type behaviour corresponding to a form-factor of the polymer coils. At higher concentrations the correlations between coils results in the structure-factor effect at small q-values, which is rather different for masses below 1000 and above 10000.

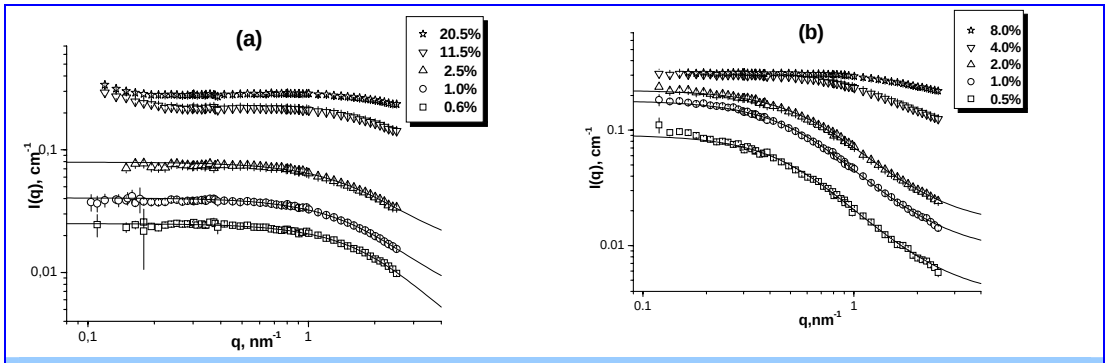

Fig. 1. Changes in SANS intensity (dots) with variation in mass fraction of PEG dissolved in D_2O, M_n is 1000 (a) and 10000 (b). Solid lines show fits in accordance with Debye formula (1) for non-interacting Gaussian coils.

Our interest in this study was the analysis of the coil form-factor. For this purpose the scattering data from low-concentrated (< 3%) solutions were first approached by the Guinier law to reveal the radius of gyration of the coil, R_g, at sufficiently small q-values ($qR_g \leq 1$). For low M_n (400 and 1000) the Guinier approximation is valid over the whole q-range covered in the experiments. This made possible to fit additionally the residual incoherent background caused by non-compensated hydrogen in PEG.

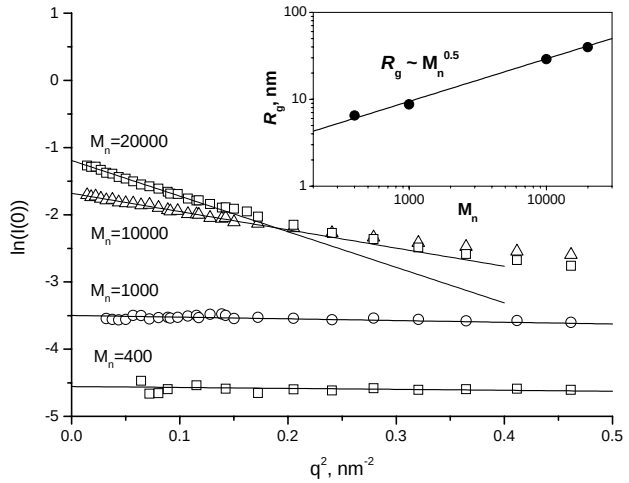

Fig. 2. Guinier plots of SANS intensity (dots) for 1% PEG solutions in D_2O with different M_n and corresponding linier approximations (lines) to regions $qR_g < 1$. Non-compensated incoherent background is subtracted. Several points with very low statistics in beginning parts of plots for M_n = 400 and 1000 are removed from treatment. Inset shows dependence of obtained radius of gyration on polymer molecular weight. Experimental errors do not exceed the size of dots.

It is important that this background was consistent for solutions with the same PEG concentrations independently of M_n. The Guinier approximations for 1% solutions of PEG with different masses are shown in **Fig.2**. The dependence of the obtained radius of gyration on the PEG molecular mass in this case (inset to Fig. 2) reveals a power-law behaviour (line in the double logarithmic scale) with an exponent of 0.48±0.02. This corresponds well to Gaussian coils (exponent 1/2) and coincides with the result for PEG with M_n= 2000 - 8000 in ionic solutions [3]. Hence, the Debye formula for the scattering from non-interacting Gaussian coils can be used at low PEG concentrations for any M_n. This is demonstrated in **Fig. 1**, where for diluted PEG solutions the fits are based on the formula:

$$I(q) = 2I_0[e^{-x} - (1-x)]/x^2 + B, \quad x = (qR_g)^2. \qquad (1)$$

Here, $I_0 = I(q \to 0)$ is the forward scattering intensity and B is the residual background. The same fit quality takes place for similar solutions with M_n of 400 and 20000. It should be noted that the relative difference in the values of the radius of gyration from the fit of the Debye formula (eq. 1) and from the Guinier appoximation is below 5%, and the Guinier approximation almost coincides with (1) in the overlapping region ($qR_g < 1$). Additionally, dependence of $q^2 \cdot I(q)$ vs. q reveals a typical behaviour for Gaussian polymer chains (not shown).

The observed scaling law $R_g \sim M_n^{0.5}$ in a wide polymer mass interval (400 – 20000) strongly confirms the Gaussian coil structure of PEG in water solutions. The scattering form-factor of the coils is well described by the Debye formula over the whole measured q-interval at the PEG concentration below 2 %. High adsorption properties of PEG for various substrates [5-7] and nanoparticles [8] also suggest a developed structure of this polymer.

References

[1] Y. Zhang, N. Kohler, M. Zhang, *Biomaterials* **23**, 1553 (2002).
[2] K.A. Rubinson, J. Hubbard, *Polymer* **50**, 2618 (2009).
[3] K.A. Rubinson, S. Krueger, *Polymer* **50**, 4852 (2009).
[4] G.D. Wignall, F.S. Bates, *J. Appl. Cryst.* **20**, 28 (1987).
[5] E. Tronel-Peyroz, H. Raous, D. Schuhmann, *J. Coll. Interface Sci.* **92**, 136 (1983).
[6] A.M. Mota, M.L. Simões Gonçalves, J.P. Farinha, J. Buffle, *Coll. Surf. A* **90**, 271 (1994).
[7] J.C. Dijt, M.A. Cohen Stuart, J.E. Hofman, G.J. Fleer, *Coll. Surf.* **51**, 141 (1990).
[8] M.V. Avdeev, A.V. Feoktystov, P. Kopčanský, G. Lancz, V.M. Garamus, R. Willumeit, M. Timko, M. Koneracká, V. Závišová, N. Tomašovičová, A. Juríková, K. Csach, L.A. Bulavin, *J. Appl. Cryst.* **43**, 959 (2010).

CONTRAST VARIATION IN SMALL-ANGLE NEUTRON SCATTERING ON WATER-BASED MAGNETIC FLUID WITH SODIUM OLEATE AND POLYETHYLENE GLYCOL STABILIZATION

M.V.Avdeev[a], A.V.Feoktystov[a,b], P.Kopcansky[c], G.Lancz[c], M.Timko[c], M.Koneracka[c], V.Zavisova[c], N.Tomasovicova[c], A.Jurikova[c], K.Csach[c], V.M.Garamus[d], R.Willumeit[d], L.A.Bulavin[b]

[a]*Frank Laboratory of Neutron Physics, Joint Institute for Nuclear Research, Dubna, Russia*
[b]*Taras Shevchenko Kyiv National University, Physics Department, Kyiv, Ukraine*
[c]*Institute of Experimental Physics, Slovak Academy of Sciences, Kosice, Slovak Republic*
[d]*Helmholtz-Zentrum Geesthacht, Geesthacht, Germany*

The structure description of complex (particularly polydisperse and multicomponent) systems is an important problem in modern nanoscience. Ferrofluids or magnetic fluids (fine stable dispersions of magnetic nanoparticles in liquids) belong to such a class of nanosystems. To ensure the long-term stability of ferrofluids in both unmagnetized and magnetized states, the magnetic nanoparticles are coated with a chemical layer, which prevents particle coagulation by attractive van derWaals and magnetic interactions. In biocompatible colloidal systems for medical applications, the chemical composition of the particle surface is of particular importance to avoid the action of the reticuloendothelial system, which is part of the immune system, in order to increase the lifetime of the magnetic nanoparticles in the blood stream. If magnetic particles in ferrofluids are coated with neutral and hydrophilic compounds such as polyethylene glycol (PEG) [1-3], the lifetime increases from minutes to hours or even days.

In present work, we investigate the above-mentioned water-based ferrofluid stabilized by sodium oleate, which is then modified by introducing biocompatible PEG. Several types of aggregates revealed in both ferrofluids complicate their reliable structure analysis. In this connection, we focus our investigation on the application of small-angle neutron scattering (SANS), which is one of the most suitable methods for studying the inner structure of colloidal particles in complex aggregate-containing systems. In particular, the contrast-variation technique (with H_2O/D_2O mixtures in the solvent) is used to reveal the scattering length density (SLD) distribution in various aggregates of non-magnetized samples at the scale of 1–100 nm.

The preparation of the ferrofluids studied here was based on a co-precipitation method that involved mixing two solutions ($FeSO_4 \cdot 7H_2O$ and $FeCl_3 \cdot 6H_2O$) with an alkaline aqueous medium (25% NH_3). The stabilization of the magnetite precipitate was achieved by the addition of sodium oleate ($C_{17}H_{33}COONa$, theoretical ratio 0.73 g to 1 g of Fe_3O_4). The system at this stage is discussed below as an initial ferrofluid and referred to as Sample 1. As a second stabilizer, PEG (M_w = 1000 g mol^{-1}) was added to the system (2.5 g per 1 g of Fe_3O_4). The experiments were carried out on the SANS-1 small-angle instrument at the FRG-1 steady-state reactor of the Helmholtz-Zentrum Geesthacht, Geesthacht, Germany (former GKSS Research Centre) [4]. No external magnetic field was applied to the samples.

The experimental data were treated in terms of the approach of [5] which, in addition to the classical contrast-variation technique [6], takes into account the polydispersity and magnetic scattering.

The experimental SANS curves for the two samples with different η are presented in **Fig.1**. The changes in the character of the curves are similar in both cases. Fluids with a low D_2O content (below 30%) show mainly the signal from magnetite. For higher D_2O content the contribution from the H-containing components becomes significant, which explains particularly the appearance of a broad peak (band) in the curves around $q \sim 0.8$ nm^{-1}. At the same time, some specific differences can be emphasized. First, the scattering from Sample 1 is significantly larger on the absolute scale. It resembles scattering from well defined particles, which is reflected in the existence of the Guinier regime at low q values.

In Sample 2, a degree of aggregation affects the curves, comparable to what is observed in water-based ferrofluids with double steric stabilization [7-10]. This is concluded from the power-law behavior of the scattering at low q values, which points to the fractal-type organization of the aggregates discussed below. The Guinier regime is not observed in the initial parts of the curves for these aggregates, which means that the aggregate size is beyond the instrument limit $D \sim 120$ nm (the estimate is derived from the minimum measured q value in accordance with the rule $D \sim 2\pi/q$).

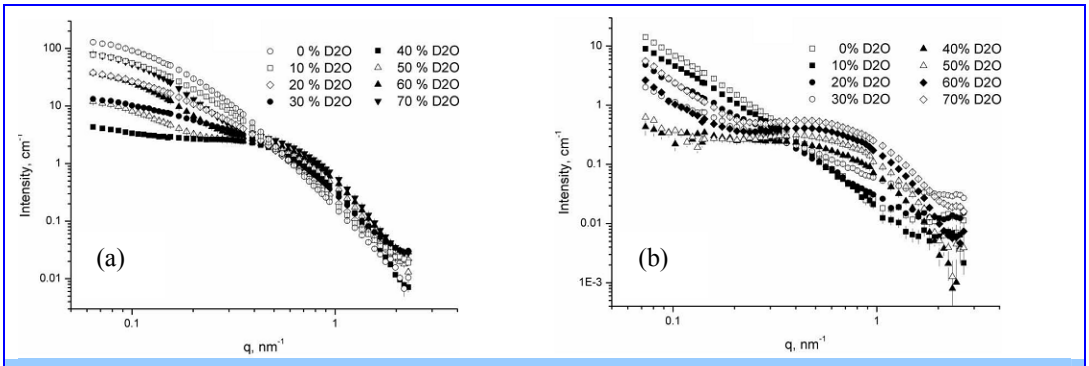

Fig. 1. Changes in the SANS curves with contrast variation for (*a*) Sample 1and (*b*) Sample 2. The percent volume fraction of D_2O in the solvent is indicated.

From the whole set of scattering curves the modified basic functions were calculated. The basic function $I_c(q)$ (Fig.2*a*) reflecting the average shape scattering differs greatly for the two samples in the initial parts of the curve (q <0.4 nm^{-1}).

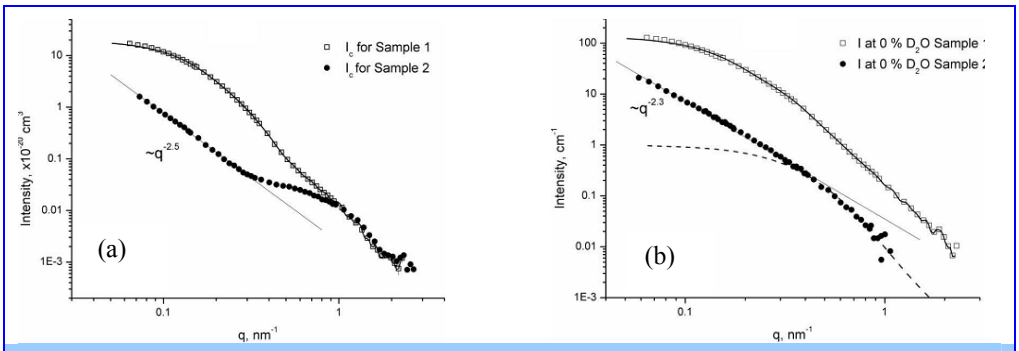

Fig. 2. (*a*) Experimentally obtained $I_c(q)$ basic functions (shape scattering) for Samples 1 and 2, compared with (b) the curves at 0% D_2O (scattering from magnetite only). Solid lines for Sample 1 correspond to IFT fits. Solid lines for Sample 2 show power-type scattering with the indicated exponents. The dashed line for the curve at 0% D_2O in (*b*) shows the scattering from separate magnetite nanoparticles (R_0 = 3.4 nm, S = 0.38).

It may be concluded that there is a transition from well defined particles in the case of Sample 1 to smaller particles and large aggregates in Sample 2. The new aggregates can be associated with fractal structures, which determine scattering of a power-law type with an exponent of about −2.5. This corresponds to a mass fractal dimension D =2.5 [11]. The behavior of the curves at high q values is similar and they show certain types of bands. For comparison, in **Fig.2*b*** the scattering curve obtained at η = 0 (light water) is given. At low q values, the character of the curves repeats those of the $I_c(q)$ functions, thus proving that magnetite particles mainly determine the shape scattering. At high q values, the curves differ significantly from the $I_c(q)$ functions. In particular, the bands disappear, which means that their origin is connected with particles composed of H-containing components.

We relate the bands above q ~ 0.3 nm^{-1} in the $I_c(q)$ functions to micelles of free sodium oleate in the solvent. At the highest q values the two functions differ by only a factor showing that the micelle concentration is about 30% higher in Sample 2 than in Sample 1. Additionally, the contribution from the micelles is more significant in the case of Sample 2, when the scattering from the magnetite particles decreases. In this case, the Guinier region for the micelles is well resolved. It was treated by indirect Fourier transform (IFT), taking into account the power-law scattering at low q values. If a spherical shape is assumed for the micelles, the resulting radius of gyration of the micelles, R_{gmic} = 1.59(5) nm, gives R = 2.05 nm according to the well known equation $R^2_{gmic} = (3/5)R^2$. The obtained value correlates well with the molecular length of sodium oleate.

So, the structures of a water-based ferrofluid with magnetite stabilized by sodium oleate and its mixture with PEG have been revealed by the contrast-variation technique in small-angle neutron scattering experiments. In particular, the addition of PEG leads to reorganization of the aggregate structure compared with the initial ferrofluid. Notably, a type of

exchange of packed and comparatively small aggregates (about 40 nm) with developed and large aggregates (above 120 nm) is observed, which is caused by the adsorption of PEG on the magnetite particles. Aggregates in both kinds of ferrofluids are stable with respect to time and temperature increase (343K).

References

[1] Timko, M., Koneracka ,M., Kopcansky ,P., Tomori, Z., Vekas, L., Jozefczak, A., Skumiel, A., Radenovic, A., Dietler, G., Bystrenova, E. & Lita, M. (2004). Indian J. Eng. Mater. Sci. 11, 276–282.

[2] Tomasovicova ,N., Koneracka ,M., Kopcansky ,P., Timko, M. & Zavisova ,V. (2006). Meas. Sci. Rev. 6, 32–35.

[3] Hong, R.Y., Ren, Z.Q., Han, Y.P., Li, H.Z., Zheng, Y. & Ding, J. (2007). Chem. Eng. Sci. 62, 5912–5924.

[4] Zhao, J., Meerwinck, W., Niinkoski, T., Rijillart, A., Schmitt, M., Willumeit, R. & Stuhrmann, H.B. (1995). Nucl. Instrum. Methods Phys. Res. Sect. A, 356, 133–137.

[5] Avdeev, M.V. (2007). J. Appl. Cryst. 40, 56–70.

[6] Stuhrmann, H.B. (1995). Modern Aspects of Small-Angle Scattering, edited by H. Brumberger, pp.221–253. Dordrecht: Kluwer Academic Publishers.

[7] Balasoiu, M., Avdeev, M.V., Aksenov, V.L., Hasegan, D., Garamus, V.M., Schreyer, A., Bica, D. & Vekas, L. (2006). J. Magn. Magn. Mater. 300, e225–e228.

[8] Wiedenmann, A., Hoell, A. & Kammel, M. (2002). J. Magn. Magn. Mater. 252, 83–85.

[9] Avdeev, M.V., Aksenov, V.L., Balasoiu, M., Garamus, V.M., Schreyer, A., Torok, Gy., Rosta, L., Bica, D. & Vekas, L. (2006). J. Colloid Interface Sci. 295, 100–107.

[10] Feoktystov, A.V., Bulavin, L.A., Avdeev, M.V., Vekas, L., Garamus, V.M. & Willumeit, R. (2009). Ukr. J. Phys. 54, 266–273.

[11] Schmidt, P.W. (1995). Modern Aspects of Small-Angle Scattering, edited by H. Brumberger, pp.1–56. Dordrecht: Kluwer Academic Publishers.

СОЗДАНИЕ МАКЕТА ТЕХНОЛОГИЧЕСКОЙ СИСТЕМЫ КРИОГЕННОГО ЗАМЕДЛИТЕЛЯ С ЭЛЕКТРОНИКОЙ УПРАВЛЕНИЯ И КОНТРОЛЯ

Ананьев В.Д., Беляков А.А., Богдзель А.А., Булавин М.В., Верхоглядов А.Е., Кулагин Е.Н., Куликов С.А., Кустов А.А., Мухин К.А., Петухова Т.Б., Сиротин А.П., Федоров А.Н., Шабалин Е.П., Шабалин Д.Е., Широков В.К.

ЛНФ, ОИЯИ

Введение

Криогенный замедлитель на основе ароматических углеводородов на мощном импульсном исследовательском реакторе ИБР-2 (КЗ) - будет уникальным импульсным источником холодных нейтронов с длиной волны более 0.3 нм, обеспечивающим проведение на современном мировом уровне научных и прикладных работ с использованием методик нейтронного рассеяния. КЗ будет входить в состав комплекса нейтронных замедлителей на реакторе ИБР-2 /1-8/.

Установка КЗ включает в себя собственно криогенный замедлитель - камеру, заполняемую рабочим веществом в виде замороженных шариков из смеси ароматических углеводородов (мезитилен + m-ксилол), систему приготовления шариков и заполнения ими камеры, замены рабочего вещества при выработке ресурса, систему охлаждения камеры и поддержания температуры шариков на уровне 30 К и другие, вспомогательные системы, обеспечивающие нормальную работу КЗ.

КЗ представляет собой весьма сложную техническую структуру, создание которой требует поэтапного решения конкретных методических и конструкторских задач. К первостепенным задачам относится обеспечение загрузки замороженных шариков в камеру замедлителя. Выбранный принцип загрузки - транспортировка шариков холодным гелием (40К -80 К) по протяженной пневмотрассе от специального дозирующего устройства до камеры. Проблема транспортировки состоит в отсутствии как экспериментальных, так и теоретических данных об упруго-пластических, адгезионных и трибологических свойствах твердого аморфного мезитилена (каковой является его 70% смесь с m-ксилолом), а также о движении одиночного шарика по цилиндрической широкой трубе с учетом трения качения и скольжения и отклонения от сферичности. Все это затрудняло расчет параметров пневмотранспортной системы и разработку дозирующего устройства. Поэтому проблему транспортировки надо было решать экспериментально – сначала на специальном лабораторном стенде для решения проблемы движения одиночного шарика /9-11/, и затем - при помощи стенда с прототипом криогенного замедлителя нейтронов. В данной работе он представлен как испытательный стенд криогенного замедлителя для исследования характеристик холодной трассы загрузки шариков твердых замороженных ароматических углеводородов (мезитилена, m-ксилола)».

Цель создания стенда и проведения научно-исследовательских работ на нем - обоснование принятого принципа доставки и загрузки рабочего вещества в камеру холодного замедлителя нейтронов на основе ароматических углеводородов и проверка работоспособности технологических систем.

В настоящее время на испытательном стенде криогенного замедлителя нейтронов реактора ИБР – 2М выполнены следующие работы:

- произведена загрузка камеры-имитатора на 30% (~300 мл шариков);
- проведена отладка технологической системы управления и контроля;
- выбран оптимальный температурный режим работы стенда;
- определена рабочая скорость гелия во внутренней трубе пневмотрассы;
- определена оптимальная скорости подачи шариков из дозирующего устройства;
- определено время полной загрузки камеры-имитатора.

Испытательный стенд криогенного замедлителя нейтронов

Пневмотрасса стенда замедлителя разработана и введена в эксплуатацию на 3-м канале экспериментального зала №2 реактора ИБР-2. Она представляет собой повторение основных узлов и системам пневмотрассы реального замедлителя **(рис.1)**.

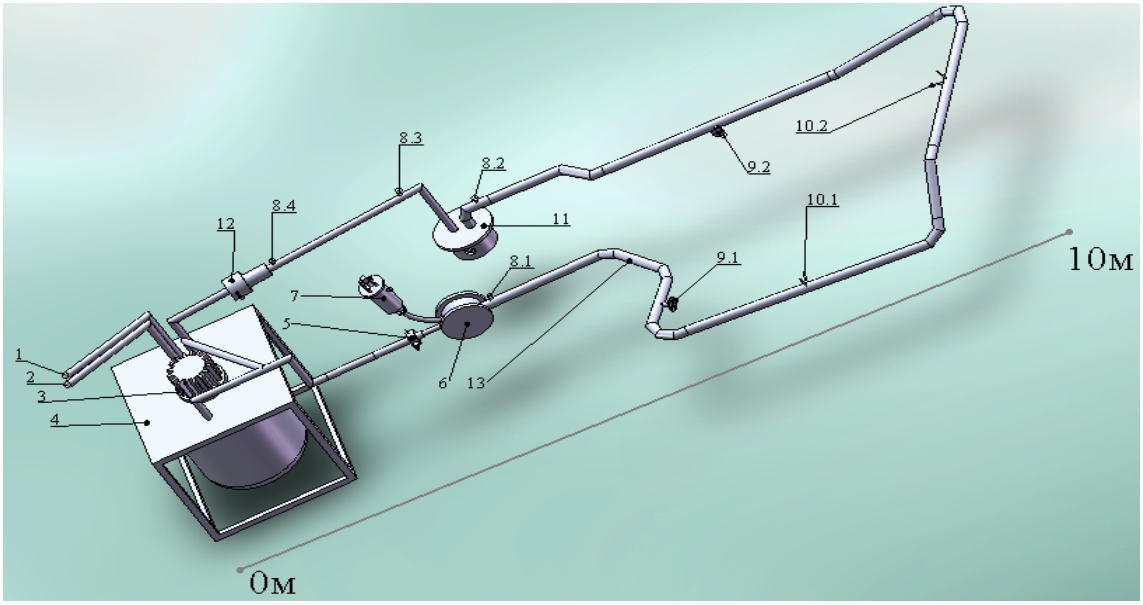

Рис.1. Трехмерный эскиз стенда криогенного замедлителя нейтронов реактора ИБР – 2М: 1-трубопровод подвода гелия к КГУ-500, 2- трубопровод отвода гелия от КГУ-500, 3-газодувка, 4-криостат, 5-узел с трубкой Пито и мановакуумметром, 6-тройник, 7-дозатор подачи шариков в пневмотракт; 8.1, 8.2, 8.3, 8.4-ТВО; 9.1, 9.2 - фланцы для откачки вакуума; 10.1, 10.2 - выводы трубок к датчикам движения шариков; 11- камера-имитатор холодного замедлителя, 12 - система подпитки гелия; 13-пневмотранспортный трубопровод.

Принцип работы стенда заключается в доставке замороженных шариков из дозатора к камере-имитатору по пневмотрассе с помощью холодного гелия при температуре 30-40К. Для подготовки стенда к работе, в межтрубном пространстве пневмотрассы (шарики транспортируются по внутренней трубе) и в криостате **(рис.2)** необходимо создать вакуум порядка 10^{-4} – 10^{-5} Torr.

Внутренний трубопровод откачивают через фланец дозатора шариков до получения форвакуума, с целью удаления воздуха и остатков мезитилена. После получения форвакуума трубопровод заполняют гелием комнатной температуры под давлением 1,03 атм. из газгольдера. Во время работы газгольдер постоянно открыт, благодаря чему давление гелия во внутренней трубе поддерживается на одном и том же уровне. Холодный гелий по трубопроводу его подвода от криогенной гелиевой машины (КГУ-500) поступает в криостат, после чего происходит захолаживание его первого контура. Значения температуры в криостате фиксируются датчиками типа ТВО (Т1-Т5, **рис.2**) и контролируются при помощи компьютера. После заполнения пневмотранспортного трубопровода гелием, он начинает циркулировать по пневмотрассе (2-ой контур криостата). Благодаря теплообменнику, температура гелия 2-го контура понижается, постепенно захолаживая внутреннюю трубу.

Температура на разных участках пневмотрассы фиксируется с помощью ТВО Т6-Т9. После получения рабочих температур 30-40К, можно переходить к процессу загрузки камеры-имитатора. Замороженные шарики, помещают в дозатор, который доставляет их во внутреннюю трубу пневмотрассы. Потоком холодного гелия шарики транспортируются к камере-имитатору, их появление в камере фиксируются Web-камерой. После окончания эксперимента, жидкий мезитилен удаляется из камеры-имитатора через специальную трубку.

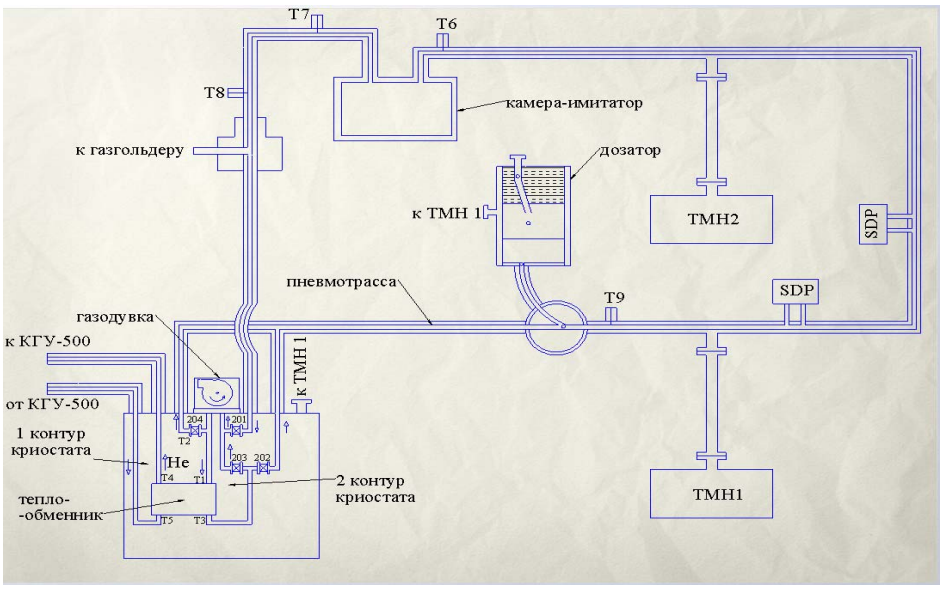

Рис.2 Технологическая схема стенда криогенного замедлителя нейтронов: ТМН и ФВН – турбомолекулярные и фор-вакуумные насосы, SDP – датчики дифференциального давления, Т – датчики температуры типа ТВО, 201-204 – вентили, регулирующие движение гелия в криостате

Технологическая система управления и контроля испытательного стенда криогенного замедлителя

На данный момент разработка системы управления и контроля стенда завершена **(рис.3)**, проводится ее отладка и оптимизация работы. Все модули системы объединены в единый блок, расположенный в экспериментальном зале, а управление и сбор данных осуществляется дистанционно с помощью ПК и специально написанного программного обеспечения.

Система управления и контроля включает в себя:

- модули контроля температуры и вакуума,
- модуль управления газодувкой (циркулятором гелия),
- модуль управления двигателем дозирующего устройства,
- модуль управления Web-камерой.

Система контроля температуры

Для контроля температуры используется комплекс из 8-ми последовательно соединенных датчиков типа ТВО (Т1-Т9, **рис.1**). Диапазон измеряемых температур составляет 15К-273К, что соответствует изменению сопротивления датчиков в диапазоне - 1,8кОм – 800Ом. Зависимость сопротивления от температуры – обратная.

Требуемая точность измерения температуры - 0,1град. Датчики подключены по 4-х проводной схеме, т.е. по 2-м проводам подводится постоянный ток, а через 2 других провода осуществляется съем напряжения, пропорционального измеряемой величине – сопротивлению датчика. Для регистрации напряжений с датчиков был выбран 8-канальный измеритель аналоговых сигналов ТМ 5103, который используется в режиме циклического просмотра измерений по всем 8 каналам на основном 4-х разрядном табло. Измеритель ТМ 5103 имеет интерфейс связи с ПК – RS232, что делает возможным его подключение к ПК по линии связи длиной до 15 м.

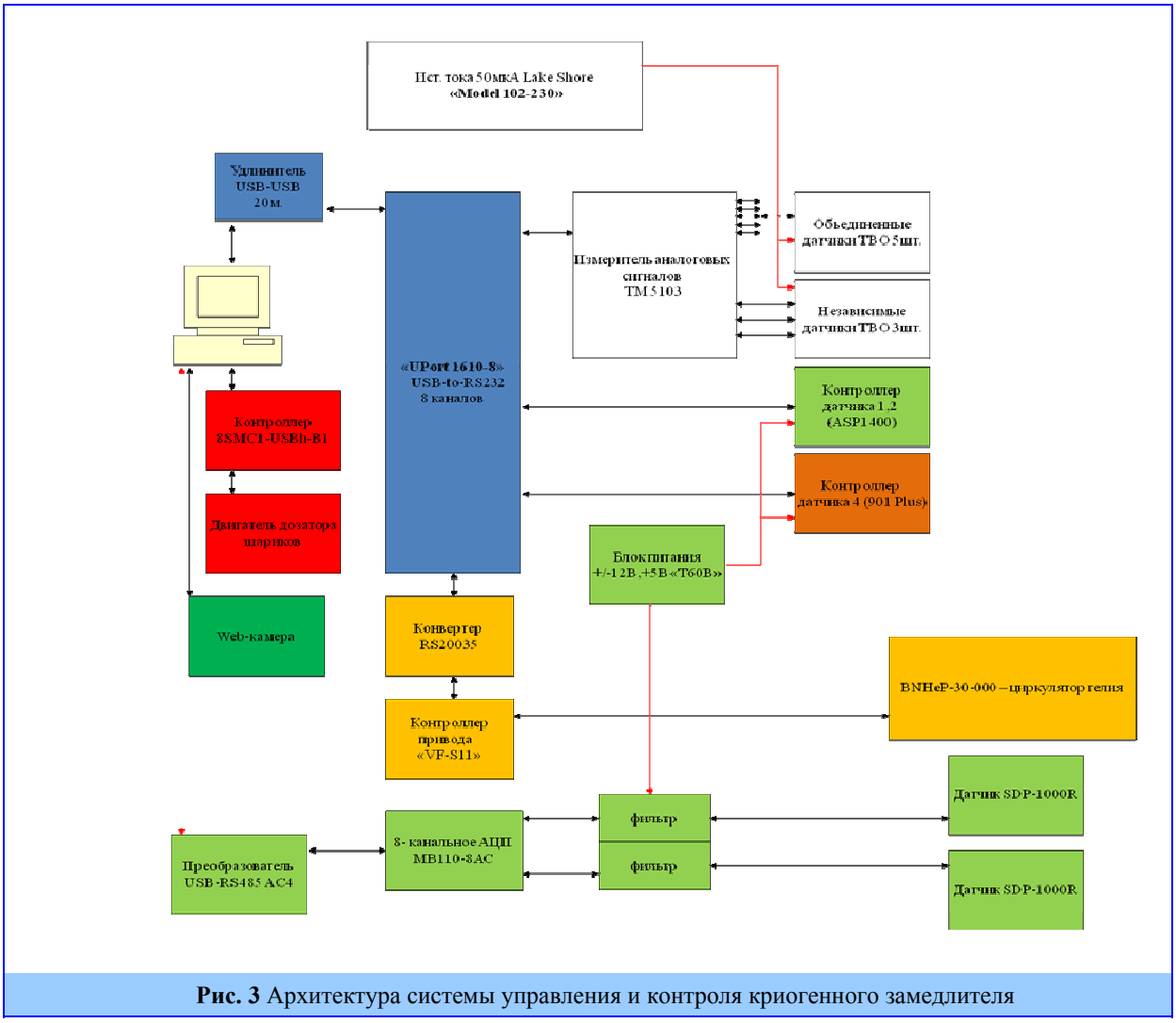

Рис. 3 Архитектура системы управления и контроля криогенного замедлителя

Система управления газодувкой (циркулятором гелия)

Газодувка (циркулятор гелия) предназначена для получения необходимой скорости движения рабочего газа во внутренней трубе. От скорости движения газа зависит скорость движения шариков по трубе, и, соответственно, время заполнения камеры макета. С одной стороны, скорость движения шариков не должна быть слишком большой, иначе они будут разрушаться, а с другой стороны, – не слишком малой, так как в этом случае время загрузки будет непозволительно большим. Характеристикой циркулятора, задающей скорость движения газа в трубе является частота вращения двигателя. В качестве частотного привода было выбрано устройство «VF-S11» фирмы Toshiba для двигателей мощностью до 400Вт.

Система управления двигателем дозирующего устройства

Дозирующее устройство («Дозатор») представляет собой цилиндр с диском у основания, на котором располагаются замороженные шарики **(рис.5)**. Цилиндр окружен вакуумно-азотной «рубашкой», предотвращающей приток тепла к диску с шариками **(рис.4)**. Верхний фланец «рубашки» имеет в верхней части специальное отверстие, через которое происходит загрузка. Диск соединен длинным штоком с шаговым электродвигателем.

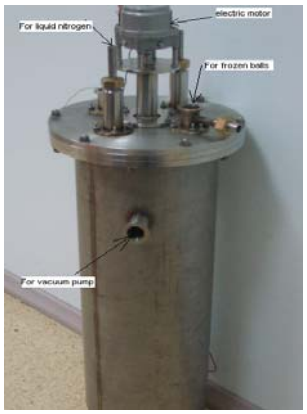

Рис.4 Дозирующее устройство

Рис.5 Цилиндр с диском

В качестве основы для системы управления дозатором шариков были выбраны контроллеры управления шаговыми двигателями фирмы Standa: 8SMC1- USBh-B1. Они позволяют в широком диапазоне регулировать скорость шагового двигателя. Для обеспечения плавности хода дозатора шаговый двигатель выбран с редуктором 1:150, что обеспечивает от нескольких оборотов в минуту до 1 оборота за несколько минут. Управление и контроль параметров работы, таких как положение, ускорение/замедление, скорость и направление движения осуществляется с персонального компьютера через USB интерфейс.

Система управления Web-камерой

Для контроля заполнения камеры макета используется Web-камера, которая в он-лайн режиме фиксирует попадание шариков внутрь камеры, через специальные стеклянные вставки **(рис.6)**

Рис. 6 Камера-имитатор макета

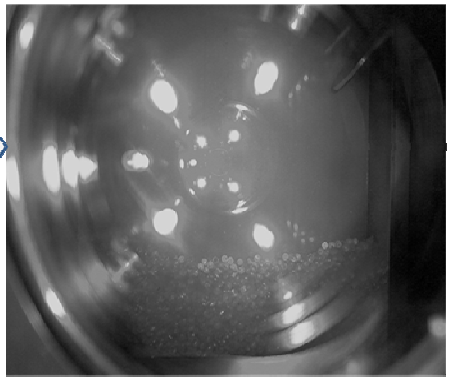

Рис. 7 Снимок шариков, сделанный Web-камерой

Web-камера записывает и передает изображение на компьютер через USB удлинитель, благодаря чему, пользователь может аблюдать за процессом загрузки шариков в режиме реального времени **(рис.7)**.

Заключение

На данный момент на макете криогенного замедлителя был проведен ряд экспериментов по загрузке камеры-имитатора. В ходе экспериментов в камеру было загружено около 300 мл шариков из необходимого количества в 1000 мл **(рис.7)**, был выбран оптимальный температурный режим работы, проведена отладка системы управления и контроля, оптимизация режимов загрузки, в частности, выбор скорости гелия во внутренней трубе, выбор скорости подачи шариков из дозатора, а также определено примерное время загрузки камеры. В ближайшее время планируются эксперименты по полной загрузке камеры, разработка системы подсчета количества шариков и

контроля возможных заторов шариков в трубе, а также выработка рекомендаций по эксплуатации реального криогенного замедлителя нейтронов.

Литература

1. С.А. Куликов, Е.П. Шабалин. Сравнение эффективности материалов холодных замедлителей нейтронов для реактора ИБР-2. Сообщение ОИЯИ Р17-2005-222.
2. S. Kulikov, E. Shabalin. Complex of neutron moderators for the IBR-2M reactor . In: Proceedings of 17th Meeting of the International Collaboration on Advanced Neutron Sources, ICANS-XVII. April 25-29, 2005. Santa Fe, New Mexico.
3. S. Kulikov, E. Shabalin. New complex of moderators for condense matter research at the IBR-2M reactor. Romanian Journal of Physics, ISSN:1221-146X, Изд:Publishing House of the Romanian Academy, V.54, 3-4, January.2009
4. Е.П. Шабалин, С.А. Куликов, В.В. Мелихов. Study of fast neutron irradiation effects in cold moderator materials. Письма в ЭЧАЯ N5 [114] 2003 стр. 82-88.
5. Е.П. Шабалин, Е.Н. Кулагин, С.А. Куликов, В.В. Мелихов Радиационные эксперименты с водородсодержащими материалами на криогенной облучательной установке УРАМ-2 реактора ИБР-2. Атомная Энергия т. 97, вып. 3, стр. 183-189, 2004
6. И. М. Баранов, И.И. Воронин, В.Г. Ермилов, Е.Н. Кулагин, С.А. Куликов, В.В. Мелихов, Р.Г. Пушкарь, Ро Ду Мин, Д.Е. Шабалин, Е.П. Шабалин. Изучение процесса выхода радиолитического водорода из экспериментального элемента холодного замедлителя на твердом мезитилене. Сообщения ОИЯИ, Р3-2004-212 (2004)
7. Е.Н. Кулагин, С.А. Куликов, В.В. Мелихов, Е.П. Шабалин. Radiation effects in cold moderator materials: Experimental study of accumulation and release of chemical energy. Nuclear Inst. and Methods in Physics Research, B, 215, (2004), 181-186.
8. С.А. Куликов, И.В. Калинин, В.М. Морозов, А.Г. Новиков, А.В. Пучков, А. Н. Черников, Е.П. Шабалин. Измерение спектров холодных нейтронов на макете криогенного замедлителя реактора ИБР-2. Письма в ЭЧАЯ, 2010. Т.7, №1 (157), с.95-100.
9. Е. П. Шабалин. О нерегулярности движения шара при пневмотранспорте в трубе. Сообщение ОИЯИ Р 3-2008-67, 12 стр.
10. Е.Н. Кулагин, С.А. Куликов, Д.Е. Шабалин, Е.П. Шабалин, О.Г. Бузыкин, А.В. Казаков. О пневмотранспортировке твердых шариков холодного замедлителя нейтронов. Сообщение ОИЯИ Р13-2008-116, 16 стр.
11. М.В.Булавин, Е.Н.Кулагин, С.А.Куликов, К.А.Мухин, Д.Е.Шабалин, Е.П.Шабалин. Моделирование пневмотранспорта твердых шариков холодного замедлителя нейтронов: распределение скорости и времени движения.. Сообщение ОИЯИ, Р13-2009-72, 16 стр.

EPITHERMAL NEUTRON ACTIVATION ANALYSIS OF THE ASIAN HERBAL PLANTS

Baljinnyam N., Jugder B[1]., Norov N[2]., Frontasyeva M.V., Ostrovnaya T.M., S.S. Pavlov

Frank Laboratory of Neutron Physics, JINR, Dubna
[1]Medical college "Monos", Ulaanbaatar, Mongolia
[2]Centre of Nuclear Research, NUM, Ulaanbaatar, Mongolia

Introduction

Herbal medicines are the staple of medical treatment in many civilizations including those of Africa, China, Egypt, India, Latin America and others (Steiner., R. P. 1986). According to the World Health Organization (WHO) estimates, 70% of the world population use herbal medicines and herbal products for primary health care (British Medical Association., 1993). Thousands of plants are used for curing various diseases in Mongolia. The larger part of treatment in Mongolian Traditional Medicine is medication. Mongolia has over 600 types of medical plants so far discovered. In addition Mongolia imports more than 100 components of traditional medicine from China and the Russian Federation (Ligaa. U., et.al., 1997).

Neutron activation analysis is a very convenient method for analyzing trace elements in all types of samples, including herbal medicine. Examples of recent work on the use of the technique are 28 elements in medicinal herbs (Sarmani S., et.al., 1998), 6] 12 elements in Chinese medicinal herbs (Yamashita C. I. et.al., 2005).

The present study was undertaken to investigate the elemental contents in 2 types of medicinal herbs commonly used in controlling and healing of different diseases.

Asian medicinal herbs Chrysanthemum (*Spiraea aquilegifolia* Pall.) and Red Sandalwood *(Pterocarpus Santalinus*) are widely used in folk and Ayurvedic medicine for healing and preventing some diseases. The modern medical science has proved that the Chrysanthemum (*Spiraea aquilegifolia* Pall.) possesses the following functions: reducing blood press, dispelling cancer cell, coronary artery's expanding and bacteriostating and Red Sandalwood *(Pterocarpus Santalinus*) is recommended against headache, toothache, skin diseases, vomiting and sometimes it is taken for treatment of diabetes. Species of Chrysanthemums were collected in the north-eastern and central Mongolia, and the Red Sandalwood powder was imported from India. Samples of Chrysanthemums (branches, flowers and leaves) (0.5 g) and red sandalwood powder (0.5 g) were subjected to the multi-element instrumental neutron activation analysis using epithermal neutrons (ENAA) at the IBR-2 reactor, Frank Laboratory of Neutron Physics (FLNP) JINR, Dubna. A total of 41 elements (Na, Mg, Al, Cl, K, Ca, Sc, V, Cr, Mn, Fe, Co, Ni, Zn, As, Se, Br, Rb, Sr, Zr, Mo, Cd, Cs, Ba, La, Hf, Ta, W, Sb, Au, Hg, Ce, Nd, Sm, Eu, Tb, Dy, Yb, Th, U, Lu) were determined. For the first time such a large group of elements was determined in the herbal plants used in Mongolia. The quality control of the analytical results was provided by using certified reference material Bowen Cabbage.

Experimental

Sample collection and preparation

Species of Chrysanthemums were collected in the north-eastern and central Mongolia, and the Red Sandalwood powder was imported from India. In the laboratory the sample of Chrysanthemums was cleaned from extraneous plant materials and dried to constant weight at 30^0-40^0 for 48 hours. The samples were not washed and not homogenized.

Chrysanthemum (*Spiraea aquilegifolia* Pall.)

Red Sandalwood *(Pterocarpus Santalinus*)

Analysis

The concentration of elements in the herbal plant samples was determined by a multi-element instrumental neutron activation analysis using epithermal neutrons (ENAA) at the IBR-2 reactor, FLNP JINR, Dubna (Frontasyeva M.V. et. al., 2000). To carry out ENAA investigations, plant samples of 0.5 g were heat-seated in polyethylene foil bags and packed in aluminum cups for short and long irradiation, respectively. The processing of the data and determination of the concentrations of elements were performed using certified reference materials and flux comparators with the help of the software developed in FLNP, JINR (Ostrovnaya T. M., et. Al., 1993)

Results and discussion

The concentrations of 41 elements were determined in 2 medicinal herbs samples using INAA. For the first time such a large group of elements was determined in the herbal plants used in Mongolia. The quality control of the analytical results was provided by using certified reference material Bowen Cabbage. The results obtained are compared to the "Reference plant" (B. Markert, 1992) data and interpreted in terms of excess of such elements as Se, Cr, Ca, Fe, Ni, Mo, and rare earth elements.

Conclusion

The data obtained in the present work are important for synthesis of new herbal drugs which can be used for the control and cure of various diseases. In order to develop a stronger basis for appreciating the curative effects of medicinal plants, there is a need to investigate their elemental content. It has been demonstrated that INAA with its multi-elemental characterization over a wide range of concentrations, blank free-nature and minimum sample preparation is the ideal analytical technique for such studies.

The authors acknowledge the financial assistance of the RFBR-Mongolia grant 08-05-90214-Mong_a.

References:

British Medical Association, Complementary Medicine: New Approaches to Good Practice, Oxford University Press, Oxford, 1993.

Frontasyeva M. V., Pavlov S. S., Analytical Investigations at the IBR-2 Reactor in Dubna, JINR Preprint, E14-2000-177, Dubna, 2000.

Ligaa U., et.al., Methods of uses of medicinal plants in Mongolian Traditional medicine and prescriptions. Artist Publishing, Ulaanbaatar: 1997, p. 9–10.

Markert B. Establishing of "Reference plant" for inorganic characterization of different plant species by chemical fingerprinting, // J. Water, Air, and Soil Pollution, Vol. 64, 1992, p. 533-538.

Ostrovnaya T. M., Nefedyeva L. S., Nazarov V. M., Borzakov S.B., Strelkova L. P., Software for INAA on the Basis of Relative and Absolute Methods Using Nuclear Data Base, Activation Analyisi in Enviroment Protection, D-14-93-325, Dubna, 1993, 319-326.

Sarmani S., Abugassa I., Hamzan A., // J. Radioanal. Nucl. Chem., 234, 1998, p. 17.

Steiner R. P. (Ed.) Folk Medicine – The Art and the Science, American Chemical Society, Washington DC, 1986, p. 223.

Yamashita C. I., Saiki M., Vasconcellos M. B. A., Sertie J. A. A., // J. Appl. Rad. Isotopes, 63, 2005, p. 841.

RADIOMETRY OF ^{137}CS AND ^{210}PB IN MOSS FROM BELARUS

Aleksiayenak Yu. V.[1], Frontasyeva M.V.[1], Florek M.[2], Faanhof A.[3]

[1]Frank Laboratory of Neutron Physics, Joint Institute for Nuclear Research, Dubna, Russia,
[2]Dept.of Nuclear Physics and Biophysics, Comenius University, Bratislava, Slovakia,
[3]South African Nuclear Energy Corporation, Pretoria, Republic of South Africa

Introduction

Mosses have been extensively used to study atmospheric deposition of trace metals on the European scale (Harmens et al, 2010), and they are equally suitable indicators of airborne radionuclides (Mattson, 1972; Sumerling, 1984; Barci-Funel, 1992; Steinnes and Njåstad, 1993; Nifontova, 1996, 1998; Sawidis, 1997; Florek, 2001; Popovic, 2008; Cevik and Celik, 2009). The south-eastern part of Belarus was severely contaminated with fallout from the 1986 accident at the Chernobyl nuclear power plant. About 70% of the total radioactive fallout occurred on Belarus territory (Kenik, 1995). Soil contamination with ^{137}Cs, ^{90}Sr and ^{239}Pu is still high, and eight years after the accident 2,640 km^2 of agricultural land was still excluded from use. Within the 40-km radius of the power plant, 2,100 km^2 of land in the Poles'e state nature reserve has been excluded from use for an indefinite period of time. Vast territories in the Gomel and Mahilyow regions were rendered uninhabitable. Roughly 7,000 km² of soil were contaminated by ^{137}Cs to levels greater than 550 GBq/km², i.e. inaccessible for human usage for a very long time. In 1995 the areas contaminated to ^{137}Cs levels exceeding 37 GBq/km² (1 Ci/km²) constituted about 23% of the country (IAEA, 2006) and in 2002 more than 1.5 million people still lived in this area.

Experimental

Sampling and sample preparation. Sixty-three samples of the moss species *Hylocomium splendens* and *Pleurozium schreberi* were collected in Belarus (Fig. 1) in order to study deposition of airborne radionuclides.

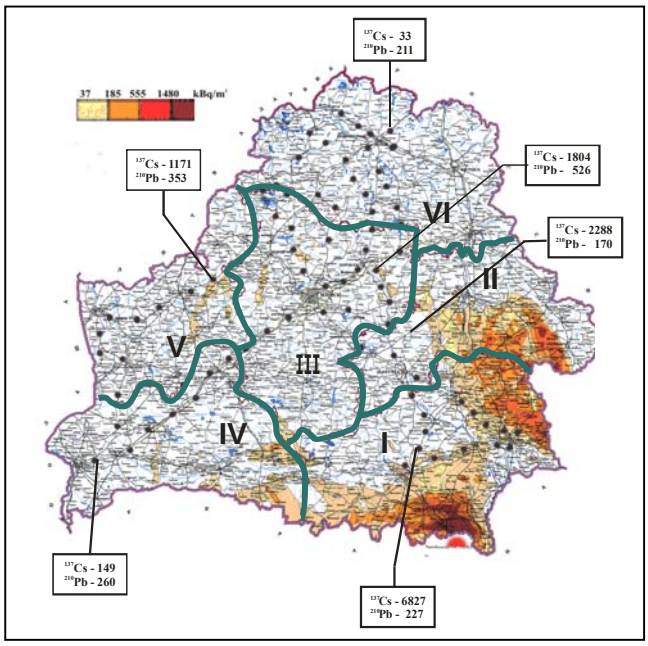

Fig. 1. Map of ^{137}Cs contamination in Belarus in 2004. with sampling sites. Maximum concentrations (Bq/kg) in different regions are given in squares

The sampling network in Belarus covers strongly contaminated (Gomel and Mahilyow) as well as relatively "clean" (Minsk, Grodno, Vitebsk) regions. Samples were dried and then pelletized prior to activity measurements. Sample weight of sample was typically around 17 gram, cylindrical geometry with height ca. 2–3 cm, and diameter about 7 cm.

Measurements. Gamma spectrometry on the moss samples was performed in the low-level background counting laboratory of the Department of Nuclear Physics and Biophysics of the Comenius University in Bratislava, Slovakia, using a Canberra

HPGe detector (177 cm^3) with a carbon window, placed in a low-level background shield. The measuring time was 24 hours or more. The counting statistics was less than 3%. The total uncertainty in determination of radionuclide activities was estimated at 15% or less. A limited suite of samples was also measured at the South African Nuclear Energy Corporation (SANEC) using an ultra low level background counting facility (160 cm3 n-type HPGe Canberra BE5030 detector mounted in a lead shield of 13 cm lead of less than 50 Bq/kg and another layer of 2 cm less than 10 Bq/kg lined with 1 mm cadmium, 2 mm copper and 4 mm Perspex). Measuring time was one hour. Data obtained in the two laboratories for samples from two localities in Belarus was compared and the results appear to be in agreement within experimental errors.

Results and Discussion

In Belarus the maximum activity of ^{137}Cs (6827 Bq/kg) was observed in the Gomel Region near the town Mazyr and the minimum one (4,83 Bq/kg) in Vitebsyevskii Region near Luzhki-Yazno. "Hot spots" were observed near town of Borisow and Yuratsishki. The ^{137}Cs activity in the moss presumably reflects the initial deposition of ^{137}Cs fallout from the Chernobyl accident. The obtained results support previous data showing particularly high deposition of ^{137}Cs in the Gomel and Mahilyow Regions from the Chernobyl accident (IAEA, 2006). Most radionuclides, deposited on soil, are located in its top layers. ^{137}Cs migration deep into the soil occurs very slowly. The median value of concentrations of ^{137}Cs in the samples from Gomel and Mahilyow regions are in ten-twenty times higher compared to other Belarus regions. The main reason why the moss samples still reflect the original distribution of Chernobyl fallout in Belarus is probably that Cs migrates progressively from the older to the younger shoots, as shown in studies of moss samples exposed to Chernobyl fallout in Norway (Gaare and Steinnes, 1996).

The results obtained in the present study confirm the spatial distribution of ^{137}Cs in Belarus due to fallout from the Chernobyl accident.

The median value of ^{137}Cs concentrations in moss samples from Gomel and Mahilyow regions are more ten times higher than present values from other Belarus regions and literature values from the outside territories (see Fig. 2) where corresponding studies have been carried out. The minimum concentrations in Belarus however are similar to those reported from the other studies. The concentrations of ^{210}Pb in moss samples collected over the territory of Belarus vary within the range 141–575 Bq/kg with a median value of 312 Bq/kg. In comparison with concentration of ^{137}Cs the range is narrow, and

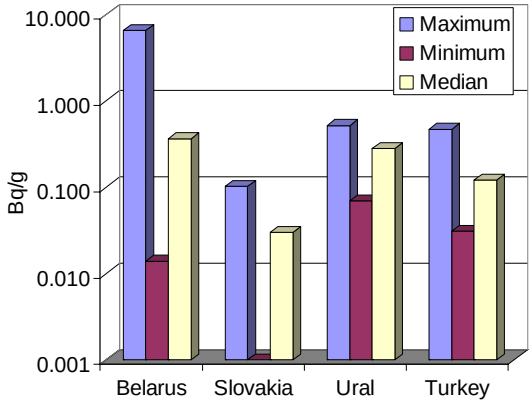

Fig. 2. Comparison of ^{137}Cs concentration in moss from different countries

differences between regions are small from region to region.

References

Barci-Funel, G., Dalmasso, J., Ardisson, G., 1992. Deposition of long-lived radionuclides after the Chernobyl accident in the forestal massif of Boreon. J. radioanal. nucl. chem. 164, 157-169

Berg, T., Steinnes, E., 1997. Use of mosses (Hylocomium splendens and Pleurozium schreberi) as biomonitors of heavy metal deposition: from relative to absolute values. Environmental Pollution. 98, 61-70.

Cevik, U., Celik, N., 2009. Ecological half-life of ^{137}Cs in mosses and lichens in the Ordu province, Turkey by Cevik and Celik. J. Environ. Radioact. 100, 23-28.

Florek, M., Frontasyeva, M., Mankovska, B., Oprea, K., Pavlov, S., Steinnes, E., , 2001. Air pollution with heavy metals and radionuclides in Slovakia studied be the moss biomonitoring technique. ISINN-9, 442-449.

Gaare, E., Steinnes, E., 1996. Use of the moss Hylocomium splendens for the mapping of radiocaesium fallout from the atmosphere. Proceedings, Nordic Radioecology Seminar, Reykjavik, 26-29 August, 367-370.

Harmens, H. et al., 2010. Mosses as biomonitors of atmospheric heavy metals deposition: Spatial patterns and temporal trends in Europe. Environmental Pollution. 158, 3144-3156.

IAEA, 2006. International Atomic Energy Agency, Environmental Consequences of the Chernobyl Accident and their Remediation: Twenty Years of Experience. Report of the UN Chernobyl Forum Expert Group "Environment". In: Radiological Assessment Reports Vienna.

Kenik, I., 1995. Belarus: a small country faces 70 percent of the fallout. DHA News. September-October, 7-8

Kulan, A., 2006. Seasonal ^{7}Be and ^{137}Cs activities in surface air before and after the Chernobyl event. Journal of Environmental Radioactivity. 90, 140-150.

Mattsson, S., 1972. Radionuclides in Lichen, Reindeer and Man. Lund, 48.

Nifontova, M., 1996. Mushrooms, lichens and mosses as biological indicators of radioactive environmental contamination. Radioecology and the restoration of radioactive-contaminated sites. 155-162.

Nifontova, M., 1998. Content of long-lived artificial radionuclides in moss-lichens cover of terrestrial ecosystems of the Ural-Siberian Region. Ecology 3, 196-200 (in Russian).

Popovic, D. et al, 2008. Radionuclides and heavy metals in Borovac, Southern Serbia. Environ. Sci. Pollut. Res. 15, 509-520.

Povinec, P., Chudy, M., Sýkora, I., Szarka, J., Pikna, M., Holý, K., 1988. Aerosol radioactivity monitoring in Bratislava following the Chernobyl accident. J. Radioanal. Nucl. Chem. Letters 126/6, 467-478.

Sawidis, Th., Heinrich, G., Chettri, M., 1997. Cesium-137 monitoring using mosses from Macedonia, N. Greece. Water, Air and Soil Pollution. 110, 171-179.

Steinnes, E., Njåstad, O., 1993. Use of mosses and lichens for regional mapping of ^{137}Cs fallout from the Chernobyl accident. J. Environ. Radioact. 21, 65-73.

Sumerling, T., 1984. The use of mosses as indicators of airborne radionuclides near a major nuclear installation. The Science of the Total Environment. 35, 251-265.

UNSCEAR, 1982. United Nations Scientific Committee on the Effects of Atomic Radiation Report. Ionizing Radiation: Sources and Biological Effects, United Nations, New York.

5. PUBLICATIONS

DEPARTMENT OF NEUTRON INVESTIGATION OF CONDENSED MATTER

1. Atomic and magnetic structures (diffraction)

1. Burzo, E. et al. Magnetic and magnetocaloric properties of some ferrimagnetic compounds // J. of Optoelectronics & Adv. Mat. 2010. V. 12, pp. 1105-1113.
2. Cornei, N. et al. Electronic phase diagram of $La_{0.54}Sm_{0.11}Ca_{0.35}Cu_xMn_{1-x}O_3$ manganites // J. of Optoelectronics & Adv. Mat. 2010. V. 12 (4), pp. 872-875.
3. Craus, M.-L. et al. Influence of Na and Cr substitutions on electronic phase diagram of $La_{0.54}Ho_{0.11}Ca_{1-x}Na_xMn_{1-y}Cr_yO_3$ manganites // Romanian Reports in Physics. 2010. V. 62 (4), (in press).
4. Craus, M.-L. et al. Influence of Co on transport properties of $La_{0.54}Ho_{0.11}Sr_{0.35}Co_xMn_{1-x}O_3$ manganites // J. of Optoelectronics & Adv. Mat. 2010. V. 12 (4), pp. 868-871.
5. Dobrea, V. et al. Some physical properties of Ni_2MnGa Heusler shape memory alloys with substitutions // J. of Optoelectronics & Adv. Mat. 2010. V. 12 (4), pp. 854-857.
6. Golosova, N. O. et al. Effect of high pressure on the crystal and magnetic structures of $La_{0.5}Ca_{0.5}CoO_3$ cobaltite // JETP Letters. 2010. V. 92, pp. 110-114. (Голосова Н. О. и др. Влияние высокого давления на кристаллическую и магнитную структуру кобальтита $La_{0.5}Ca_{0.5}CoO_3$ // Письма в ЖЭТФ. 2010. Т. 92 (2), с. 114–118).
7. Gonchar', L. É. et al. Effect of pressure on the magnetic properties of lanthanum manganite // JETP. 2010. V. 111, pp. 194-198. (Гончарь, Л. Э. и др. Влияние давления на магнитные свойства манганита лантана // ЖЭТФ. 2010. Т. 138, с. 221-225).
8. Kozlenko, D. P. et al. Structural and magnetic phase transitions in $Pr_{0.15}Sr_{0.85}MnO_3$ at high pressure // Eur. Phys. J. B. 2010. V. 77, V. 3, pp. 407-411.
9. Kozlenko, D. P. et al. Competition between ferromagnetic and antiferromagnetic ground states in multiferroic $BiMnO_3$ at high pressures // Phys. Rev. B. 2010. V. 82, pp. 014401.
10. Kozlenko, D. P. et al. Spin fluctuations and structural modifications in frustrated multiferroics RMnO3 (R = Y, Lu) at high pressure // High Pressure Research. 2010. V. 30 (2), pp. 252-257.
11. Lushnikov, S. et al. Structure of Thermally Desorbed $CeNi_3$-Based Hydrides // Inorganic Materials. 2010. V. 46, No. 8, pp. 836-841. (Лушников, С. А. и др. Структура термодесорбированных гидридов на основе $CeNi_3$ // Неорг. Материалы. 2010. Т. 46 (8), с. 932-938).
12. Pomjakushin, V. Yu. et al. Evidence for strong effect of quenched correlated disorder on phase separation and magnetism in $(La_{1-y}Pr_y)_{0.7}Ca_{0.3}MnO_3$ // J. Phys.: Condens. Matter. 2010. V. 22, pp.115601 (1-5).
13. Бескровный, А. И. и др. Температурные зависимости параметра порядка для нитрита натрия, внедренного в пористые стекла и опалы // Физика твердого тела. 2010. Т. 52 (5), с. 1021-1025.
14. Козленко, Д. П. и др. Структурные и магнитные фазовые переходы в Pr0.7Ca0.3MnO3 при высоких давлениях // Письма в ЖЭТФ. 2010. Т. 92, с. 654-658.

2. Nanostructured materials (small-angle scattering)

15. Белушкин, А. В. и др. Исследование структурных аспектов формирования оптических свойств наносистемы GeO2−Eu2O3−Ag // Физика твердого тела, 2010. Т. 52 (7), с. 1278-1284. (Belushkin, A. V. et al. Investigation of the structural aspects in the formation of optical properties of the GeO2-Eu2O3-Ag nanosystem // Phys. Solid State. 2010. Vol. 52. (7), pp. 1366-1371).
16. Rajewska, A. Aggregation in heavy water micellar dilutes solutions of three nonionic classic surfactants C10E7 and C12E7 and C14E7 study by SANS method // AIP Conference Proceedings. 2010. V. 1202, pp. 171-174.
17. Кривандин, А. В. и др. Исследование структуры альфа-кристаллина методом малоуглового рассеяния нейтронов с вариацией контраста // Сообщения ОИЯИ, 2010. Р14-2010-65.
18. Balasoiu, M. et al. Particle Concentration Effects on the Ferrofluids based Elastomers Microstructure // J. of Industrial and Engineering Chemistry. 2010 (in press).
19. Balasoiu, M. et al. Magnetic field and particle concentration competitive effects on ferrofluid based silicone elastomer microstructure // J. of Crystallography Reports. 2010 (in press).
20. Balasoiu, M. et al. Structural investigation of biogenic ferrihydrite nanoparticles dispersion // J. of Optoelectronics & Adv. Mat.: Rapid Communications. 2010. V. 4 (12), pp. 2136-2139.
21. Balasoiu, M. et al. Structural investigation of biogenic ferrihydrite nanoparticles dispersion // Preprint JINR, 2010. E14-2010-148.
22. Belushkin, A. V., Kozlenko, D. P. Structural organization of nanomaterials and nanosystems: neutron scattering insight // Adv. Nat. Sci.: Nanosci. Nanotechnol. 2010. V. 1, pp. 023002 (8).
23. Cherny, A. Yu. et al. Scattering from generalized Cantor fractals // J. Appl. Cryst. 2010. 43, pp. 790–797.
24. Kuklin, A. I. et al. Do the size effects exist // Rom. J. Phys. 2011. V. 56 (1–2) (in press).
25. Stan, C. et al. Preliminary Investigations on Fe3O4-Ferrofluids at Different Temperatures by Means of Magnetic Measurements // U. P. B. Sci. Bull. 2010 (in press)
26. Белушкин, А. В. и др. Исследование структурных аспектов формирования оптических свойств наносистемы GeO2-Eu2O3-Ag // Препринт ОИЯИ, 2010. Р14-2009-165.
27. Черный, А. Ю. и др. Малоугловое рассеяние на детерменированных фрактальных системах // Поверхность. Рентгеновские, синхротронные и нейтронные исследования. 2010. №11, с. 35-39. (Cherny, A. Yu. et al. Small angle scattering from deterministic fractal systems // J. of Surface Investigations, X-ray, Synchrotron & Neutron Techniques, 2010. V. 4 (6), pp. 903-907).

3. Soft matter, liquids (small angle scattering and diffraction)

28. Avdeev, M. V. et al. Structure of water-based ferrofluids with sodium oleate and polyethylene glycol stabilization by small-angle neutron scattering: contrast-variation experiments // J. Appl. Cryst. 2010. V. 43. pp. 959–969.
29. Avdeev, M. V. et al. Structure and in Vitro Biological Testing of Water-Based Ferrofluids Stabilized by Monocarboxylic Acids // Langmuir. 2010. V. 26, pp. 8503–8509.
30. Avdeev, M. V. et al. On structural features of fullerene C60 dissolved in carbon disulfide: Complementary study by small-angle neutron scattering and molecular dynamic simulations // J. Chem. Phys. 2010. V. 132, pp. 164515.
31. Balasoiu, M. et al. Microstructure of stomaflex based magnetic elastomers // Phys. Solid State. 2010. V. 52, pp.917-921.
32. Balasoiu, M. et al. Hierarchical structure investigations of biogenic ferrihydrite samples // Rom. J. Phys. 2010. V. 55 (7-8), pp. 782-789
33. Balgavý, P. et al. Why and How to Measure Lipid Bilayer Thickness, in Advances in Medicine and Biology / Ed. by Berhardt, L. V. 2010. V. 4.
34. Bulavin, L. A. et al. Structure transformations in the triple liquid system tetradecyltrimethylammonium bromide-D2O-NaBr // Ukr. J. Phys. 2010. V. 55 (4), pp. 410-414.
35. Bulavin, L. A. et al. Neutron studies of the NaBr impurity influence on micelle formation in the heay water-tetradecyltrimethylammonium bromide systems // Ukr. J. Phys. 2010. V. 55 (3), pp. 288-292.
36. Gallová, J. et al. Influence of cholesterol and β-sitosterol on structural characteristics of the EYPC bilayers // J. Membr. Biol. 2010 (in press).
37. Kyrey, T. O. et al. Study of solvatochromism in liquid fullerene containing systems of various polarity // Bulletin of the University of Kyiv Series: Physics & Mathematics. 2010, in Ukrainian (in press).
38. Kyzyma, O. A. et al. Solvatochromism and Fullerene Cluster Formation in C60/N-methyl-2-pyrrolidone // Fullerenes, Nanotubes, and Carbon Nanostructures. 2010. V. 18, pp.458-461.
39. Kyzyma, O. A. et al. Aggregate development in C60/N-metyl-2-pyrrolidone solution and its mixture with water as revealed by extraction and mass spectroscopy // Chem. Phys. Lett. 2010. V. 493, pp. 103–106.
40. Lancz, G. et al. SANS study of poly(ethylene glycol) solutions in D2O // Acta Phys. Polonica. 2010. V. 118 (5), pp. 980-982.
41. Nagornyi, A. et al. Determination of optimal conditions for experiment of small-angle neutron scattering on ferrofluids with a low concentration of magnetite // Bulletin of University of Kyiv Series: Physics & Mathematics. 2010, in Ukrainian (in press).
42. Petrenko, V. I. et al. Micelle formation in aqueous solutions of dodecylbenzene sulfonic acid studied by small-angle neutron scattering // Coll. Surf. A. 2010. V. 369, pp. 160–164.
43. Petrenko, V. I. et al. The interaction of long-chain n-alcohols with fluid lipid DOPC bilayers: a neutron diffraction study. // General Physiology and Biophysics. 2010, V. 29, pp. 355-361.
44. Raikher, Yu. L. et al. Magnetic properties of biomineral nanoparticles produced by Klebsiella oxytoca bacteria // Phys. Solid State. 2010. V. 52 (2), pp. 277-284.
45. Ryabova, N. Y. et al. Investigation of stratum corneum lipid model membranes with free fatty acid composition by neutron diffraction // European Biophysics J. 2010. V. 39, pp. 1167-1176.
46. Tomchuk, O. V. et al. Small-angle neutron scattering by fractal clusters in water suspensions of detonation nanodiamonds // Bulletin of the University of Kyiv Series: Physics & Mathematics. 2010, in Ukrainian (in press).
47. Tropin, T. V. et al. Nucleation theory models for describing kinetics of cluster growth in C60/NMP solutions // Phys. Status Solidi B. 2010. V. 247 (11-12), pp. 3022-3025.
48. Tropin, T. V. et al. On the dependence of the properties of glasses on cooling and heating rates // J. Non-Cryst. Solids. 2010 (in press).
49. Závišová, V. Et al. Biocompatible magnetic fluid stabilized with poly (ethylene glycol) // J. Magn. Magn. Mater. 2010 (in press).
50. Авдеев, М. В. и др. Нейтронография наносистем // Энциклопедия ЮНЕСКО «Нанонаука и Нанотехнологии». 2010. С. 804-837.
51. Авдеев, М. В. и др. Малоугловое рассеяние нейтронов в структурных исследованиях магнитных жидкостей. // Обзор УФН. 2010. Т. 180 (10), с. 1009-1034. (Avdeev, M. V. et al. Small-angle neutron scattering in structure research of magnetic fluids // Review. Phys. Uspekhi. 2010 (in press).
52. Авдеев, М. В. и др. Модели кластерообразования фуллеренов в растворах // Обзор. Ж. Физ. Химии. 2010. Т. 84 (8), с. 1405-1416. (Avdeev, M. V. et al. Models of fullerene cluster formation in solutions // Rus. J. Phys. Chem. A. V. 84(8). 2010, pp.1273-1283).
53. Авдеев, М. В. и др. Исследование микроструктуры активированных углей методом малоуглового рассеяния медленных нейтронов // ФТТ. 2010. Т. 52 (5), с. 923. (Avdeev, M. V. Et al. Investigation of the microstructure of activated carbons by the small-angle slow neutron scattering method // Phys. Solid State. 2010. V. 52 (5), pp. 985-987).
54. Аксенов, В. Л., Киселев, М. А.. Дополнительность нейтронных и синхротронных структурных исследований в реальном времени: применение в молекулярной биологии // Кристаллография. 2010. Т. 55 (7). (в печати) (Aksenov, V. L, Kiselev, M. A. Complementarity of neutron and synchrotron structural research in real time: applications for molecular biology // Cryst. Reports. 2010 (in press).
55. Аксенов, В. Л. и др. К вопросу об образовании кластеров фуллерена С60 в азот-содержащих растворителях // Физ. Тверд. Тела. 2010. Т. 52, с. 992-995 (Aksenov, V. L. et al. Formation of C60 Fullerene Clusters in Nitrogen-Containing Solvents // Phys. Solid State. 2010. V. 52 (5), pp. 1059–1062).
56. Булавін, Л. А. и др. Комплексне дослідження міцелоутворення в водній системі з катіонним ПАР // Доповіді національної академії наук України, ISSN:1025-6415.
57. Исаев-Иванов, В. В. и др. Сравнительный анализ нуклеосомной структуры клеточных ядер – малоугловое нейтронное рассеяние // Физика Твердого Тела. 2010. Т. 52 (5), с. 996-1005. (Isaev-Ivanov V.V. et al. Comparative Analysis of the Nucleosome Structure of Cell Nuclei by Small-Angle Neutron Scattering // Physics of the Solid State. 2010. V. 52 (5), pp. 1063–1073).
58. Киселев, М. А. и др. Структурные исследования липидных мембран на синхротронном источнике СИБИРЬ-2 // Кристаллография. 2010. Т. 55 (3), с. 500-506. (Kiselev, M. A. et al. Structural Studies of the Lipid Membranes at the Siberia-2 Synchrotron Radiation Source // Cryst. Reports. 2010. V. 55 (3), pp. 466-472).
59. Киселев, М. А. Методы исследования липидных наноструктур на нейтронных и синхротронных источниках

// ЭЧАЯ. 2010 (принято в печать).

60. Кривандин, А. В. и др. Исследование структуры α-кристаллина методом малоуглового рассеяния нейтронов с вариацией контраста // Биохимия. 2010. Т. 75 (11), с.1499-1507

61. Нагорный, А. В. и др. Анализ малоуглового рассеяния нейтронов на сильно разбавленных магнитных жидкостях // Поверхность. Рентгеновские, синхротронные и нейтронные исследования. 2010 (принято в печать).

62. Петренко, В. И. и др. Анализ структуры водных феррожидкостей методом малоуглового нейтронного рассеяния // Физ. Тверд. Тела. 2010. Т. 52 (5). с. 913–916. (Petrenko, V. I. et al. Analysis of the Structure of Aqueous Ferrofluids by the Small-Angle Neutron Scattering Method // Phys. Solid State. 2010. V. 52 (5), pp. 974–978.)

63. Порохова, А. В. и др. Модуляция размера наномагнетита с покрытием монокарбоновыми кислотами, диспергированного в неполярный растворитель // Известия вузов. Серия физическая. 2010. Т. 53 (3/2), с.176-179.

64. Рогачев, А. В. и др. Структура кремнийорганических дендримеров высоких генераций // Физика Твердого Тела. 2010. Т. 52 (5), с. 979-983. (Rogachev, A. V. et al. Structure of Organosilicon Dendrimers of Higher Generations // Phys. Solid State. 2010. V. 52 (5), pp. 1045–1049).

65. Рябова, Н. Ю. и др. Влияние холестерина и церамида-VI на структуру многослойных липидных мембран при водном обмене // Кристаллография. 2010. Т. 55 (3), с. 516-525. / Ryabova, N. Yu. et al. Influence of Cholesterol and Ceramide VI on the Structure of Multilamellar Lipid Membranes at Water Exchange // Cryst. Reports. 2010. V. 55 (3), pp. 479-487.

66. Рябова, Н. Ю. и др. Исследование структуры многослойных липидных мембран методом дифракции нейтронов в реальном времени // Физика твердого тела 2010. Т. 52 (5), с. 984-991. (Ryabova, N. Y. et al. Investigation of the Structure of Multilayer Lipid Membranes by Real-Time Neutron Diffraction // Phys. Solid State. 2010. V. 52 (5), pp. 1050-1058).

67. Рябова, Н. Ю. и др. Структура и гидратация модельных липидных мембран на основе церамида-6. Исследования методом дифракции нейтронов в реальном времени // Дис. канд. физ.-мат. наук: 01.04.07. – Дубна: ОИЯИ. 2010. 130 с.

68. Соловьёв, Д. В. и др. Рентгенографические и P–V–T исследования системы вода–димиристоилфосфатидилхолин // Поверхность. Рентгеновские, синхротронные и нейтронные исследования. 2010 (принято в печать).

4. Thin films (reflectometry, polarized neutrons)

69. Aksenov, V. L., Khaidukov, Yu. N., Nikitenko, Yu. V., Peculiarities of magnetic states in “Ferromagnet-Superconductor” heterostructures due to proximity effects // J. Phys.: Conference Series. 2010, V. 211, pp. 012022-012027.

70. Bodnarchuk, I., et al. On the effect of gravity on the resolution for time-of-flight specular neutron reflectivity. // Nucl. Instr. Methods A, 2010 (in press).

71. Bryk, V., Goncharov, A., Grigorova, T., et al. Formation mechanism, structure and adsorption characteristics of microporous nanocrystalline (V,Ti)-N-He thin film composites // J. of Surface Investigations, X-ray, Synchrotron and Neutron Techniques. 2010 (in press).

72. Ignatovich, V. K., Nikitenko, Yu. V., Fraerman, A. A..Transport of Polarized Neutrons through Magnetic Noncoplanar Layered Systems // J. of Experimental and Theoretical Physics, 2010. V. 110 (5), pp. 775-782.

73. Ignatovich, V. K., Nikitenko, Yu. V., Radu, F. // Neutron refraction in oscillating magnetic field, NIM. 2010. V. 620, pp. 410-413.

74. Ignatovich, V. K., Nikitenko, Yu. V. A time-odd correlation in a neutron reflectometry experiment // J. of Experimental and Theoretical Physics. 2010, V. 110 (3), pp. 417-425.

75. Ignatovich, V. K., Nikitenko, Yu. V., Radu, F. Interaction of Neutrons with Layered Magnetic Media in Oscillating Magnetic Field // Physica B. 2010 (in press).

76. Khaidukov, Yu. N., Aksenov, V. L., Nikitenko, Yu. V., et. al. Magnetic Proximity Effects in V/Fe Superconductor/Ferromagnet Single Bilayer Revealed by Waveguide-Enhanced Polarized Neutron Reflectometry // J. Supercond. Nov. Magn. 2010 (in press).

77. Khaidukov, Yu. N., Nikitenko, Yu. V. Magnetic non-collinear neutron wave resonator. // NIM A. 2010, accepted.

78. Khaidukov, Yu. N., Nikitenko, Yu. V., Bottyan, L., et al. Feasibility of Study Magnetic Proximity Effects in Bilayer “Superconductir-Ferromagnet” Using Waveguide Enhanced Polarized Neutron Reflectometry // Cryst. Reports, 2010, V. 55 (7), pp. 1235-1241.

5. Atomic and magnetic dynamics (inelastic neutron scattering)

79. Goremychkin, E. A., Osborn, R., Sashin, I. L., et al. Transition from Heavy-Fermion to Mixed-Valence Behavior in Ce1-x YxAl3: A Quantitative Comparison with the Anderson Impurity” // Phys. Rev. Lett. 2010. V. 104, pp.176402.

80. Kazimirov, V. Yu., Smirnov, M. B., Bourgeois, L., et al. Lattice dynamics of Ni and Mg hydroxides // Solid State Ionics. 2010, V. 181, pp. 1764-1770.

81. Mielcarek, J., Nowak, D. M., Pajzderska, A., et al. A hybrid method for estimation of molecular dynamics of diazepam-density functional theory combined with NMR and FT-IR spectroscopy // Ind. J. Pharm. 2010 (in press).

82. Sawka-Dobrowolska, W., Bator, G., Sobczyk, L., et al. The (2:1) complex of picric acid with tetramethylpyrazine: The structure, IR spectra and tunnel splitting of methyl groups // J. Mol. Struct. 2010, V. 975, pp.298-302,

83. Благовещенский, Н. М., Морозов, В.А., Морозов, В. М., и др. Микродинамические особенности жидких металлов из экспериментов по нейтронному рассеянию. // Труды регионального конкурса научных проектов в области естественных наук на 2009, 2010, Вып. 15., с. 206-211.

84. Благовещенский, Н. М., Новиков, А. Г., Рожкова, Н. Н. Квазиупругое рассеяние нейтронов водной дисперсией наноалмазов // ФТТ. 2010, Т. 52 (5), с. 904.

85. Благовещенский, Н. М., Новиков, А. Г., Савостин, В. В. Коллективная микродинамика жидкого лития: исследование методом неупругого рассеяния нейтронов // ФТТ. 2010. Т. 52 (5), с. 908.

86. Дубовский, О. А., Орлов, А. В., Семенов, В. А. Солитонная микродинамика генерации зародышей новых фаз и структурных фазовых переходов в кристаллических материалах ядерных реакторов // Труды регионального конкурса научных проектов в области естественных наук. 2010. Вып.15, с. 88-92.

87. Калинин, И. В., Кац, Е., Коза, М., и др. Сосуществование сверхтекучего и твердого гелия в аэрогеле // ЖЭТФ. 2010, Т. 138 (2), с. 243-248

88. Калинин, И. В., Лаутер, В. В., Пучков, А. В. Исследование сверхтекучести в твердом гелии, помещенном в пористую среду // Труды регионального конкурса научных проектов в области естественных наук. 2010. Вып.15, с. 55-59.

89. Лисичкин, Ю. В., Новиков, А. Г., Сахарова, Л. А. Расчет характеристик рассеяния нейтронов водой, находящейся в околокритическом и сверхкритическом состояниях // Известия ВУЗов. Серия «Ядерная энергетика». 2010. Вып. 2, с. 23-37.

90. Мазитов, Р. М., Семенов, В. А., Лебедев, Ю. А., и др. Плотность фононных состояний наноструктурной меди // Письма в ЖЭТФ. 2010 (принято в печать).

91. Семенов, В. А., Козлов, Ж. А., Крачун, Л., и др. Спектр частот тантала при температурах 293-2300К // ФТТ. 2010. Т. 52 (5), с. 926.

92. Семенов, В. А., Козлов, Ж. А., Морозов, В. М., и др.. Неупругое рассеяние медленных нейтронов мононитридом урана при температурах 293 – 1273К // Препринт ФЭИ-3176, Обнинск, 2010, 12 с.

93. . Nowicka-Scheibe, J., Grech, E., Sawka-Dobrowolska, W., et al. Structure and vibrational spectra of squaric acid complexes with 4,4'- and 5,5'-dimethyl-2,2'-bipyridine // J. Mol. Struct. 2010. V. 976, pp. 30-35

6. Applied studies (texture, stresses, geological materials)

94. Bruno, G. et al. Micro and macroscopic thermal expansion of stabilized Aluminum Titanate // J. Europ. Ceramic Soc. 2010 (in press).

95. Bruno, G. et al. On the Stress free Lattice Expansion of Cordierite // Acta Mater. 2010. V. 58, pp. 1994-2003.

96. Frischbutter, A. et al. Neutron time-of-flight experiments with a composite from a tectonic thrust front - Residual strain-stress relations, depending on time, characterizing an othogneiss from the Penninian stack of nappes south of the Gotthard Massif (Laventina gneiss) // Z. geol. Wiss. 2010 (in press).

97. Lokajicek, T. et al. The determination of the elastic properties of an anisotropic polycrystalline graphite using neutron diffraction and ultrasonic measurements // Carbon. 2010 (in press).

98. Lychagina, T. A. et al. Texture investigation of Carrara marble // GeNF - Experimental Report. GKSS. 2010.

99. Matthies, S. On the combination of self-consistent and geometric mean elements for the calculation of the elastic properties of textured multi-phase samples // Solid State Phenomena. 2010. V. 160, pp. 87-93.

100. Mosch, S. Optimized extraction of dimension stone blocks // Environ Earth Sci, special issue. doi 10.1007/s12665-010-0825-7, 2010.

101. Nikitin, A. N., Vasin, R. N. A simultaneous application of neutron diffraction and acoustic emission methods for investigation of physical properties of rocks during polymorphic phase transitions // Neutron News. 2010. V. 21, (4), pp. 20-24.

102. Taran, Yu. V. et al. Residual stresses in biaxially fatigued austenitic stainless steel sample of cruciform geometry // PEPAN Letters (JINR). 2010 (in press).

103. Ullemeyer, K. et al. Evaluation of intrinsic velocity - pressure trends from low-pressure P wave velocity measurements in rocks containing microcracks. 2010 (in press).

104. Балагуров, А. М. и др. Определение тензора остаточных напряжений в сильно-текстурированном цилиндре из циркониевого сплава Э-110 методом дифракции нейтронов // Вопросы атомной науки и техники. 2010 (принято в печать).

105. Никитин, А. Н. и др. Распространение квазипродольных волн на границе раздела изотропной и анизотропной среды: теоретическое и экспериментальное исследование // Физика Земли. 2010 (принято в печать).

106. Никитин, А. Н. и др. Учет тепловых и транспортных свойств кристаллической соли при проектировании хранилищ радиоактивных отходов в галоидных формациях // Кристаллография. 2010. Т. 55 (3), с. 486-494.

107. Сумин, В. В. и др. Результаты измерения остаточных деформаций в корпусе реактора ВВЭР-1000 // Физика твёрдого тела. 2010. Т. 52 (5), с. 930–933.

7. Instruments and Methods

108. Avdeev, M. V. et al. Project of the new multifunctional reflectometer GRAINS with horizontal sample plane at the IBR-2M pulsed reactor in Dubna // J. Phys.: Conf. Ser. 2010. V. 251, pp. 012060.

109. Erhan, R. V. et al. A concept for the modernization of a SANS instrument at the IBR-2M pulsed reactor // Nuclear Instruments and Methods in Physics Research Section A: Accelerators, Spectrometers, Detectors and Associated Equipment, doi:10.1016/j.nima. 2010.

110. Gahramanov, I, Asgerov, E. Trace-map technique for the Pell sequence // Central European Journal of Physics (CEJP). 2010 (in press).

111. Kozhevnikov, S. V. et al. Combination of a reflectometer and a nonmagnetic waveguide for experiments with polarized neutron microbeam // Crystallography (in press).

112. Kozhevnikov, S. V. et al. Magnetic layered structure for the production of polarized neutron microbeams // Physica B. (in press).

113. Ott, F., Kozhevnikov, S. V. Off-specular data representations in neutron reflectivity // J. Appl. Cryst. 2010 (in press).

114. Балагуров, А. М., и др. Дифрактометр для исследований переходных процессов в реальном времени на реакторе ИБР-2М // Сообщение ОИЯИ Р13-2010-116. Дубна. 2010.

115. Бокучава, Г. Д. и др. Нейтронный фурье-дифрактометр ФСД для исследования механических напряжений в материалах и промышленных изделиях // Поверхность. 2010. Т.11, с. 9-21. (G.D. Bokuchava et al. Neutron Fourier diffractometer FSD for residual stress studies in materials and industrial components // Journal of Surface Investigation. X-ray, Synchrotron and Neutron Techniques. 2010. V. 4 (6), pp. 879-890).

116. Дубовский, О. А., Орлов, А. В.. Излучение пучков сверхзвуковых солитонных волн - генераторов реструктуризации нанокристаллов при бомбардировке атомами и самоорганизация динамической суперрешетки комплексов солитонных колебаний атомов // ФТТ. 2010. Т. 52 (5), с. 846.

117. Калинин, И. В. и др. Измерение спектров холодных нейтронов на макете криогенного замедлителя реактора ИБР – 2М // Письма в ЭЧАЯ. 2010. №1 (157), с. 95-100.

118. Кожевников, С. В. , Отт, Ф. Представление данных

незеркального рассеяния нейтронов // Физика твёрдого тела. 2010. Т. 52 (8), с. 1457-1466. (Kozhevnikov, S. V., Ott, F. Representation of Data on Off-Specular Neutron Scattering // Physics of the Solid State. 2010. V. 52 (8), pp. 1561–1570.)

119. Кожевников, С. В. , Отт, Ф. Представление данных незеркального рассеяния нейтронов // Физика твёрдого тела. 2010. Т. 52 (8), с. 1457-1466.

120. Куклин, А. И. и др. Анализ спектров и потоков от криогенных и тепловых замедлителей нейтронов реактора ИБР-2 по результатам моделирования и экспериментов на установке малоуглового рассеяния ЮМО // Физика элементарных частиц и атомного ядра. 2010 (принято в печать).

121. Лохматов, В. И. и др. Механический монохроматор для спектрометра малоуглового рассеяния на реакторе SAFARI-1 // ФТТ. 2010. Т. 52 (5), с. 950.

122. Мирон, Н. Ф. и др. Нейтронный рефлектометр на тепловых нейтронах с переменной длиной волны // Поверхность. Рентгеновские, синхротронные и нейтронные исследования. 2010 (принято в печать).

Patents

123. Никитенко, Ю. В. Заявка на изобретение: «Способ определения магнитно-неколлинеарной мощности нанослоя».

124. Никитенко, Ю. В. Заявка на изобретение: «Способ определения пространственного распределения намагниченности нанослоя».

Conferences

125. Aksenov, V. L., Tropin, T. V., Avdeev, M. V. Kinetics of cluster growth in fullerene C60 solutions in nitrogen-containing solvents, International Conference on Theoretical Physics, DUBNA-NANO2010. 5-10 July, 2010, Dubna, Russia, poster report.

126. Avdeev, M. V., Feoktystov, A. V., Aksenov, V. L. Small-angle neutron scattering in structure research of ferrofluids, Workshop. Nanofluid IV. November 29 – December 1, 2010, Stara Lesna, Slovakia, invited lecture.

127. Avdeev, M. V., Aksenov, V. L., Bulavin, L. A. Neutron scattering in research and diagnostics of modern ferrofluids, 5th International Conference Physics of Liquid Matter: Modern Problems PLMMP 2010. 21-23May, 2010, Kyiv, Ukraine, invited report.

128. Avdeev, M. V., Feoktystov, A. V., Aksenov, V. L. Small-angle neutron scattering in structure research of ferrofluids, Workshop. Nanofluid IV. November 29 – December 1, 2010, Stara Lesna, Slovakia, invited lecture.

129. Avdeev, M. V., Feoktystov, A. V. Contrast variation in small-angle neutron scattering experiments with polydisperse and superparamagnetic systems: basic functions approach, Central European Training School CETS2010. May 31 – June 2, 2010, Hungary, Budapest, invited lecture.

130. Avdeev, M. V., Vekas, L., Hajdu, A. et al. Aggregate structure in biocompatible aqueous magnetic fluids with steric and electrostatic stabilization, 8th International Conference on the Scientific and Clinical Applications of Magnetic Carriers.Rostock, Germany, poster report.

131. Avdeev, M. V. Structural aspects of biocompatible ferrofluids by scattering methods: Stabilization, properties control and applications Helmholtz-Russia Joint Research Groups Seminar. March 1, 2010, Moscow, Russia,oral report.

132. Balagurov, A. M., Kudryashev, V. A. Correlation Fourier diffractometry for long-pulse neutron sources: a new concept. ICANS-XIX. March 8–12, 2010, Grindelwald, Switzerland. Oral talk.

133. Balagurov, A. M. Advanced neutron scattering and nanostructures. Rusnanotech-2010. 01-03 November, 2010, Moscow, Russia, invited talk.

134. Balagurov, A. M., Bokuchava, G. D., Papushkin, I. V., et al. Neutron diffraction potentialities at the IBR-2 pulsed reactor for non-destructive testing of structural materials. ECNDT-10th. 7-11 June, 2010, Moscow, Russia.

135. Balagurov, A. M. Advanced neutron scattering for nanostructures and material science. SAIP-55. 27 September – 01 October, 2010, Pretoria, South Africa. Invited talk.

136. Balagurov, A. M. Advanced neutron diffraction at pulsed sources: new ideas, new technique, and new science. Czech Technical University. 7 April, 2010, Prague, lecture.

137. Balasoiu, M. and Barsan V. UNESCO Chair on Sustainable Development in Magurele-Bucharest: the first steps. International Conference “Sustainable Development in Conditions of Globalization: Implementation of UNESCO Strategy for the Second Half of the UN Decade of Education for Sustainable Development”. 7-8 December, 2010, Moscow, Russia.

138. Balasoiu, M., Arzumanian, G. M., Stolyar, S. V., et al. Biogenic Ferrihydrite Nanoparticles Structure Investigations, International conference Dubna-Nano2010, JINR. 5-10 July, 2010, Dubna, Russia.

139. Balasoiu, M., Bica, I., Lebedev, V. T., et al. Small angle neutron scattering analysis of ferrofluid based elastomer microstructure, International Conference on Magnetic Fluids ICMF12, Sendai, Japan, Book of abstracts, Elsevier.

140. Balasoiu, M., Bica, I., Raikher, Yu. L., et al. Particle concentration effect on microstructure of ferrofluid-based silicone rubber elastomer, IV Euro-Asian Symposium"Trends in MAGnetism" Nanospintronics EASTMAG 2010. 28 June - 2 July, 2010, Ekaterinburg, Russia, Mo-G-02P.

141. Balasoiu, M., Bica, I., Raikher, Yu. L., et al. Magnetic field and particle concentration competitive effects on ferrofluid based silicone elastomer microstructure, RNIKS-2010. 16-19 November, 2010, Moscow, Russia.

142. Balasoiu, M., Bica, I., Raikher, Yu. L., et al. Magnetic Field And Particle Concentration Competitive Effects On Ferrofluid Based Elastomer Microstructure, International conference Dubna-Nano2010, JINR. 5-10 July 2010, Dubna, Russia

143. Balasoiu, M., Ishchenko, L., Stolyar, S., et al. Small Angle X-Ray Scattering Investigations of Water Based Dispersions of Biogenic Ferrihydrite Particles, 5th International Conference "Physics of liquid matter: modern problems", Taras Shevchenko Kyiv National University. May 2010, Kyiv, Ukraine, p. 303

144. Bobrikov, A. I., Balagurov, A. M. Magnetostructural transitions in complex manganese oxides. ICSM-2010. 25 April – 1 May, 2010, Antalia, Turkey, poster presentation.

145. Cherny, A. Yu., Anitas, E. M., Kuklin, A. I., et al. The Scattering From Generalized Cantor Fractals, International conference Dubna-Nano2010. JINR, 5-10 July 2010, Dubna, Russia.

146. Craus, M.-L., Cornei, N., Pui, A. Crystalline structure and electronic phases of La0.54Nd0.11Sr0.35Mn1-xCoxO3 manganites. 7th International Conference on Inorganic

Materials. 12-14 September, 2010, Biaritz, France, poster presented.

147. Craus, M.-L., Cornei, N., Mîță, C. On magnetic/crystalline structure of La0.54(Sm/Nd)0.11Ca0.35Mn1-xCuxO3 nanomanganites, The 2nd National conference with international participation on nanostructured multifunctional materials, NMM – 2010. 4-5 November, 2010, Iaşi, ROMANIA, poster presented.

148. Craus, M.-L., Cornei, N., Islamov A. et al. Transport phenomena in La0.54Ho0.11Sr0.35Mn1-xCuxO3 manganites, 23rd General Conference of the Condensed Matter Division of the European Physical Society. 30 August - 3 September, 2010, Warshaw, Poland, poster accepted.

149. Craus, M.-L., Cornei, N., Mîță, C., et al. Transport phenomena in La0.54Ho0.11Sr0.35Mn1-XCuXO3 manganites, The 2nd National conference with international participation on nanostructured multifunctional materials, NMM – 2010. 4-5 November, 2010 Iaşi, ROMANIA, poster presented.

150. Craus, M.-L., Mata, C., Cornei, N., et al. Influence of Mn substitution with V on magnetic and crystalline structure of La0.54Ho0.11Sr0.35Mn1-XVXO3 manganites. 7th International Conference on Inorganic Materials. 12-14 September, 2010, Biaritz, France, poster presented.

151. Craus, M.-L., Simkin, V., Cornei N., et al. Influence of Mn substitution with Fe/Co on magnetic structure and transport mechanisms in some manganites The 16 th ICIT Conference on Progres in Criogenics and Isotopes Separation. 13-15 October, 2010, oral report; Calimanesti Caciulata, Romania, appeared in Progress of Cryogenics and Isotopes Separation. 2010. V.13 (1), pp. 47-53.

152. Craus, M.-L., Simkin, V., Cornei, N., et al. Influence of Mn substitution with Fe/Co on magnetic structure and transport mechanisms in some manganites); The 16 th ICIT Conference on Progres in Criogenics and Isotopes Separation, October 13-15, 2010, Calimanesti Caciulata, Romania(Plenary lecture; appeared in Progress of Cryogenics and Isotopes Separation. 2010. V.13 (1), pp. 27-34.

153. Feoktystov, A. V., Avdeev, M. V., Bulavin, L. A., et al. Structure of water-based ferrofluids for biological applications, 5th International Conference Physics of Liquid Matter: Modern Problems PLMMP 2010. 21–23 May, 2010, Kyiv, Ukraine, oral report.

154. Feoktystov, A. V., Avdeev, M. V., Bulavin, L. A., et al. New developments in applications of SANS contrast variation for structure research of magnetic fluids. Workshop “Structural aspects of biocompatible ferrofluids: stabilization, properties control and application”. 28–29 January, 2010, Geesthacht, Germany, poster report.

155. Feoktystov, A. V., Avdeev, M. V., Garamus, V. M., et al. New developments for structure analysis of polydisperse ferrofluids by contrast variation technique in small-angle neutron scattering. 15th International Seminar on Neutron Scattering Investigation in Condensed Matter. 13–15 May, 2010, Poznań, Poland, oral report.

156. Frischbutter, A., Walther, K., Scheffzuek, Ch. Neutronenflugzeitdiffraktion in Dubna - Angewandt auf Geomaterialien vom Gotthard–Basistunnel (Schweiz). Abstract at Deutsche Tagung fuer Forschung mit Synchrotronstrahlung, Neutronen und Ionenstrahlen an Großgeraeten, SNI 2010. 24-26 February, 2010, Berlin, Germany.

157. Ishchenko, L. A., Stolyar, S. V., Ladygina, et al. Magnetic properties and application of biomineral particles produced by bacterial culture, International Conference on Magnetic Fluids ICMF12, Sendai, Japan, Book of abstracts, Elsevier.

158. Ivankina, T. I., Kern, H., Lokajicek, T., et al. Bulk elastic anisotropy of a foliated biotite gneiss from the Outokumpu deep drill hole: 3D velocity calculations and laboratory seismic measurements. 32nd General Assembly of European Seismological Commission. 6-10 September, 2010, Montpellier, France.

159. Kiselev, M., Ermakova, E., Gruzinov, A., et al. Nanostructure of the Model Stratum Corneum Membranes. 4th Japan – Russia International workshop MSSMBS'10 “Molecular Simulation Studies in Material and Biological Sciences”. 24-29 September, 2010, Dubna, Russia.

160. Kiselev, M. A., Ermakova, E. V., Gruzinov, A. Yu., et al. Nanostructure of model membranes of the stratum corneum. Why pharmacy needs in neutron and X-ray diffraction? XVIII международная конференция по использованию синхротронного излучения, СИ-2010. 19-22 июля, 2010, Новосибирск, Россия. Книга тезисов.

161. Kiselev, M. A. Lipid nanostructures. International Conference on Theoretical Physics. Dubna-Nano2010. July 5-10, JINR, Dubna, Russia. Books of abstract of the International Conference on Theoretical Physics. 5-10 July, 2010, JINR Dubna, Russia.

162. Kuklin, A. I., Islamov, A. Kh., Kovalev, Yu. S., et al. Sample environment for studies of nanostructured materials at the YuMO small angle neutron scattering two-detector system spectrometer. Nanotechnology International forum, Rusnanotech. 1-3 November, 2010, Moscow, Russia.

163. Kuklin, A. I., Rogachev, A. V., Cherny, A. Yu., et al. NANOSCALE SIZE EFFECTS. 5th International Conference "Physics of liquid matter: modern problems", Taras Shevchenko Kyiv National University, 2010, Kyiv, Ukraine.

164. Kuklin, A. I., Rogachev, A. V., Cherny, A. Yu., et al. NANOSCALE SIZE EFFECTS. 5th International Conference on Theoretical Physics DUBNA-NANO2010, JINR, Bogolubov Laboratory of Theoretical Physics, 2010, Dubna, Russia, Book of abstracts.

165. Craus, M.-L., Mihai Lozovan, Nicoleta Cornei. Correlation between average radius of A places and magnetic/crystalline structure of La0.54(Sm/Nd)0.11Ca0.35Mn1-xCuxO3 manganites, 23 rd General Conference of the Condensed Matter Division of the European Physical Society. 30 August - 3 September 2010, Warshaw, Poland, poster presented.

166. Mohorianu, S., Craus, M.-L. Perovskites-like magnetic materials properties prediction by innovative computational simulation IT-based techniques. The 4-th National Conference of Applied Physics. 19-20 November, 2010, Iasi, Romania. Oral talk.

167. Murugova, T. N., Muranov, K. O., Poliansky, N. B., et al. Fifth International Conference "Physics of liquid matter: modern problems", Taras Shevchenko Kyiv National University, 2010, Kyiv, Ukraine. Study of alpha-crystallin structure by small angle x-ray and neutron scattering.

168. Nagornyi, A. V., Petrenko, V. I., Avdeev, M. V., et al. Analysis of small-angle neutron scattering from very diluted magnetic fluids 5th International Conference Physics of Liquid Matter: Modern Problems PLMMP 2010. 21–23 May, 2010, Kyiv, Ukraine, poster report.

169. Nikitin, A. N., Ivankina, T. I., Kruglov, A. A., et al. Propagation of quasi-longitudinal and quasi-transverse elastic waves at an interface between isotropic and anisotropic media: theoretical and experimental investigations. 32nd General Assembly of European Seismological Commission. 6-10 September, 2010, Montpellier, France.

170. Nikolayev, D. I., Lychagina, T. A. "The technique for treatment of texture synchrotron experimental results", DESY. 31 March, 2010, Hamburg, Germany.

171. Petrenko, V. I., Avdeev, M. V., Bulavin, L. A., et al. Nematic-isotropic phase transition in solutions of mono-carboxylic acids

in non-polar solvents studied by SANS, 5th International Conference Physics of Liquid Matter: Modern Problems PLMMP 2010. 23-26 May, 2010, Ukraine, Kyiv, poster.

172. Rajewska, A. Aggregation in heavy water mixed micellar solutions of nonionic cationic classic surfactants study by SANS method. VIII International Conference on X-ray Investigations of Polymer Structure, XIPS – 2010. 8-10 December, 2010, Wroclaw, Poland, Book of Abstracts.

173. Rajewska, A. Structure of the mixed micellar solutions of nonionic with anionic classic surfactant study by SANS method. International Soft Matter Conference. 5-8 July, 2010, Granada, Spain.

174. Rogachev, A. V., Cherny, A. Yu., Ozerin, A. N., et al. Investigation of the dendrimer solutions by small angle scattering method, 5th International Conference "Physics of liquid matter: modern problems", Taras Shevchenko Kyiv National University, 2010, Kyiv, Ukraine. Study of alpha-crystallin structure by small angle x-ray and neutron scattering.

175. Scheffzuek, Ch., Hempel, H., Frischbutter, A. et al. Proben-Rotations-Einrichtung zur simultanen Textur- und Strainmessung mit dem Diffraktometer EPSILON-MDS am Reaktor IBR-2M. Abstract at Deutsche Tagung fuer Forschung mit Synchrotronstrahlung, Neutronen und Ionenstrahlen an Großgeraeten, SNI 2010. 24-26 February, 2010, Berlin, Germany.

176. Scheffzuek, Ch., Walther, K., Frischbutter, A., et al. Reconstruction of the beamline 7A of the IBR-2M for the diffractometers EPSILON-MDS and SKAT. Talk at the 31th PAC for Condensed Matter Physics. 18-19 January, 2010, Dubna, Russia.

177. Scheffzuek, Ch., Walther, K., Frischbutter, A., et al. Stand der Umbauarbeiten an der beamline 7A der gepulsten Neutronenquelle IBR-2M, JINR Dubna. Usermeeting, 1 October, 2010, Kiel, Germany.

178. Scheffzuek, Ch., Walther, K., Frischbutter, A., et al. Status des Strain-Meßplatzes EPSILON-MDS an der gepulsten Neutronenquelle IBR-2M des JINR Dubna und einige Anwendungsbeispiele. User meeting. 1 October, 2010, Kiel, Germany.

179. Snegir, S. V., Karpenko, V. B., Filonenko, O. M., et al. Aggregation of fullerene C60 dissolved in solvents with varied permittivity. Mass-spectrometry aspects. International Symposium “Modern problems of surface chemistry and physics”. 18-21 May, 2010, Kyiv, Ukraian, oral report.

180. Solovyov, D. V., Kuklin, A. I., Utrobin, P. K, et al. Studies of water – dimyristoylphosphatidylcholine system under hydrostatic pressure. 5th International Conference "Physics of liquid matter: modern problems", Taras Shevchenko Kyiv National University, 2010, Kyiv, Ukraine.

181. Stan, C., Cristescu, C. P., Balasoiu, M., et al. Preliminary Investigations Of Fe3O4-Ferrofluids at Different Temperatures by Means of Magnetic Measurements. The 4-th National Conference on Applied Physics. 19-20 November 2010.

182. Sumin, V. Eighth European Conference “Residual stresses – ECRS8”. 26-28 June, 2010, Trento, Italy, oral report.

183. Sumin, V. V., Bokuchava, G. D., Papushkin, I. V., et al. Neutron Diffraction Potentialities for Non-Destructive Testing of Structural Materials. The 10th European Conference on NDT, 7-11 June, 2010, Moscow, Russia, oral talk.

184. Tropin, T. V., Avdeev, M. V., Kyzyma, O. A., et al. Solutions of fullerene C60 in N-methyl-2-pyrrolidone: comparison of cluster growth models results with experiment, 5th International Conference "Physics of liquid matter: modern problems" (PLMMP-2010). 21-24 May, 2010, Kiev, Ukraine, oral report.

185. Vasin, R. N. Workshop “Combined Analysis Using X-ray and Neutron Scattering”. 28 June – 4 July, 2010, Caen, France.

186. Walther, K., Scheffzuek, Ch., Frischbutter, A. Strain- und Texturdiffraktometer an der Langzeit-Neutronen-Impulsquelle IBR-2M in Dubna. Abstract at Deutsche Tagung fuer Forschung mit Synchrotronstrahlung, Neutronen und Ionenstrahlen an Großgeraeten, SNI 2010. 24-26 February, 2010, Berlin, Germany.

187. Авдеев, М. В., Благовещенский, Н. М., Новиков, А. Г., и др. Исследование пористой структуры трепела методом малоуглового нейтронного рассеяния. Тезисы доклада на XXI Совещании по использованию рассеяния нейтронов в исследовании конденсированного состояния, РНИКС-2010. 16-19 ноября 2010, РНЦ КИ, Москва, Россия, с.142.

188. Авдеев, М. В. Малоугловое рассеяние нейтронов в высокодисперсных наносистемах, Семинар, посвященный 10-летию кафедры нейтронографии Физ. Факультета МГУ. 24 апреля 2010, НИИЯФ МГУ, Дубна, приглашенный доклад.

189. Авдеев, М. В. Малоугловое рассеяние нейтронов в магнитных жидкостях: медико-биологические приложения, XXI Совещание по использованию рассеяния нейтронов в исследованиях конденсированного состояния. 16-19 ноября, 2010, Москва, Россия, приглашенный доклад.

190. Авдеев, М. В. Малоугловое рассеяние нейтронов, Школа «Современная нейтронография: междисциплинарные исследования наносистем и материалов». 25 октября – 1 ноября 2010, Дубна, Россия, приглашенная лекция.

191. Авдеев, М. В. Малоугловое рассеяние нейтронов. III Высшие курсы стран СНГ для молодых ученых, аспирантов и студентов старших курсов по современным методам исследований наносистем и материалов «Синхротронные и нейтронные исследования наносистем», СИН-нано-2010. 4-17 июля, 2010, Москва-Дубна, Россия, приглашенная лекция.

192. Авдеев, М. В. Применение магнитных наночастиц в биомедицине, Семинар НОЦ МГУ по нанотехнологиям. 22 марта 2010, Москва, МГУ, Россия, приглашенная лекция.

193. Авдеев, М. В. Современная нейтронография: исследования наносистем. Всероссийский молодежный инновационный форум Селигер 2010. 2010, Россия, приглашенная лекция.

194. Авдеев, М. В. Спектрометры нейтронов, Школа «Приборы и методы экспериментальной ядерной физики. Электроника и автоматика экспериментальных установок». 11-13 ноября 2010, Дубна, Россия, приглашенная лекция.

195. Akserov, E. Eigth Advanced Summer School on Modern Mathematical Physics. 5-15 September, 2010, JINR, Dubna, Russia.

196. Akserov, E. Twentieth International Baldin Seminar on High Energy Physics Problems "Relativistic Nuclear Physics and Quantum Chromodynamics". 4-9 October, 2010. JINR, Dubna, Russia.

197. Аскеров, Э. Международная Школа НИЯУ МИФИ по теоретической физике им. В.М. Галицкого, 20 – 26 сентября, 2010, МИФИ, Москва, Россия, без доклада.

198. Балагуров, А. М. Спектрометры на реакторе ИБР-2М: статус и перспективы. РНИКС-XXI. 16-19 ноября, 2010, Москва, Россия, приглашенный доклад.

199. Белушкин, А. В., Кичанов, С. Е., Козленко, Д. П., и др. Исследование структурных аспектов оптических свойств наносистемы GeO2-Eu2O3-Ag. Тезисы докладов XXI Совещания по использованию рассеяния нейтронов в исследованиях конденсированного состояния (РНИКС-2010). 16-19 ноября, 2010, Москва, Россия.

200. Благовещенский, Н. М., Новиков, А. Г., Савостин, В. В. Исследование атом-атомной и структурной релаксации в жидких щелочных металлах с помощью формализма функции памяти. Тезисы доклада на XXI Совещании по использованию рассеяния нейтронов в исследовании конденсированного состояния, РНИКС-2010. 16-19 ноября 2010, РНЦ КИ, Москва, Россия.

201. Благовещенский, Н. М., Новиков, А. Г., Савостин, В. В. Контроль концентрации примесей в жидких металлах методом нейтронного рассеяния. Тезисы доклада на XXI Совещании по использованию рассеяния нейтронов в исследовании конденсированного состояния, РНИКС-2010. 16-19 ноября 2010, РНЦ КИ, Москва, Россия.

202. Бокучава, Г. Д. О возможностях изучения макро- и микронапряжений в объемных материалах на различных нейтронных дифрактометрах (HRFD, FSD, HRPT, D7A). 25 февраля 2010, ЛНФ ОИЯИ, Дубна, Россия.

203. Васин, Р. Н. Геофизические исследования с использованием нейтронографии. Всероссийская научная школа для молодежи «Современная нейтронография: фундаментальные и прикладные исследования функциональных и наноструктурированных материалов». 25 октября – 2 ноября 2010, Россия.

204. Голосова, Н. О., Козленко, Д. П., и др. Влияние высокого давления на кристаллическую и магнитную структуру кобальтита La0.5Ca0.5CoO3. Тезисы докладов XXI Совещания по использованию рассеяния нейтронов в исследованиях конденсированного состояния (РНИКС-2010), 16-19 ноября 2010, Москва, Россия.

205. Дубовский, О. А., Орлов, А. В. Генерация высокоамплитудных солитонных волн в кристаллических материалах 1D,2D,3D размерности при облучении атомами, ионами и нейтронами. Тезисы доклада на XXI Совещании по использованию рассеяния нейтронов в исследованиях конденсированного состояния, РНИКС – 2010. 16-19 ноября 2010, РНЦ КИ, Москва, Россия.

206. Калинин, И. В., Кац, Е., Коза, М., и др. Исследование неравновесной сверхтекучей фазы в гелии под давлением. Тезисы доклада на XXI Совещании по использованию рассеяния нейтронов в исследованиях конденсированного состояния, РНИКС – 2010. 16-19 ноября 2010 г., РНЦ КИ, Москва, Россия.

207. Кизима, Е. А.. Кинетика кластерообразования в полярных растворах фуллерена С60 по данным экстракции и масс-спектрометрии, XIV научная конференция молодых ученых и специалистов ОИЯИ, 1-6 февраля, 2010г, Дубна, Россия, устный доклад.

208. Кирей, Т. А., Кизима, А. А., Гарамус, В. М., и др. Кластерная организация фуллерена с60 в смеси полярный−слабополярный растворитель.РНИКС - 2010, XXI. Совещание по использованию рассеяния нейтронов в исследованиях конденсированного состояния. 16-19 ноября 2010, Москва, Россия, стендовый доклад.

209. Киселев, М. А. Развитие методов нейтронографии и рентгенографии для определения наноструктуры и свойств липидных систем. XXI Совещание по использованию рассеяния нейтронов в исследованиях конденсированного состояния.РНИКС – 2010. 16-19 ноября 2010, РНЦ КИ, Москва, Россия.

210. Киселев, М. А. Развитие методов нейтронографии и рентгенографии на современных нейтронных и синхротронных источниках для определения наноструктуры и свойств липидных систем. IV Сисакяновские чтения «Проблемы биохимии, радиационной и космической биологии». 5-9 сентября, 2010, ОИЯИ, Дубна-Алушта.

211. Кичанов, С. Е., Козленко, Д. П., Билски, П., и др. Структура и атомная динамика резорцинола при высоких давлениях и температурах. XIV научная конференция молодых ученых и специалистов.1-8 февраля 2010, Дубна, Россия, устный доклад.

212. Кожевников, С. В. “Magnetic layered structure for the production of polarized neutron microbeams”.International conference “Polarized Neutrons for Condensed Matter Investigations”. 5-8 July 2010, Delft, The Netherlands, стендовый доклад.

213. Кожевников, С. В. Channeling and tunneling in neutron waveguides. Conference on neutron reflectometry SUPER ADAM. 25-26 October, 2010, Grenoble, France, poster.

214. Кожевников, С. В. Combination of a reflectometer and a nonmagnetic waveguide for experiments with polarized neutron microbeam. XXI Совещание по использованию рассеяния нейтронов в исследованиях, РНИКС-2010. 16-19 ноября, Москва, Россия, устный доклад.

215. Кожевников, С. В. Magnetic waveguides for the production of polarized neutron microbeams. Third User Meeting. 15 October 2010, Garching, Germany, стендовый доклад.

216. Козленко, Д. П. Современная нейтронография: исследования функциональных материалов. Всероссийский образовательный форум Селигер – 2010. 12-19 июля 2010, Россия.

217. Козленко, Д. П. Современная нейтронография: исследования функциональных материалов. Всероссийская научная школа для молодежи “Современная нейтронография: фундаментальные и прикладные исследования функциональных и наноструктурированных материалов”. 25 октября – 2 ноября 2010, Дубна, Россия.

218. Козленко, Д. П., Кичанов, С. Е., Лукин, Е. В., и др. Структурные и магнитные фазовые переходы в мультиферроиках BiMnO3 и BiFeO3 при высоких давлениях, XXI Совещание по использованию рассеяния нейтронов в исследованиях конденсированного состояния (РНИКС-2010). 16-19 ноября 2010, Москва, Россия, устный доклад.

219. Круглов, А. А. Аномалии физических полей при сейсмических процессах. XVIII междисциплинарный семинар «Система «Планета Земля». 3 февраля 2010, МГУ, Москва, Россия.

220. Кудряшев, В. А., Балагуров, А. М., Бокучава, Г. Д., и др. Новый фурье-дифрактометр на реакторе ИБР-2М и возможности корреляционного метода Фурье на источниках с длинным импульсом. РНИКС-XXI. 16-19 ноября 2010, Москва, Россия, устный доклад.

221. Локаичек, Т., Рудаев, В., Иванкина, Т. И., и др. Семинар ИФЗ им. О.Ю. Шмидта РАН «Анизотропия и текстура горных пород литосферы при высоких давлениях по данным акустических и нейтронографических исследований». 19 ноября 2010, Москва, Россия.

222. Лукин, Е. В., Белушкин, А. В., Кичанов, С. Е., и др. Исследование структурных аспектов оптических свойств наносистемы GeO2-Eu2O3-Ag. XIV научная конференция молодых ученых и специалистов. 1-8 февраля 2010, Дубна, Россия, устный доклад.

223. Лукин, Е. В., Кичанов, С. Е., Козленко, Д. П., и др. Исследование кристаллической и магнитной структуры мультиферроика BiFeO3, XXI Совещание по использованию рассеяния нейтронов в исследованиях конденсированного состояния (РНИКС-2010). 16-19 ноября 2010, Москва, Россия, стендовый доклад.

224. Матвеев, В. А., Бокучава, Г. Д., Журавлев, В. В., и др. Адаптация дифрактометра FSS для работы на реакторе ИБР-2М. РНИКС-XXI. 16-19 ноября 2010, Москва, Россия,

стендовый доклад.

225. Миронова, Г. М. Дифрактометр для исследований переходных процессов в реальном времени на реакторе ИБР-2М. XXI Совещание по использованию рассеяния нейтронов в исследованиях конденсированного состояния, РНИКС-2010. 16-19 ноября, 2010, РНЦ КИ, Москва, Россия.

226. Миронова, Г. М. О полноте спектральной информации в эксперименте по времени пролета на импульсном источнике нейтронов. XXI Совещание по использованию рассеяния нейтронов в исследованиях конденсированного состояния, РНИКС-2010. 16-19 ноября, 2010, РНЦ КИ, Москва, Россия.

227. Муругова, Т. Н., Муранов, К. О., Полянский, Н. Б., и др. Исследование структуры альфа-кристаллина с помощью малоуглового рентгеновского и нейтронного рассеяния, абстракты XLIV Зимней школы ПИЯФ, Секция физика конденсированных сред. 2010, Рощино, Россия.

228. Нагорный, А. В., Булавин, Л. А., Авдеев, М. В., и др. Моделирование малоуглового рассеяния нейтронов на магнитных жидкостях с учетом анизотропии частиц, XXI Совещание по использованию рассеяния нейтронов в исследованиях конденсированного состояния, РНИКС-2010. 16-19 ноября, 2010, Москва, Россия, стендовый доклад.

229. Никитенко, Ю. В. Interaction of neutrons with layered magnetic media in oscillating magnetic field.PNCMI-2010). 5-8 июля, 2010, Делфт, Нидерланды, устный доклад.

230. Никитенко, Ю. В. Прохождение поляризованных нейтронов через неколлинеарные и некомпланарные магнитные слоистые структуры. Нанофизика и наноэлектроника. 15-19 марта, Нижний Новгород, Россия, устный доклад.

231. Новиков, А. Г., Пучков, А. В. О модернизации спектрометра ДИН-2ПИ. XXI Тезисы совещания по использованию рассеяния нейтронов в исследовании конденсированного состояния. РНИКС-2010. 16-19 ноября 2010, РНЦ КИ, Москва, Россия, с.157.

232. Орлов, А. В., Дубовский, О. А. Солитонная микродинамика фазовых переходов в кристаллических материалах и фононы нового типа на границе раздела фаз. Тезисы доклада на XXI Совещании по использованию рассеяния нейтронов в исследованиях конденсированного состояния, РНИКС – 2010. 16-19 ноября 2010, РНЦ КИ, Москва, Россия, с.34.

233. Петренко, В. И., Авдеев, М. В., и др. Структурные особенности растворов поверхностно-активных веществ, используемых для стабилизации магнитных жидкостей, XXI Совещание по использованию рассеяния нейтронов в исследованиях конденсированного состояния. 16-19 ноября 2010, Москва, Россия, стендовый доклад.

234. Петренко, В. И. Структура растворов поверхностно-активных веществ, используемых для стабилизации магнитных жидкостей, XIV научная конференция молодых ученых и специалистов ОИЯИ. 1-6 февраля 2010, Дубна, Россия, устный доклад.

235. Раевска, А. Изучение структуры смешанных мицеллярных растворов на основе неионного и катионного ПАВ методом малоуглового рассеяния нейтронов. XXI Совещание по использованию рассеяния нейтронов в исследованиях конденсированного состояния (РНИКС-2010). Тезисы докладов. 16 – 19 ноябрь, 2010, Москва, Россия.

236. Рубцов, А. Б., Боднарчук, В. И., Игнатович, В. К., и др. Изучение возможностей создания супернзеркал с периодической структурой. РНИКС -2010, XXI Совещание по использованию рассеяния нейтронов в исследованиях конденсированного состояния. 16-19 ноября, 2010, Москва, Россия, стендовый доклад.

237. Рябова, Н. Ю. Исследование модельных липидных мембран Oral Stratum Corneum на основе церамида-6. XXI Совещание по использованию рассеяния нейтронов в исследованиях конденсированного состояния, РНИКС-2010. 16-19 ноября, 2010, РНЦ КИ, Москва, Россия.

238. Рябова, Н. Ю. Школа «Современные фундаментальные, медицинские и биотехнологические аспекты исследования биологических мембран». 3-7 октября 2010, МФТИ, Долгопрудный, Россия, без доклада.

239. Сахарова, Л. А., Лисичкин, Ю. В., Туманов, А. А. Молекулярная динамика воды, адсорбированной на поверхности кремнезема (по данным нейтронной спектроскопии). Тезисы доклада на XXI Совещании по использованию рассеяния нейтронов в исследовании конденсированного состояния, РНИКС-2010. 16-19 ноября 2010, РНЦ КИ, Москва, Россия.

240. Семенов, В. А., Дубовский, О. А., Орлов, А. В. Солитонный механизм микродинамики и теплопроводности нитрида урана при высоких температурах. Тезисы доклада на XXI Совещании по использованию рассеяния нейтронов в исследованиях конденсированного состояния, РНИКС – 2010. 16-19 ноября 2010, РНЦ КИ, Москва, Россия.

241. Сумин, В. В., Балагуров, А. М., Васин, Р. Н., и др. Определение тензора остаточных напряжений в сильно-текстурированном цилиндре из циркониевого сплава Э-110 методом дифракции нейтронов. Всероссийская научно-техническая конференция «Материалы ядерной техники» (МАЯТ-2010). 26 сентября – 02 октября, 2010, Краснодарский край, Туапсе, Россия.

242. Тропин, Т. В., Авдеев, М. В., Коробов, М. В., и др. Кинетика роста кластеров в полярных растворах фуллерена С60, VI Международная научная конференция «Кинетика и механизм кристаллизации. Самоорганизация при фазообразовании». 21-24 сентября, 2010, Иваново, Россия, стендовый доклад.

243. Тропин, Т. В., Авдеев, М. В., Аксенов, В. Л. Модели кластерообразования фуллеренов в растворах, XXI Совещание по использованию рассеяния нейтронов в исследованиях конденсированного состояния, РНИКС-2010. 16-19 ноября, 2010, Москва, Россия, стендовый доклад.

244. Тропин, Т. В. Растворы фуллерена С60 в N-метил-2-пирролидоне: сравнение кинетической модели роста кластеров с экспериментом, XIV научная конференция молодых ученых и специалистов ОИЯИ, ОМУС-2010. 1-6 февраля, 2010, ОИЯИ, Дубна, Россия, устный доклад.

245. Феоктистов, А. В., Авдеев, М. В., Аксенов, В. Л., и др. Обобщенный подход в структурном анализе полидисперсных магнитных жидкостей методом малоуглового рассеяния нейтронов с вариацией контраста, XXI Совещание по использованию рассеяния нейтронов в исследованиях конденсированного состояния, РНИКС-2010. 16-19 ноября 2010, Москва, Россия, стендовый доклад.

246. Феоктистов, А. В., Авдеев, М. В. Магнитные наночастицы в растворах для медикобиологических применений. III Высшие курсы стран СНГ для молодых ученых, аспирантов и студентов старших курсов по современным методам исследований наносистем и материалов «Синхротронные и нейтронные исследования наносистем», СИН-нано-2010. 4-17 июля 2010, Москва-Дубна, Россия, приглашенная лекция.

247. Khaidukov, Yu. N. Experimental observation of the inverse proximity effect in the superconductor ferromagnet bilayer.

International Conference on Superconductivity and Magnetism. 25-30 April, 2010, Antalia, Turkey, oral presentation.

248. Khaidukov, Yu. N. Polarization of the Cooper-pairs on the superconductor/ferromagnet interface. Совещание "Superconductivity Explored by Neutron Scattering Experiments". 21-23 October, 2010, Grenoble, France, oral presentation.

249. Khaidukov, Yu. N. Magnetic proximity effect by waveguide-enhanced PNR. Совещание "Neutron reflectometry: the next generation and beyond". 25-26 October, 2010, Grenoble, France, poster.

250. Khaidukov, Yu. N. Waveguide-enhanced polarized neutron reflectometry: a new approach in the study of magnetic proximity effects.Совещание пользователей реактора FRM-2. 15 October, 2010, Munchen, Germany, Мюнхен, oral presentation.

251. Аскеров, Э. Перспективы использования ядерной энергии в мирных целях, ИРП НАНА. 8 – 10 ноября 2010, Баку, Азербайджан, без доклада.

DEPARTMENT OF IBR-2 SPECTROMETERS COMPLEX

252. Kulikov, S. A. et al. Full scale model of pelletized cold neutron moderators for the IBR-2M reactor // Proceedings of International Collaboration on Advanced Neutron Sources (ICANS XIX). PSI, Grindelwald, Switzerland, ISSN 1019-6447, 2010.

253. Куликов, С. А. и др. Измерение спектров холодных нейтронов на макете криогенного замедлителя реактора ИБР-2М. // Письма в журнал «Физика элементарных частиц и атомного ядра» (Письма в ЭЧАЯ). 2010. Т. 7 (157), с. 95-100.

254. Кудряшев, В. А. и др. «овый фурье-дифрактометр на реакторе ИБР-2М и возможности корреляционного метода Фурье на источниках с длинным импульсом // XXI СОВЕЩАНИЕ по использованию рассеяния нейтронов в исследованиях конденсированного состояния (РНИКС–2010) г. Москва, РНЦ «Курчатовский институт» 16–19 ноября 2010 г., Тезисы докладов.

255. Матвеев, В. А. Адаптация дифрактометра FSS для работы на реакторе ИБР-2М // XXI СОВЕЩАНИЕ по использованию рассеяния нейтронов в исследованиях конденсированного состояния (РНИКС–2010) г. Москва, РНЦ «Курчатовский институт» 16–19 ноября 2010 г., Тезисы Докладов.

256. Bodnarchuk, I., Manoshin, S. et al. On the effect of gravity on the resolution for time-of-flight specular neutron reflectivity // Nuclear Inst. and Methods in Physics Research Section A. 2010 (submitted).

257. Erhan, R. V., Manoshin, S. et al. A concept for the modernization of a SANS instrument at the IBR-2M pulsed reactor // Nucl. Instr. and Methods in Phys. Research Section A. 2010 (in press).

258. Manoshin, S., Belushkin, A. V. and Ioffe, A. The VITESS polarized neutron suite: completed and allows for the simulation of any polarized neutron scattering instrument // The 8th international workshop on Polarised Neutrons in Condensed Matter Investigations Delft, the Netherlands, 5 - 8 July 2010, Proceeding of abstracts.

259. Белушкин, А. В. и др. Разработки газонаполненных позиционно-чувствительных детекторов тепловых нейтронов в ЛНФ ОИЯИ // Физика Твердого Тела. 2010. Т. 52 (5), с. 961-963,

260. Пантелеев, Ц. Ц. и др. Нейтронный спектрометр на базе протонного телескопа с электронной коллимацией протонов отдачи // Препринт ОИЯИ 313-2010-124, Дубна. 2010.

261. Bogdzel, A. A. et al. High-Speed Neutron Counter // Neutron News. V. 21 (3), pp. 25-26.

262. Кириллов, А. С. и др. Архитектура систем контроля и управления экспериментальных установок на реакторе ИБР-2М // XXI Совещание по использованию рассеяния нейтронов в исследованиях конденсированного состояния, РНИКС-2010. 16-19 ноября 2010, РНЦ «Курчатовский институт», Москва, Тезисы докладов.

263. Churakov, A. V. Measurement of thermal neutrons bunches profile on installation IREN // ISINN-18, Dubna, May 29-31. 2010. Book of abstract.

264. Черников, А. Н. и др. Шахтный криостат для охлаждения камер высокого давления с алмазными и сапфировыми наковальнями // Поверхность. Рентгеновские, синхротронные и нейтронные исследования. 2010. № 11, с. 1–6.

265. Trofimov, V. Design and performance of a double stage He4/He3 refrigerator with the cryosorption pumps // International Cryogenic Engineering Conference 23 - International Cryogenic Materials Conference ICEC23-ICMC2010. July 19-23 2010, Wroclaw, Poland. Abstracts.

266. Chernikov, A. N. Development of laboratory cryostats in the cryogenics research group of FLNP JINR // XVIII International Seminar on Interaction of Neutrons with Nuclei (ISINN-18), FLNP JINR, 26-29 May, 2010, Dubna, Russia. Abstracts.

267. Шевлюга, В. М. Спектральные возможности сверхвысоковакуумного сканирующего туннельного микроскопа GPI CRYO // Тезисы докладов XX Всероссийской научной конференции "Рентгеновские и электронные спектры и химическая связь" РЭСХ-2010, Новосибирск, 24-28 мая 2010, с. 206.

268. Черников, А. Н. Шахтные криостаты для нейтронных исследований в диапазоне температур 6-300К // Тезисы докладов XXI Совещания по использованию рассеяния нейтронов в исследованиях конденсированного состояния, РНИКС-2010. 16-19 ноября 2010, РНЦ «Курчатовский институт», Москва.

269. Глазков, В. П. Нейтронно-синхротронные исследования при высоких давлениях // Тезисы докладов XXI Совещания по использованию рассеяния нейтронов в исследованиях конденсированного состояния, РНИКС-2010. 16-19 ноября 2010, РНЦ «Курчатовский институт», Москва.

NUCLEAR PHYSICS DEPARTMENT

1. Experimental investigations

270. Gledenov, Yu. M. et al. Cross-section measurement and analysis for the 149Sm(n, α)146Nd reaction at 6 MeV neutron energy region // Physical Review C. 2010. V. 82, pp. 014601.

271. Gledenov, Yu. M. Cross sections of the 67Zn(n,α)64Ni reaction at 4.0, 5.0, and 6.0 MeV // Physical review C. 2010. V. 82, pp. 054619.

272. Gledenov, Yu. M. et al. Cross-section measurement for the 67Zn(n,α)64Ni reaction at 6.0 MeV // . J. Eur. Phys A. 2010. V. 43 (1-4).

273. Zhang, G. Cross section measurement for the 95Mo(n, α)92Zr reaction at 4.0, 5.0 and 6.0 MeV // Appl. Radiation & Isotopes. 2010. V. 68, pp. 180-183.

274. Весна, В. А. и др. Новый вариант интегрального метода измерений малых эффектов в экспериментах на выведенных пучках атомного реактора при частоте переключения знака эффекта выше основных частот спектра флуктуаций мощности реактора // Журнал технической физики. 2010. Т.80 (11), с.140-148.

275. Skoy, V. R. et al. Multicrystal Scintillation Detector for Investigation of Angular Correlations in (n,γ) Reactions // IEEE Trans. on Nucl. Science. 2010. V. 57 (3), pp. 1391-1395.

276. Pyatkov, Yu. V. et al. Collinear cluster tri-partition of 252Cf (sf) and in the 235U (nth, f) reaction // The European Physical Journal A - Hadrons and Nuclei. V. 45 (1), pp. 29-37, doi: 10.1140/epja/i2010-10988-8.

277. Пятков, Ю. В. и др. Канал тройного коллинеарного кластерного распада в реакции 235U(n_th, f) // Ядерная физика. 2010. Т. 73 (8), с.1350-58.

278. Pyatkov, Yu. V. et al. Collinear Cluster Tri-Partition 252Cf(sf) and in Neutron-Induced Fission of 235U(n_th), f) // Europhysics News. 2010. V. 41 (4), pp. 14.

279. Данилян, Г. В. и др. Поиск Т-нечетных корреляций в эмиссии мгновенных нейтронов деления ядер поляризованными нейтронами // ЯФ. 2010. Т. 73 (7), с. 1155.

280. Суховой, А. М. и др. Прецизионная модельная аппроксимация Дубненских данных по плотности уровней ядер области 40≤A≤200 ниже Bn // ЯФ. 2010. Т. 73 (9), с. 1554-1562.

281. Sukhovoj, A. M. et al. Precise model approximation of the Dubna data on nuclear level density in region 40≤A≤200 below Bn // Physics of atomic nucleus. 2010. Т. 73 (9), с. 1507-1515.

282. Суховой, А. М., Хитров, В. А. Возможность реализации непрямого эксперимента по определению сечениявзаимодействия нуклона с произвольным ядром в широкой области энергииего возбуждения // ЯФ. 2010. Т. 73 (10), с. 1683-1692.

283. Sukhovoj, A. M., Khitrov, V. A. The possibility to realize indirect experiment on determination of nucleon interaction cross section with exated nucleus // Physics of atomic nucleus. 2010. Т. 73 (10), с. 1635-1644.

284. Pokotilovski, Yu. N. Limits on short-range spin-dependent forces from spin relaxation of polarized ^{3}He // Phys. Lett. B. 2010. V. 686, pp. 114-117.

285. Sobolev, Yu. et al. Cubic boron nitride: A new perspective material for ultracold neutron applications // Nucl. Instr. Meth. A. 2010. V. 614, pp. 461-7.

286. Pokotilovski, Yu. N. Options for the neutron lifetime measurement in traps // Phys. At. Nucl. 2010. V. 73, pp. 725-736.

287. Новопольцев, М. И. и др. Корреляционная времяпролётная спектрометрия ультрахолодных нейтронов // ПТЭ. 2010. №5, с. 22-27.

288. Bunatian G. G. et al. On the E-LINAC - based neutron yield // Preprint JINR E3-2010-144. 2010 (submitted to "ЯФ").

289. Nesvizhevsky, V. et al. Application of Diamond Nanoparticles in Low-Energy Neutron Physics // Materials 3. 2010. pp. 1768-1781. doi:10.3390/ma3031768.

290. Cubitt, R. et al. Quasi-specular reflection of cold neutrons from nano-dispersed media at above-critical angles // NIM A. 2010. V. 622, pp. 182-185.

291. Gould, C.R. et al. Reanalysis of recent neutron diffusion and transmission measurements in nuclear graphite // Nuclear Science and Engineering. 2010. V. 165, pp. 200.

292. Gillis, R.C. et al. A Measurement of the parity-violating gamma-asymmetry in in n-p capture // J. Phys. Rev. 2010. Conf. Ser. V. 239, pp. 012012.

293. Зейналова, О. В. и др. Спектроскопия продуктов деления 252cf(sf) с применением цифровой обработки сигналов // Известия РАН, серия физическая. 2010. Т. 74 (6), с. 837-841.

294. Zeynalov, Sh. et al. Comparison of digital and analogue data acquisition systems for nuclear spectroscopy // Nuclear Instruments and Methods in Physics Research A. 2010. V. 624, pp. 684–690.

2. Theoretical investigations

295. Utsuro, M. et al. Handbook of Neutron Optics // Wiley VCH. 2010. Berlin. 45.

296. Игнатович, В. К. Рассеяние на магнитных наноцилиндрах и метод искаженных волн в неколлинеарных полях // ТМФ. 2010. Т. 163, № 1, с. 140-155.

297. Ignatovich, V. K., Scattering by magnetic nanocylinders and the method of distorted waves in noncollinear fields // Theoretical and Mathematical Physics.2010. 163, № 1. pp. 517-530.

298. Ignatovich, V.K, Nikitenko Yu.V. A Time-odd correlation in a neutron reflectometry experiment // ЖЭТФ. 2010. Т. 137, № 3. pp. 473-482// JETP, V. 110. N. 3. pp. 417-425.

299. Игнатович, В. К. и др. Прохождение поляризованных нейтронов через магнитные некомпланарные слоистые системы // ЖЭТФ. 2010. Т. 137. № 5, с 886-894; V. K. Ignatovich et al. Transmission of Polarized Neutrons through Magnetic Noncoplanar Layered Systems // JETP 110. N. 5. pp. 775–782.

300. Ignatovich, V. K, Nikitenko Yu.V. A Time-odd correlation in a neutron reflectometry experiment // JETP. 2010. V. 110. N. 3. pp. 417-425.

301. Ignatovich, V. K. et al. Neutron refraction in oscillating magnetic field // Nucl.Instr.Meth. A. 2010. V. 628. N. 2-3. pp. 410–413.

302. Ignatovich, V. K. Comment on ``Observation of the Goos-H" anchen shift with neutrons`` // Phys.Rev.Lett. 2010. V. 105.pp. 01890.

303. Ignatovich, F. V., Ignatovich, V. K. On Fresnel Reflection and Evanescent Gain // OPN. 2010. V. 21. N. 5.pp. 6.

304. Ignatovich, F. V. and Ignatovich V.K. An experiment on a ball-lightning model. 2010. // JINR E4-2010-83.

305. Игнатович, В. К., Ф.В.Игнатович Оптика анизотропных сред // припринт ОИЯИ Р4-2010-119.

306. Lyuboshitz, V. L, Lyuboshitz, V. V. Spin correlations in the $\Lambda\Lambda$ and $\Lambda\overline{\Lambda}$ systems generated in relativistic heavy-ion collisions // Ядерная физика. 2010.Т. 73 (5), с. 836 – 845. Physics of Atomic Nuclei. V. 73 (5). 2010. pp. 805 - 814.

307. Lyuboshitz, V. L., Lyuboshitz, V. V. Spin structure of the “forward” nucleon charge-exchange reaction $n + p \rightarrow p + n$ and the deuteron charge-exchange breakup // Материалы сессии-конференции секции ядерной физики ОФН РАН. ИТЭФ, г. Москва, 23 – 27 ноября 2009 г. // Ядерная

физика, т. 74 (2), 2011 (направлено печать).

308. Кобзев, А. П., Механизм излучения Вавилова – Черенкова // Физика элементарных частиц и атомного ядра. 2010. Т. 309.

41. Вып.3, с.830 – 867. A.P.Kobzev The Mechanism of Vavilov – Cherenkov Radiation // Physics of Particles and Nuclei. 2010. V. 41. No. 3. pp. 452 – 470.

3. Applied research

310. Гуляев, В. В. и др. Изменение морфологии, элементного и фазового состава поверхности ниобата лития после плазмохимического и радикального травления // Вестник воронежского государственного технического университета. 2010. Т. 6 (9).

311. Bunatian, G. G. et al. On the usage of electron beam as a tool to produce radioactive isotopes in photo-nuclear reactions // Communication of JINR E6-2009-182, 2010 (submitted to "NIM A").

312. Bunatian, G. G. et al. The usage of electron beam to produce radio isotopes through the uranium fission by gamma-rays and neutrons // Communication of JINR E6-2010-86.

313. Adam, W. J. et al. Study of Deep Subcritical Electronuclear Systems and Feasibility of Their Application for Energy Production and Radioactive Waste Transmutation // Preprint JINR. 2010. E1-2010-61.

314. Frontasyeva, M. V. et al. Algae for the production of pharmaceuticals // Chapter to the book "Bioprocesses Sciences and Technology", ed. by Columbus, F. 2010. PP. 119-142. ISBN 978-1-61122-950-9.

315. Фронтасьева, М. В. Нейтронный активационный анализ в науках о жизни // Обзор: Физика элементарных частиц и атомного ядра. 2010 (принято печать). (Frontasyeva, M. V. Neuitron activation analysis for the Life Sciences // A review. Accepted by "Physics of Elementary Particles and Atomic Nuclei". 2010)

316. Frontasyeva, M. V. et al. NAA for applied investigations at FLNP JINR: present and future. // J. of Radioanalytical and Nuclear Chemistry. 2010. V. 286 (2), pp. 519-524. Doi: 10.1007/s10967-010-0814-z.

317. Tsibakhashvili, N., Meerten, van, Th. G. NAA for studying detoxification of Cr and Hg by Arthrobacter globiformis 151B // J. of Radioanalytical and Nuclear Chemistry. 2010. V. 286 (2), pp. 533–537. Doi: 10.1007/s10967-010-0815-y.

318. Popovic, D. et al. Concentration of trace elements in blood and feed of homebred animals in Southern Serbia // Env. Sci. & Pollution Research. 2010. V. 17 (5), pp. 1119-1128.

319. Marinova, S. et al. Air pollution studies in Bulgaria using the moss biomonitoring technique, NAA and AAS // Ecol. Chem. & Engineering. 2010. V. 17 (1), pp. 37-52.

320. Dimovska, S. et al. Distribution of some natural and man-made radionuclides in soil from the city of Veles (Republic of Macedonia) and its environs // Radiation Protection Dosimetry. 2010. V. 138, pp. 144-157.

321. Stafilov, T. et al. Heavy metal contamination of surface soils around a lead and zinc smelter in the Republic of Macedonia // J. of Hazardous Materials, Elsevier. 2010. V. 175 (1-3), pp. 896-914.

322. Nguyen Viet H. et al. Atmospheric heavy metal deposition in Northern Vietnam: Hanoi and Thainguyen case study using the moss biomonitoring technique, INAA and AAS // Env. Sci. & Pollution Research. 2010. V. 17. (5), pp. 1045-1052.

323. Marinova, S. et al. The moss techniques for air pollution study in Bulgaria // AIP Conference Proceedings. 2010. V. 1203, pp. 777-782.

324. Frontasyeva, M. V. et al. Some results of application of INAA and AAS in the environmental research in Slovakia // Acta Physica Universitatis Comenianae. 2010 V. L-LI . pp. 155-161.

325. Merešová, J. et al. Air pollution studies in Slovakia using aerosol filters and biomonitoring technique // Ekológia (Bratislava). 2010. V. 29 (3), pp. 294-306.

326. Горелова, С. В. и др. Оценка возможности использования древесных растений для биоиндикации и биомониторинга выбросов предприятий металлургической промышленности // Проблемы биогеохимии и геохимической экологии. 2010. № 1(12), с. 155-163. (Gorelova, S. V. et al. Assessment of possibility to use woody plants for bioindication and biomonitoring emissions of metallurgical industry // Problems of Biogeochemistry and Geochemical Ecology. 2010. N. 1(12), pp. 155-163).

327. Grabovsky, V. et al. Low background measurements of bottom sediments of the Carpathian Rivers: technogenic and natural factors // Problems of Nuclear Power Plants Safety and of Chornobyl. 2010. V. 14, pp. 126-134.

328. Biziuk, M. et al. Nuclear Activation Methods in the estimation of environmental pollution and the assessment of the industrial plant impact on the citizens of Gdansk (Poland) // LANL: Analytical Letters. 2010. V. 43 (7), pp. 1242-1256.

329. Ильченко, И. Н. и др. Концентрации токсичных, потенциально токсичных и эссенциальных элементов в крови московских женщин и риск развития низкой массы тела // Профилактическая медицина. 2010. Т. 13 (1), с. 7-12. (Ilchenko, I. N. et al. Concentrations of toxic, potentially toxic and essential elements in blood of Moscow women and risk of development of low body mass index // Preventive Medicine. 2010. V. 13 (1), pp. 7-12).

330. Harmens, H. et al. Air Pollution and Vegetation: ICP Vegetation Annual Report 2009/2010. 2010. 40 pp.

331. Holy, M. et al. First thorough identification of factors associated with Cd, Hg and Pb concentrations in mosses sampled in the European Surveys 1990, 1995, 2000 and 2005 // J. of Atmospheric Chemistry. 2010. V. 63 (2), pp. 109-124.

332. Schröder, W. et al. Are cadmium, lead and mercury concentrations in mosses across Europe primarily determined by atmospheric deposition of these metals // J. of Soils and Sediments. 2010. V. 10, pp. 1572–1584. Doi 10.1007/s11368-010-0254-y.

333. Harmens, H. et al. Mosses as biomonitors of atmospheric heavy metal deposition: spatial and temporal trends in Europe // Environmental Pollution. 2010. V. 158 (10), pp. 3144-3156.

334. Aleksiayenak, Yu.V. et al. Atmospheric deposition of radionuclides in Belurus: 20 years after Chernobyl // Proceedings of the XVII International Seminar on Interaction of Neutrons with Nuclei. 2010. E3-2010-36, pp. 78-84, Dubna.

335. Duliu, O.G. et al. Epithermal neutron activation analysis of some geological samples of different origin // Proceedings of The 7th International Conference of the Balkan Physical Union, edited by A. Angelopoulos and T. Fildisis, American Institute of Physics. 2010. Proceedings Series # CP1203. pp. 489-494.

336. McIntyre, G. et al. Modulated Crystal structures of phases VII and V in (NH4)3H(SO4)2 // Neutron Laue Diffrection. 2010 (accepted for publication in Crystallography).

337. Tsibakhashvili, N. et al. Microbial synthesis of silver nanoparticles // International Journal of NANO RESEARCH. 2010 (submitted).

338. Duliu, O.G. et al. On the heavy elements content of sediments and rocks from two semiclosed ecosystems: proglacial lake Bâlea (Fagaras Mountanins) and crater lake St. Ana (Harghita Mountains) // Geologica Carpathica. 2010 (submitted).
339. Gorelova, S.V. et al. Revitalization of urban ecosystems through vascular plants: preliminary results from the BSEC-PDF project // International Journal AGROCHIMICA: Proceedings of International Conference on Environmental Pollution and Clean Bio/Phytoremediation, CEPR. 2010 (submitted).
340. Spiric, Z. et al. Multielement atmospheric deposition study in Croatia // International Journal of Environmental Analytical Chemistry. 2010 (submitted).
341. Aleksiayenak, Yu.V. et al. Distribution of 137Cs and 210Pb in moss collected from Belarus and Slovakia // J. of Env. Radioactivity. 2010 (submitted).
342. Krmar, M. et al. Airborne radionuclides in mosses collected at different latitudes // J. of Env. Radioactivity. 2010 (submitted).
343. Duliu, O.G. et al. On the elemental and mineralogical composition of some sediments collected from the anoxic shelf of the Black Sea // Geo-Marine Letters (Springer). 2010 (submitted).
344. Baljinnyam, N. et al. Epithermal neutron activation analysis of the Asian herbal plants // American Institute of Physics Conference Proceedings Series. 2010 (submitted).
345. Borzakov, S. B. et al. The Investigation of the Rare Metal Content in the Geological Samples from Mongolia on the IREN Facility // American Institute of Physics Conference Proceedings Series. 2010 (submitted).

Reports at Schools and Conferences

346. Gledenov, Yu. M., Sedysheva, M. V., Stolupin, V. A., et al. Cross Section Measurement for the 143Nd(n,α)140Ce Reaction at 4.0, 5.0 and 6.0 MeV. In: Proc. of the 17 International Seminar on Interaction of Neutron with Nuclei (ISINN-17), Dubna, 2010) E3-2010-36, pp. 323-330.
347. Guohui Zhang, Hao Wu, Jiaguo Zhang, et al. Cross Section Measurement for the 95Mo(n,α)92Zr Reaction at 4.0, 5.0 and 6.0 MeV. In: Proc. of the 17 International Seminar on Interaction of Neutron with Nuclei (ISINN-17), Dubna, 2010) E3-2010-36, pp. 331-336.
348. Khuukhenkhuu, G., Gledenov, Yu. M., Sedysheva, M. V., et al. Analysis of averaged (n,p) reaction cross sections for fission neutron spectrum. In: Proc. of the 17 International Seminar on Interaction of Neutron with Nuclei (ISINN-17), Dubna, 2010) E3-2010-36, pp. 337-341.
349. Gledenov, Yu. M., Guohui Zhang, Koehler, P. E., et al. Investigation of (n,α) Reaction for Rare-Earth Elements in the MeV Neutron Energy Region. ND2010 Intern.Conf. on Nuclear Data for Science & Technology. 26-30 April, 2010, Jeju Island, Korea. Abstract Book, p. 17.
350. Guohui Zhang, Gledenov, Yu. M., Jiaguo Zhang, et al. 64Zn and 67Zn (n,α) Reactions in the MeV Neutron Energy Region. ND2010 Intern.Conf. on Nuclear Data for Science & Technology. 26-30 April, 2010, Jeju Island, Korea. Abstract Book, p. 210.
351. Khuukhenkhuu, G., Gledenov, Yu. M., Odsuren, M., et al. Statistical Model Analysis of (n,p) Cross Sections Averaged over the Fission Neutron Spectrum. ND2010 Intern.Conf. on Nuclear Data for Science & Technology. 26-30 April, 2010, Jeju Island, Korea. Abstract Book, p. 254.
352. Khuukhenkhuu, G., Gledenov, Yu. M., Sedysheva, M. V., et al. (n,α) reaction cross section and alpha decay probability of nucleus. In: Abstracts of the 18 International Seminar on Interaction of Neutron with Nuclei (ISINN-18), Dubna, 2010. E3-2010-49, p. 34.
353. Lee, M., Kim, K. S., Yang, S. C., et al. Measurement of neutron total cross-sections for Dy with a new DAQ system based on FADC. 18th Int. Seminar on Interaction of Neutrons with Nuclei, Dubna, Russia, 26-29 May, 2010.
354. Кобзев, А. П., Вахтель, В. М. Глубинное разрешение ядерно – физической аналитической методики РОР. XVIII Международная конференция по электростатическим ускорителям и пучковым технологиям. 19-22 октября 2010г. Обнинск.
355. Huran, J., Balalykin, N. I., Shirkov, G. D., et al. Nanocrystalline Diamond/amorphous Composite Carbon Films Prepared by PECVD Techno;ogy for Photocathode Applications. 8-th International Conference on Advanced Semiconductor Devices and Microsystems. 25-27 October, 2010, Smolenice, Slovakia.
356. Bohacek, P., Huran, J., Valovich, A., et al. N-doped Nanocrystalline Silicon Carbide Films Prepared by PECVD Technology. 8-th International Conference on Advanced Semiconductor Devices and Microsystems. 25-27 October, 2010, Smolenice, Slovakia.
357. Gagarski, A., Goennenwein, F., Guseva, I., et al. First observation of the ROT-effect of LCP emission asymmetry in the 239Pu ternary fission induced by the cold polarized neutrons, in Proc. XVII International Seminar on Interaction of Neutron with Nuclei (ISINN-17), Dubna, 27-29 May, 2009, Dubna, 2010, p.17.
358. Kopatch, Yu., Prokhorova, E., Itkis, J., et al. Search for Angular Correlations Between Fragment Spins and Prompt Neutrons in Spontaneus Fission of 252Cf , In: Proc. of the 17 International Seminar on Interaction of Neutron with Nuclei (ISINN-17), Dubna, 2010. p.71.
359. Gönnenwein, F., Gagarski, A., Petrov, G., et al. Tri And Rot Effects In Ternary Fission: What Can Be Learned?, in Proc. International Symposium on Exotic Nuclei (EXON-2009), Sochi, Russia, 28 September – 2 October, 2009, AIP, 2010, p. 338.
360. Kamanin, D. V., Pyatkov, Yu. V., Kuznetsova, E. A., et al. Collinear Cluster Tripartition as a Neutron Source—Evaluation of the Setup Parameters, n Proc. International Symposium on Exotic Nuclei (EXON-2009), Sochi, Russia, 28 September – 2 October, 2009, AIP, 2010. pp. 385.
361. Kamanin, D. V., Pyatkov, Yu. V., Kopach, Yu. N., et al. Collinear Cluster Tripartition in the Light Nuclear Charge and Neutron Multiplicity Measurements in Proc. International Symposium on Exotic Nuclei (EXON-2009), Sochi, Russia, 28 September – 2 October, 2009, 11/ 1/2010. pp.105.
362. Sukhovoj, A. M., Khitrov, V. A. Estimation of maximum permissible errors in the total gamma-spectra intensities at determination from them of level density and radiative strength functions, In: XVII International Seminar on Interaction of Neutrons with Nuclei, Dubna, May, 2009, E3-2010-36, Dubna, 2010. pp. 268-281.
363. Sukhovoj, A. M., Khitrov, V. A., Mezentseva, Zh. V. The possibility of experimental determination of interaction cross-section of nucleon with excited nucleus, In: XVII International Seminar on Interaction of Neutrons with Nuclei, Dubna, May 2009, E3-2010-36, Dubna, 2010. pp. 282-295.
364. Sukhovoj, A. M., Khitrov, V. A. Partial density of n-quasi-particle excitations and experimental estimation of coefficient of vibration enhancement of neutron resonances density, In: XVII International Seminar on Interaction of Neutrons with

Nuclei, Dubna, May, 2009, E3-2010-36, Dubna, 2010. pp. 296-307.

365. Sukhovoj, A. M., Khitrov, V. A. On problems of experimental determination of reliable values of nucleus parameters at low excitation energy -- 60Ni as an example, In: XVII International Seminar on Interaction of Neutrons with Nuclei, Dubna, May 2010, Abstracts, E3-2010-49, Dubna, 2010. p. 46.

366. Sukhovoj, A. M., Khitrov, V. A. Some practical limits on achievable precision of some of nuclear-physics parameters determination, In: XVII International Seminar on Interaction of Neutrons with Nuclei, Dubna, May 2010, Abstracts, E3-2010-49, Dubna, 2010. p. 47.

367. Sukhovoj, A. M., Khitrov, V. A. Parameters of the best approximation for distribution of the reduced neutron widths. Specific of full-scale method of analysis, In: XVII International Seminar on Interaction of Neutrons with Nuclei, Dubna, May 2010, Abstracts, E3-2010-49, Dubna, 2010. p. 48.

368. Sukhovoj, A. M., Khitrov, V. A. Parameters of the best approximation for distribution of the reduced neutron widths. Actinides, In: XVII International Seminar on Interaction of Neutrons with Nuclei, Dubna, May, 2010, Abstracts, E3-2010-49, Dubna, 2010. p. 49.

369. Sukhovoj, A. M., Khitrov, V. A. Parameters of the best approximation for distribution of the reduced neutron widths. The most probable density of neutron resonances in actinides, In: XVII International Seminar on Interaction of Neutrons with Nuclei, Dubna, May 2010, Abstracts, E3-2010-49, Dubna, 2010. p. 50.

370. Enik, T. L., Mitsyna, L. V., Nikolenko, V. G., et al. Preparation for testing experiment on IREN neutron beam. In: Proceedings of XVII Int. Seminar on Interaction of Neutrons with Nuclei, Dubna, 27-29 May, 2009, E3-2010-36, 2010. pp.162.

371. Popov, A. B. An influence of hypothetical extra-short-rage interaction on the scattering anisotropy of cold neutrons by noble gases. In: Proceedings of XVII Int. Seminar on Interaction of Neutrons with Nuclei, Dubna, 27-29 May, 2009, E3-2010-36, 2010. p. 383.

372. Ignatovich, V. K. Nikitenko, Yu. V. T-odd correlation in a neutron reflectometry experiment. In: XVII nternational Seminar on Interaction of Neutrons with Nuclei, Dubna, May, 2009, E3-2010-36, Dubna, 2010. pp. 237-246.

373. Ignatovich, V. K. Reflection of neutrons from a magnetic mirror with helicoidal magnetization and a dispute with aps of usa on linear algebra . Ucn2010 International Workshop on UCN and Fundamental Neutron Physics, RCNP, April, Osaka, Japan.

374. Ignatovich, V. K. On epr paradox, bell□s inequalities and experiments that prove nothing. (oral), contradictions of the quantum scattering theory (poster), Advances in Foundations of Quantum Mechanics and Quantum Information with atoms and photons, QUANTUM 2010, Inrim, May, Turin, Italy.

375. Stephenson, S. L., Crawford, B. E., Yager-Elorriaga, D. A., et al. Problem In The nn- Experiment At The YAGUAR Reactor // Neutron Spectroscopy, Nuclear Structure, Related Topics; ISINN-17 Dubna, 27-29 May, 2009, JINR Report E3-2010-36, pp. 390-395.

376. Strelkov, A. Low-background counters of ultracold neutrons. GRANIT 2010, Les Houches – France, 14-19 February 2010.

377. Muzychka, A. Large-size real-time position-sensitive detectors with 100 micrometer resolution. GRANIT 2010, Les Houches – France, 14-19 February, 2010.

378. Lychagin, E. Nanoparticle reflectors for cold and very cold neutrons. GRANIT 2010, Les Houches – France, 14-19 February, 2010.

379. Lychagin, E. Reflectors for GRANIT source of ultracold neutrons. GRANIT 2010, Les Houches – France, 14-19 February, 2010.

380. Verkhogliadov, A. E., Lychagin, E. V., Muzychka, A. Yu., et al. Poster “A method of “External cold neutron source” for UCN production in superfluid 4He” // Neutron Spectroscopy, Nuclear Structure, Related Topics; ISINN-18 Dubna, 26-29 May, 2010.

381. Музычка, А. Ю. Эксперимент по прямому измерению сечения nn- рассеяния на реакторе ЯГУАР // XXI совещание по использованию рассеяния нейтронов в исследованиях конденсированного состояния РНИКС-2010, Москва, 16-19 ноября 2010.

382. Shvetsov, V. N., Sharapov, E. I., Stephenson, S. L., et al. Comparison of calculated and measured yields of medical isotopes produced by electron bremsstrahlung. Proceedings of the XVII International Seminar on Interaction of Neutrons with Nuclei: ISINN-17, Dubna, E3-2010-36, JINR, Dubna, 2010, p. 172.

383. Crawford, B. E., Furman, W. I., Lychagin, E. V. et al. A Model of the gamma-ray induced outgassing in the n-n scattering expreriment at YAGUAR. XVIIIШ International Seminar on Interaction of Neutrons with Nuclei: ISINN-18 Abstracts, E3-2010-49, JINR, Dubna, 2010. p. 21.

384. Gan, K., Micherdzinska, A. M., Opper, A. M., et al: nHe-4 Collaboration. Computer simulation of systematic effects for neutron spin rotation in liquid helium. American Physical Society Meeting, February 13-16, 2010, Abstracts p. H8-005.

385. Furman, W. Quantum aspects of low energy nuclear fission, In “Seminar on Fission, Het Pand, World Scientific, Ed. J. Wagemans, p. Seminar on fission VII, Het Pand, Belgium, 16-20 May 2010, W.S. Ed. J. Wagemans and C. Wagemans.

386. Belloni, F., Milazzo, P. M., Calviani, M. et al. Neutron-induced fission cross sections of 233U and 243Am in the energy range 0.5 Mev En 20 MeV @ n_TOF / n_TOF Collaboration In Proc. 12th International Conference on Nuclear Reaction Mechanisms, Villa Monastero, Varenna, Italy, 15- 9 June 2009, pp. 231-238.

387. Furman, W., Baldin, A., Chinenov, A. et al. Time-dependent spectra of neutrons emitted by interaction of 1 and 4 GeV deuterons with massive natural uranium and lead targets. Proc. Int. Conf. “Nuclear Data for Science and Technology”, Jeju island, Korea, 26-29 April, 2010, ND1067, in press.

388. Guerrero, C.: nTOF Collaboration. Study of Photon Strength Functions of Actinides: the case of U-235, Np-238 and Pu-241, Proc. Int. Conf. “Nuclear Data for Science and Technology”, Jeju island, Korea, 26-29 April, 2010, ND1067, in press.

389. Calviani, M.: nTOF Collaboration. Fission cross-section measurements of U-233, Cm-245 and Am-241,243 at the CERN n_TOF facility, Proc. Int. Conf. “Nuclear Data for Science and Technology”, Jeju island, Korea, 26-29 April, 2010, ND1067, in press.

390. Furman, W., Andrukhovich, S., Baldin, A.et al. Energy and time-dependent neutron spectra in interaction of 1 and 4 GeV deuterons with massive uranium and lead targets. Talk at ISINN18, Dubna, 25-29 May, 2010.

391. Furman, W., Baldin, A., Gundorin, N.et al. Massive 238U target as new type of ADS core – first results and perspectives. Invited talk at 8-th Asian ADS Symposium , Suwon, Korea, 25-26 October 2010.

392. Фурман, В. И., Нейтроно-производящие подкритические системы, инициируемые ускорителями, Приглашенный обзорный доклад на РНИКС-2010, Москва, РНЦ КИ. 16 ноября 2010.

393. Baldin, A., Furman, V., Gundorin, N. et al., Basic principles

of relativistic nuclear technology (RNT) and first results of experiments on its physical justification, 20th Baldin International Seminar on High Energy Physics Problems «Relativistic Nuclear Physics and Quantum Chromodynamics», 4-9 October 2010, Dubna.

394. Hambsch, F.-J., Oberstedt, S., Al-Adili, A., et al. Investigation of the fission process at irmm. International Conference on Nuclear Data for Science and Technology, 26-30 April 2010, Jeju Island, 2010, S.Korea.

395. Zeynalov, Sh., Hambsch, F.-J., Oberstedt, S., et al. Netron emission in fission of 252CF(SF). International Conference on Nuclear Data for Science and Technology, 26-30 April 2010, Jeju Island, 2010, S.Korea.

396. Hambsch, F.-J., Oberstedt, S., Zeynalov, Sh. Prompt neutron emission in fission of 252Cf(SF), SEMINAR ON FISSION, 17-20 May, Gent University, Belgium.

397. Zeynalov, Sh. Recent achievements in application of Dpp to fission fragment spectroscopy. Technical Meeting on Instrumentation for Digital Spectroscopy (TM-39362), Organized by International Atomic Energy Agency, Vienna, Austria, 11-15 October 2010.

398. Zeynalov, Sh., Zeynalova, O., Hambsch, F.-J., et al. Recent results from investigation of prompt fission neutron (PFN) emission in spontaneous fission of 252Cf. NEMEA-6 international workshop, organized by EC-JRC-IRMM, Krakow, Poland, 21-26 october 2010.

399. Зейналова, О., Зейналов, Ш., Хамбш, Ф.-Й., и др. Двойная позиционно-чувствительная ионизационная камера с использованием backgammon и времяпроекционного методов, LX Международная конференция «Ядро—2010. Методы ядерной физики для фемто- и нанотехнологий» (LX Совещание по ядерной спектроскопии и структуре ядра). 6–9 июля 2010 года, Петергоф, Санкт-Петербургский государственный университет.

400. Lyuboshitz, V. L., Lyuboshitz, V. V. Low-energy elastic scattering of a polarized neutron on a polarized deuteron. Talk at ISINN-18 (Dubna, 26-29 May, 2010); Proceedings of ISINN-18, Dubna, 2011 – to be published.

401. Lyuboshitz, V. L., Lyuboshitz, V. V. Sign of the singlet length of (np)-scattering, neutron radiative capture by the proton and problem of the virtual level of the (np) system" . Talk at the International Conference on Nuclear Physics "NUCLEUS-2010" –60-th International Meeting on Nuclear Spectroscopy and Nuclear Structure, Saint-Petersburg, Peterhof, Russia, 6-9 July, 2010.

402. Lyuboshitz, V. L., Lyuboshitz, V. V. Low-energy elastic scattering of a polarized neutron on a polarized proton. Poster presentation at the International Conference on Nuclear Physics "NUCLEUS-2010" – 60-th International Meeting on Nuclear Spec-troscopy and Nuclear Structure, Saint-Petersburg, Peterhof, Russia, 6-9 July, 2010.

403. Lyuboshitz, V. L., Lyuboshitz, V. V. Sign of the singlet (np)-scattering length, neutron radiative capture by the proton and problem of the virtual level of the (np) system. Talk at the 21-st European Conference on Few-Body Problems in Physics – EFB21 (Salamanca, Spain, 29 August – 3 September, 2010); will be published in Proceedings of EFB21, Few-Body Systems, 2011.

404. Lyuboshitz, V. L., Lyuboshitz, V. V. The medium with polarized nuclei and effects of low-energy neutron refraction and reflection. Proceedings of the XVII International Seminar on Interaction of Neutrons with Nuclei – ISINN-17 (Dubna, 27-30 May, 2009), JINR E3-2010-36, Dubna, 2010, pp. 247 - 259.

405. Lyuboshitz, V. L., Lyuboshitz, V. V. Spin correlations of the electron and positron in the two-photon process $\gamma\gamma \rightarrow e + e$ -. Proceedings of the XIII Advanced Research Workshop on High Energy Spin Physics – DSPIN-09 (Dubna, 1-5 September, 2009) , JINR E1,2-2010-13 , Dubna, 2010, pp. 91-94 .

406. Lyuboshitz, V. L., Lyuboshitz, V. V. Spin correlations in the $\Lambda\Lambda$ and $\Lambda\overline{\Lambda}$ systems generated in relativistic heavy-ion collisions. Proceedings of the 13-th International Conference on Elastic and Diffractive Scattering – EDS'09 (CERN, Geneva, Switzerland, 29 June – 3 July, 2009) , CERN-Proceedings-2010-002, Geneva, 2010, pp. 365 – 371.

407. Lyuboshitz, V. V., Lyuboshitz, V. L. On the coherent inelastic binary and multiparticle processes in the ultrarelativistic hadron–nucleus, photon–nucleus and nucleus–nucleus interactions. Talk at the XVIII International Workshop on Deep Inelastic Scattering and Related Subjects – DIS 2010, Florence, Italy, 19-23 April, 2010.

408. Lyuboshitz, V. L., Lyuboshitz, V. V. Possible effect of mixed phase and decon-finement upon spin correlations in the $\Lambda\overline{\Lambda}$ pairs produced in relativistic heavy ion collisions. Talk at the XVIII International Workshop on Deep Inelastic Scattering and Related Subjects – DIS 2010, Florence, Italy, April 19-23, 2010.

409. Lyuboshitz, V. L., Lyuboshitz, V. V. Possible effect of mixed phase and decon-finement upon spin correlations in the $\Lambda\overline{\Lambda}$ pairs generated in relativistic heavy-ion collisions. Talk at the XX International Baldin Seminar on High Energy Physics Problems – ISHEPP-20, Dubna, 4-9 October, 2010.

410. Lyuboshitz, V. L., Lyuboshitz, V. V. Possible effect of mixed phase and decon-finement upon spin correlations in the $\Lambda\overline{\Lambda}$ pairs generated in relativistic heavy-ion collisions. Poster presentation at the 35-th International Conference on High Energy Physics – ICHEP 2010, 35-th Rochester Conference, Paris, France, 22-28 July, 2010.

411. Lyuboshitz, V. L., Lyuboshitz, V. V. Spin correlations of muons and tau leptons produced in the annihilation processes $e + e - \rightarrow \mu + \mu -$, $e + e - \rightarrow \tau + \tau -$ ". Poster presentation at the 21-st European Conference on Few-Body Problems in Physics – EFB21, Salamanca, Spain, 29 August – 3 September , 2010.

412. Lyuboshitz, V. L., Lyuboshitz, V. V. Polarization effects in the reactions $p + 3He \rightarrow \pi + + 4He$, $\pi + + 4He \rightarrow p + 3He$ and quantum character of spin correlations in the final (p, 3He) system. Poster presentation at the 21-st European Conference on Few-Body Problems in Physics – EFB21, Salamanca, Spain, 29 August – 3 September, 2010.

413. Frontasyeva, M. V., Gorelova, S. V., Yurukova, L., et al. Revitalization of urban ecosystems through vascular plants: preliminary results from the BSEC-PDF project. Book of Abstracts, International Conference on Environmental Pollution andClean Bio/Phytoremediation, CEPR, 16-19 June, 2010, Pisa, Italy.

414. Gorelova, S. V., Garifzyanov, A. R., Frontasyeva, M. V., et al. Physiological stability as a factor for selection of woody plants for phytoremediation and biomonitoring. Book of Abstracts, Conference on Environmental Pollution and Clean Bio/Phytoremediation, CEPR, 16-19 June, 2010, Pisa, Italy.

415. Frontasyeva, M. V., Pavlov, S. S., Culicov, O., et al. Assessment of exposure to toxic/potentially toxic elements in women of fertile age with different nutritional status in one selected district of Moscow using nuclear and related analytical techniques. Book of Abstracts of The 4th International Symposium on Trace Elements and Minerals in Medicine and Biology, FESTEM, St. Petersburg, Russia, 9-13 June, 2010.

416. Frontasyeva, M. V. NAA FOR Life Sciences at FLNP JINR: present and future. Book of Abstracts, ISINN-18, 26-29 May,

2010, Dubna, p. 25.

417. Baljinnyam, N., Jugder, B., Ganbold, G., et al. Epithermal neutron activation analysis of the Asian herbal plants. Book of Abstracts, ISINN-18, 26-29 May, 2010, Dubna, p. 15.

418. Gorelova, S. V., Frontasyeva, M. V., Lyapunov, S. M., et al. Biogeochemical variability of bushes in technogenic stress conditions using studied by instrumental neutron activation analysis. Book of Abstracts, ISINN-18, 26-29 May, 2010, Dubna, p. 27.

419. Сватюк, Н. И., Стец, М. В., Маслюк, В. Т., и др. Кластерный и факторный анализ данных радиоэкологических исследований рек Закарпатья. Сборник абстраектов. VIII конференции по физике высоких энергий, ядерной физике и ускорителям, Харьков, 2010, с. 38-39.

420. Frontasyeva, M. V. Radioanalytical investigations at FLNP JINR for Life Sciences. Book of Abstracts, Int. Conf. on Radiochemistry. Marianske Lazne, Czech Rep., 18-21 April, 2010.

421. Tsibakhahsvili, N., Mosulishvili, L., Kirkesali, E., et al. NAA for studying detoxification of Cr and Hg by Arthrobacter globiformis. Book of Abstracts, Int. Conf. on Radiochemistry. Marianske Lazne, Czech Rep., 18-21 April, 2010.

422. Pantelica, A., Culicov, O., Frontasyeva, M. V., et al. Elemental concentrations in vegetable species from industrial zones in Romania determined by INAA. Book of Abstracts, Int. Conf. on Radiochemistry. Marianske Lazne, Czech Rep., 18-21 April, 2010.

423. Frontasyeva, M. V., Nguyen-Viet, H., Trinh Thi M., et al. Atmospheric heavy metal deposition in Northern Vietnam: Hanoi and Thainguyen case study using the moss biomonitoring technique, INAA and AAS. Book of Abstracts, The 23rd Task Force Meeting UNECE ICP Vegetation, 1-3 February, 2010, Tervuren, Belgium.

424. Spiric, Z., Frontasyeva, M. V., Steinnes, E., et al. Multielement atmospheric deposition study in Croatia. Book of Abstracts, The 23rd Task Force Meeting UNECE ICP Vegetation, 1-3 February, 2010, Tervuren, Belgium.

425. Stafilov, T., Šajn, R., Pančevski, Z., et al. Distribution of heavy metals in surface soil due to industrial pollution, Invited Lecture, Serminar “Microanalytical techniques in applied Earth sciences”, Belgrade, 2010.

426. Stafilov, T., Šajn, R., Pančevski, Z., et al. Contamination of topsoil in veles region, republic of macedonia, 3rd Slovenski geološki kongres, Bovec, 16-18 September, 2010, Abstracts, pp. 46-47.

427. Dimovska, S., Stafilov, T., Šajn, R., et al. Distribution of some natural and man-made radionuclides in soil from the city of Veles (Republic of Macedonia) and its environs, XXI Congress of Chemists and Technologists of Macedonia, Book of Abstracts, ACE-14, Ohrid, 2010. p. 60.

428. Stafilov, T., Barandovski, L., Pančevski, Z., et al. Monitoring of the pollution with heavy metals using INAA, ICP-AES and AAS. The results from the studies in the Republic of Macedonia. Book of Abstracts, International Symposium on In Situ Nuclear Metrology as a Tool for Radioecology (INSINUME’2010), 20-23 October 2010, Dubna, Russia, p. 88.

6. PRIZES

Kozlenko D.P.

The Grant of the President of the Russian Federation on the state support of scientific research activities of young D.Sci. scientists (МД-696.2010.2).

The Commendation Letter from the Governor of the Moscow region for great scientific and technical achievements and a significant contribution to the development of the scientific and industrial complex of the Moscow region.

Project “Cryogenic moderator-cold neutron source for investigation of nanostructures”

Winner in the «IX contest “Russian innovations”» category “Promising project”

Winner in CIS Open contest “Young innovation projects in the field of humanitarian, natural and technical sciences”

JINR PRIZES

Scientific and technical applied research:

First Prize

«New theoretical and experimental investigations of seismic properties of the Earth’s lithosphere on the basis of neutron diffraction data»
Authors: T.I. Ivankina, V. K. Ignatovich, H. Kern, T. Lokajicek , A. N. Nikitin, L.T.N. Phan, K. Ullemeyer, R. N. Vasin.

Encouraging prize

«Investigations of cluster formation in liquid solutions of fullerenes».
Authors: M.V. Avdeev, V.L. Aksenov, E.A. Kyzyma, T.V, Tropin, A.A. Khokhryakov, L.A. Bulavin, L. Rosta, M.V. Korobov, V.B. Priezzhev, J.W.P Schmelzer.

Experimental physics research:

Second Prizes

«Solution of the scientific problems, related to the creation of the transdermal vesicular drug carriers, by neutron and X-ray scattering».
Authors: M.A. Kiselev, A.M. Balagurov, E.V. Zemlyanaya, E.V. Ermakova, N.Yu. Ryabova, A.M. Kisselev, P. Lesieur, T. Hauss, R. Neubert, V. L. Aksenov

“Measurement of the P-odd asymmetry in emission of tritons in the 6Li(n,α)3H reaction and γ-quanta in the 10B(n,α)7Li*→γ→7Li(g.st.) reaction with cold polarized neutrons”.
Authors: Yu.M. Gledenov, P.V. Sedyshev, V.A. Vesna, E.V. Shulgina, V.V. Nesvizhevsky, T. Soldner.

FLNP PRIZES

Nuclear Physics:

First Prize

Limits on new spin-dependent interactions from longitudinal spin relaxation of polarized ultracold neutrons and polarized ^{3}He
Authors: Yu.N. Pokotilosvky, V.K. Ignatovich

Second Prize

Investigation of prompt fission neutron emission
Author: Sh. Zeinalov

Third Prize

Precise model approximation of the Dubna data on nuclear level density in region 40≤A≤200 below Bn
Authors:A. M. Sukhovoj, V. A. Khitrov

Applied and Methodical Investigations:

Second Prize

The effect of gravity on the resolution for time-of-flight specular neutron reflectivity
Authors: I.A. Bodnarchiuk, S.A. Manoshin, S.P. Yaradaikin, V.Yu. Kazimirov, V.I. Bodnarchiuk

Second Prize

Low energy fission investigation using digital signal processing
Authors: O.V. Zeinalova, Sh. Zeinalov

Condensed Matter Physics:

First Prize

Competition between ferromagnetic and antiferromagnetic ground states in multiferroic $BiMnO_3$ at high pressures
Authors: D.P. Kozlenko, S.E. Kichanov, A.V. Belushkin, B.N. Savenko

Second Prize

Structure research of magnetic fluids using small-angle neutron scattering
Authors: M.V. Avdeev, V.L. Aksenov, V.I. Petrenko, A. Feoktistov

Third Prize

Investigation of influence of the charge transfer on the dynamic properties of the methyl group
Author: A. Pawlukojć

AYSS PRIZES

Methodological and scientific-technical research:
Second Prize R.V. Erhan

Scientific and technical applied research:
Second Prize V.M. Milkov

JINR YOUTH GRANTS

Winners of the competition among the PhD researchers:
R.N. Vasin
T.N. Murugova

Winners of the competition among the researchers:
N.O. Golosova
I.I. Zinkovskaya
N.Yu. Ryabova
A.V. Churakov

Winners of the competition among the specialists:
Yu.K. Bulycheva
A.Ye. Verkhoglyadov
A.V. Kutergin

Winners of the competition among the workers:
D.V. Kokunov

I.M. FRANK FELLOWSHIPS (FLNP)

In Neutron Nuclear Physics
K.N. Vergel

In Condensed Matter Physics
Ye.V. Ermakova

In Methodical Investigations
M.V. Bulavin

F.L. SHAPIRO FELLOWSHIPS (FLNP)

In «Polarized Neutrons»
A.V. Feoktistov

In «Neutron Spectroscopy»
N.V. Rebrova

F.L. SHAPIRO FELLOWSHIPS (UC)

A.V.Nagornyi
A.V. Belozerov

Ye.S. Reshunova
K.A. Mukhin

7. SEMINARS

Date	Authors	Title
28.01.2010	I.Natkaniec (Henryk Niewodniczański INP of the PAS, Krakow, FLNP JINR)	On the history and main results of the collaboration initiated by Prof. E.A. Janik in 1960 during the preparation for the start-up of the fast pulsed IBR reactor
06.04.2010	V.L. Aksenov, B.L. Aranzon, A.I. Babayev, G.Ye. Belovitskii, V.I. Luschikov, Yu.Ts. Oganesyan, A.V. Strelkov	Memorial Seminar dedicated to F.L. Shapiro, one of the founders and scientific leaders of FLNP
25.10.2010	Acad. D.V.Shirkov (JINR)	N.N.Bogolyubov – a scientist and a teacher
25.10.2010	Corr. Memb. of RAS V.V. Kvardakov (RR Centre “Kurchatov Institute”)	Investigations of functional and nanostructured materials using the synchrotron radiation and neutron scattering techniques
26.10.2010	A.P. Menushenkov (National Research Nuclear University “MEPhI”)	Spectroscopy of X-ray absorption in condensed matter physics and physics of nanostructures
26.10.2010	N.N. Salaschenko (Institute for Physics of Microstruc-tures of the RAS, Nizhny Novgorod)	Problems of precision X-ray optics
27.10.2010	Corr. Memb. of RAS V.I. Agol	Viruses: their place in the nature, diversity, hypotheses explaining their origin
27.10.2010	Corr. Memb. of RAS Ye.A. Gudilin (Moscow State University)	Studying Chemistry using HTSC
28.10.2010	Acad. V.M. Buznik (Innovation Centre “Chernogolovka” of RAS)	Fluoropolymer nanomaterials
28.10.2010	Acad. Yu.Ts.Oganesyan (JINR)	Island of stability of superheavy elements
30.10.2010	Acad. L.A. Bulavin (National Academy of Sciences of Ukraine)	Liquids and liquid systems. Nanofluids

8. ORGANIZATION AND USER INTERACTION

8.1. STRUCTURE OF LABORATORY AND SCIENTIFIC DEPARTMENTS

Directorate:	
Director	*A.V. Belushkin*
Deputy Director	*V.N. Shvetsov*
Deputy Director	*Deleg Sangaa*
Deputy Director	*S.V. Kozenkov*
Chief engineer:	*A.V. Vinogradov*
Scientific Secretary	*O.A. Culicov*
Laboratory Scientific Leader	*V.L. Aksenov*
Advisor to Directorate	*V.D. Ananiev*

Reactor and Technical Departments	**Head**
IBR-2 reactor	Chief engineer: *A.V.Dolgikh*
Mechanical maintenance division	*A.A.Belyakov*
Electrical engineering department	*V.A.Trepalin*
Design bureau	*A.A.Kustov*
Experimental workshops	*A.N.Kuznetsov*

Scientific Departments and Sectors	**Head**
Department of neutron investigation of condensed matter	*D.P. Kozlenko*
Nuclear physics department	*V.N. Shvetsov*
Department of IBR-2 spectrometers complex	*S.A. Kulikov*

Administrative Services
Secretariat
Finances
Personnel

Scientific Secretary Group
Secretariat
Translation
Graphics

DEPARTMENT OF NEUTRON INVESTIGATION OF CONDENSED MATTER

Sub-Division	Title	Head
Sector 1: Neutron Diffraction. Head: *A.M. Balagurov*		
Group No.1	HRFD	*A.M. Balagurov*
Group No.2	DN-2	*A.I. Beskrovnyi*
Group No.3	DN-12	*B.N. Savenko*
Group No.4	Geomaterials	*A.N. Nikitin*
Group No.5	SKAT /Epsilon	*Ch. Scheffzük*
Sector 2: Neutron Optics. Head: *M.V. Avdeev*		
Group No.1	Physics of Surfaces	*Yu.V. Nikitenko*
Group No.2	Physics of Nanostructures	*M.V. Avdeev*
Small angle scattering group		*A.I. Kuklin*
Inelastic scattering group		*I.Natkaniec*

NUCLEAR PHYSICS DEPARTMENT

Sub-Division	Title	Head
Sector 1. Correlation γ-spectroscopy and development of experimental installations. Head: *N.A.Gundorin*		
Sector 2. Investigation of neutron properties. Head: *Ye.V. Lychagin*		
Sector 3. Neutron activation analysis. Head: *M.V.Frontasyeva*		
Group No.1	Analytical	*M.V. Frontasyeva*
Group No.2	Experimental	*S.S. Pavlov*
Group No.4	**Fission**	*Yu.N. Kopatch*
Group No.5	**Proton and α-decay**	*Yu.M. Gledenov*
Group No.6	**Polarized neutrons and nuclei**	*V. P. Skoy*

DEPARTMENT OF IBR-2 SPECTROMETERS COMPLEX

Sub-Division	Title	Head
Group No.1	Detectors	*A.V. Churakov*
Group No.2	Electronics	*A.A. Bogdzel*
Group No.3	Information technologies	*A.S. Kirilov*
Group No.4	Sample environment and choppers	*A.P. Sirotin*
Group No.5	Cryogenic investigations	*A.N. Chernikov*
Group No.6	Methodical developments	-
Group No.7	Cold moderators	*S.A. Kulikov*

8.2. MEETINGS AND CONFERENCES

In 2010, FLNP organized the following meetings:

- *18th International Seminar on Interaction of Neutrons with Nuclei: "Fundamental Interactions & Neutrons, Nuclear Structure, Ultracold Neutrons, Related Topics", May 26-29.*
- *Anniversary Workshop "50 years from the IBR reactor's startup", June 23.*
- *III Higher Courses of CIS for young scientists, post-graduate and graduate students on advanced methods of research in nanosystems and materials "Synchrotron and Neutron Investigations of Nanosystems (SYN-nano-2009), July 04-17.*
- *II All-Russian Scientific School for Young Scientists and Students "Modern Neutron Diffraction Studies: Interdisciplinary Research of Nanosystems and Materials", October 25 – November 02.*
- *All-Russian Scientific School for Young Scientists and Students "Instruments and Methods of Experimental Nuclear Physics. Electronics and Automatics of Experimental Facilities", November 11-13.*

In the year 2011, FLNP will organize:

- *19th International Seminar on Interaction of Neutrons with Nuclei: "Fundamental Interactions & Neutrons, Nuclear Structure, Ultracold Neutrons, Related Topics".*
- *IV Higher Courses of CIS for young scientists, post-graduate and graduate students on advanced methods of research in nanosystems and materials "Synchrotron and Neutron Investigations of Nanosystems (SYN-nano-2011)" (if a grant of the Intergovernmental Foundation for Educational, Scientific and Cultural Cooperation of the CIS (IFESCCO) is available).*
- *IV All-Russian Scientific School for Young Scientists and Students "Modern Neutron Diffraction Studies: Interdisciplinary Research of Nanosystems and Materials" (if a grant of the Russian Ministry of Education and Science is available).*
- *II All-Russian Scientific School for Young Scientists and Students "Instruments and Methods of Experimental Nuclear Physics. Electronics and Automatics of Experimental Facilities" (if a grant of the Russian Ministry of Education and Science is available).*
- *International Conference "Stress and Texture Investigations by Means of Neutron Diffraction".*
- *User Meeting of the YuMO small-angle neutron scattering spectrometer dedicated to the 75th anniversary of the birth of Yu.M.Ostanevich.*
- *3rd Joint seminar-school JINR-Romania on neutron physics for investigations of nuclei, condensed matter and life sciences.*

8.3. EDUCATION

The objective of the FLNP educational program is the training of specialists in the field of neutron methods for condensed matter and nuclear physics research and in the field of electronics and automatics of experimental installations. More then 20 students from different Russian universities performed their term and diploma works in FLNP during the 2010.

The FLNP successfully collaborated with the JINR University Centre in organization of summer practical work for students from JINR Member States (Czech Republic, Slovakia, Romania, Poland) and Associated countries (Egypt, South Africa). Lessons and excursions at FLNP facilities for teachers of physics from Russia and JINR Member States were organized, too.

Three above mentioned scientific schools for advanced training of young scientists were organized in the Frank Laboratory of Neutron Physics in 2010. Participants the Schools had ample opportunity to establish new scientific contacts with other researchers to enrich their experimental ideas with new research methods. During the guided excursion to the IBR-2 high-flux pulsed reactor, the participants became familiar with this unique facility and the variety of neutron-scattering investigations carried out at FLNP. The Schools were not confined only to the lectures and practical laboratory work. The participants were encouraged to present their own investigations in poster sessions and short oral presentations.

These Schools continued the tradition of the FLNP Schools for young scientists devoted to the fundamental and applied aspects of neutron research in the fields of condensed-matter physics, materials science and related topics.

8.4. COOPERATION

List of Visitors from Member States of JINR and from Non-Member States of JINR in 2010

From Member States of JINR		From Non-Member States of JINR	
Country	**Nr of visitors**	**Country**	**Nr of visitors**
Azerbaijan	2	Germany	13
Bulgaria	2	Latvia	1
Czech Rep.	10	India	1
Mongolia	2	Slovenia	3
Poland	9	Hungary	1
Romania	7	Great Britain	1
Rep. of Korea	4	USA	2
Ukraine	5		

8.5. FINANCE

Financing of the FLNP Scientific Research Plan in 2010

No.	Theme	Financing plan, $ th.	Expenditures For 12 months, $ th.	In % of planned budget
I	**Condensed matter physics**	9430.0	10575.2	112.1
	-1069-	2410.4	2085.5	86.5
	-0851-	5564.2	6991.1	125.6
	-1075-	1455.4	1798.6	123.6
II	**Neutron nuclear physics**	2135.5	2118.6	99.2
	-1036-	2135.5	2118.6	99.2
	TOTAL:	**11565.5**	**12993.8**	**112.3**

8.6. PERSONNEL

Distribution of the Personnel per Department as of 31.12.2010

Theme	Departments	People
-1104-	Nuclear Physics Department and IREN Department	84
-1069-	Department of neutron investigation of condensed matter	74
-1075-	Department of IBR-2 spectrometers complex	41
-0851-	IBR-2 reactor	51
	Mechanical and Technical Department Electric and Technical Department Central Experimental Workshops Nuclear Safety Group Design Bureau	48 28 38 6 6
	FLNP infrastructure: Directorate Services and Management Department Scientific Secretary Group Supplies Group	 10 22 5 4
Total		**416**

Personnel from the JINR Member States (besides the RF) as of 31.12.2010

Country	People	of which young specialists (<35 years)	Country	People	of which young specialists (<35 years)
Azerbaijan	4	4	Mongolia	4	2
Bulgaria	3	1	Poland	5	
China	1		Romania	6	2
DPRK	2		Ukraine	7	6
Georgia	2		Uzbekistan	1	1
Germany	2				
Moldavia	2	2	**TOTAL**	**39**	**18**